Biologie

Characterization of type-III secreted bacterial virulence factors that interfere with Rho-GTPase signalling

Inaugural-Dissertation
zur Erlangung des Doktorgrades
der Naturwissenschaften im Fachbereich Biologie
der Mathematisch-Naturwissenschaftlichen Fakultät
der Westfälischen Wilhelms-Universität Münster

vorgelegt von
Stefan Arens

aus Unna

-2013-

Dekan:	Prof. Dr. Dirk Prüfer
Erste Gutachterin:	Prof. Dr. Theresia Stradal
Zweiter Gutachter:	Prof. Dr. Klemens Rottner
Tag der mündlichen Prüfung:	02.12.2013
Tag der Promotion:	03.12.2013

Zusammenfassung

Infektionskrankheiten sind vor allem in Entwicklungsländern eine große Bedrohung des menschlichen Lebens. Immerhin sind 10 % aller krankheitsbedingten Tode weltweit auf sie zurückzuführen. Verursacht werden diese Krankheiten durch Bakterien, wie zum Beispiel *Salmonella enterica*, *Shigella flexneri* oder enteropathogene und enterohämorragische *Escherichia coli*, die meist auf dem fäkal-oralem Weg in den Organismus gelangen. Im Darm heften sich die Bakterien an Epithelzellen oder dringen in diese ein und beginnen sich zu vermehren. Ein typisches Symptom einer solchen Infektion ist schwere Diarrhö. Es ist die Aufgabe der Wissenschaft, die komplexen Mechanismen hinter der Wirt-Pathogen Interaktion zu entschlüsseln, um Infektionen begegnen zu können.

Damit Bakterien eine Infektion etablieren können, müssen sie den Verteidigungsmechanismen des Wirtes entkommen. In der Regel wird dies dadurch erreicht, dass die Bakterien Signalwege der Wirtszelle manipulieren und sich so eine spezielle Nische schaffen, in der sie überleben können. Die Manipulation wird oft mit Hilfe eines Sekretionssystems erreicht, das es den Bakterien erlaubt Virulenzfaktoren in das Zytoplasma der Wirtszelle einzubringen. Hier interagieren die bakteriellen Proteine dann mit ihren wirtseigenen Zielen, wie beispielsweise den kleinen Rho GTPasen und rufen so unter anderem Veränderungen am Aktin-Zytokelett der Zelle hervor.

Obwohl die Zahl der verschiedenen Effektorproteine im Reich der Bakterien groß ist, lassen sie sich doch auf Grund bestimmter Charakteristika in einzelne Gruppen einordnen. Eine besondere Gruppe unter den Virulenzfaktoren stellt die sogenannte WxxxE Familie dar. Zu ihren Mitgliedern gehören IpgB1 und IpgB2 (*S.flexneri*), SifA und SifB (*S.enterica*) sowie Map und EspT (EPEC). Sie alle teilen ein konserviertes WxxxE Motiv und die meisten besitzen GEF Aktivität, die es ihnen ermöglicht Rho GTPasen zu aktivieren. Die WxxxE Familie ist zurzeit Gegenstand intensiver Forschung. Durch ihre Interaktion mit Rho GTPasen erhalten Bakterien Zugriff auf eine Vielzahl zelluläre Prozesse, allen voran Aktin-Zytokelett Organisation und Vesikel Transport. Aktuelle Untersuchungen deuten jedoch darauf hin, dass diese bakteriellen Virulenzfaktoren noch weiter Interaktionspartner unter den Wirtsproteinen haben müssen, um den Bakterien die Generierung eines optimalen Lebensraums zu ermöglichen.

Das finale Ziel dieser Arbeit war es daher, weitere Interaktionen zwischen Wirts- und bakteriellen Proteinen aufzudecken, die möglicherweise die Komplexität von Wirt-Pathogen Interaktionen erklären.

Mit Hilfe von biochemischen Methoden wie *pull down assays* und Co-Immunpräzipitationen, sowie mittels mikroskopischer Verfahren konnten deutliche Hinweise auf eine Interaktion zwischen dem humanen, mit RhoA interagierendem Protein Rhophilin1 (RHPN1) und dem Virulenzfaktor Map aus EPEC, der GEF Aktivität gegenüber Cdc42 besitzt, gefunden werden. In diesem Zusammenhang zeigen wir auch, dass RHPN1 mit der kleinen GTPase Rac1, zusätzlich zu RhoA, interagieren kann. Des Weiteren zeigen wir hier, dass RHPN1 zumindest teilweise an Mitochondrien lokalisiert und stellen erst Hinweise zur Verfügung, die darauf hindeuten, dass RHPN1 in der Lage ist Autophagie von membranassoziierten EPEC in Infektionsversuchen zu induzieren.

In parallelen Ansätzen zeigen wir, dass der bakterielle Virulenzfaktor IpgB2 aus *S.flexneri* in der Lage ist, mit dem Bardet-Biedl Syndrom Protein 4 (BBS4) in Interaktion zu treten. Schlussendlich scheint der *S.enterica* Effektor SifA mit der kleinen GTPase Rab9 interagieren zu können. Diese beiden ersten Erkenntnisse sind nun Gegenstand eigenständiger Projekte.

Zusammengefasst unterstreicht diese Arbeit, dass das Funktionsspektrum der untersuchten Virulenzfaktoren weit über die einfache Aktivierung von GTPasen hinausgeht. Die Fähigkeit mit weiteren Wirtsproteinen interagieren zu können, ermöglicht letztlich die Etablierung von bakteriellen Infektionen beziehungsweise verdeutlicht die Verteidigungsmechanismen der Zelle. Der spannende Zusammenhang zwischen EPEC Infektion und Autophagie wird zurzeit weiter verfolgt, um unser Verständnis des komplexen Zusammenspiels von Wirtszelle und diesem bedeutendem Pathogen auszubauen.

Summary

Infectious diseases are a serious threat of human life, especially in developing countries. They cause at least 10 % of all death on diseases worldwide. Bacteria like *Salmonella enterica*, *Shigella flexneri*, or enteropathogenic and enterohemorrhagic *Escherichia coli* cause such diseases. Usually they enter the host organism via the fecal-oral route. In the intestine they attach to, or invade epithelia cells and begin to reproduce. Severe diarrhea is a typical symptom of those infections. In order to fight infections, it is the task of science to decrypt the complex mechanisms of host pathogen interaction.

Prior to establishment of an infection, bacteria have to overcome the defense system of the host. Commonly, bacteria can accomplish this by manipulating the host´s signaling pathways, leading to the formation of a replication niche where the bacteria can survive. Often bacteria utilize a secretion system to inject virulence factors into the host cell cytoplasm, which in turn start manipulation of the host targets. Common targets are small GTPases that control rearrangements of the actin cytoskeleton.

Although the number of different effector proteins among the bacteria is huge, it is possible to group them on the basis of certain characteristics. A special group of virulence factors is the so called WxxxE family. IpgB1 and IpgB2 (*S.flexneri*), SifA and SifB (*S.enterica*), as well as Map and EspT (EPEC) are family members. All of them contain a conserved WxxxE motive, and the majority of them embodies bacterial GEFs, which are able to activate Rho GTPases. Currently, the WxxxE family is subject of extensive research. By targeting Rho GTPases, bacteria gain access to a variety of cellular processes, like actin cytoskeleton organization or vesicle transport. Current research indicated that these bacterial virulence factors must have additional interactors among the host´s proteins to allow bacteria the generation of an optimal environment.

The ultimate goal of this work was to identify further interactions between host- and bacterial proteins that may explain the complexity of host pathogen interaction.

By using biochemical methods like pull down assays and co-immunoprecipitations as well as microscopic techniques we reveal evidence for an interaction between the human RhoA interactor rhophilin1 (RHPN1) and the virulence factor Map from EPEC, which embodies a bacterial GEF for Cdc42. Within this framework we also show that RHPN1 is able to bind, to the small GTPase Rac1 in addition to RhoA. Furthermore we here show an at least partial localization of RHPN1 to mitochondria

and provide initial evidence for RHPN1 being able to induce autophagy of EPEC attached to the plasma membrane by using infection assays.

In a parallel effort, we show that the bacterial virulence factor IpgB2 from *S.flexneri* is able to get in contact with the Bardet-Biedl Syndrom Protein 4 (BBS4). Finally, the *S.enterica* effector protein SifA targets the small GTPase Rab9. These two initial findings are now subjects of independent projects.

In conclusion, this work underpins once more that the spectrum of functions of the analyzed virulence factors goes far beyond the simple activation of GTPases. The ability to interact with further host proteins finally allows establishment of an infection or reflects cell defense mechanisms. The exiting link between EPEC infection and autophagy is currently followed to further our understanding of the complex interplay of host cells with this important pathogen.

Content

Abbreviations

®	registered trademark symbol
%	percent
°C	degree Celsius
2D	two dimensional
α	anti
Å	ångström
A	ampere
aa	amino acid(s)
A/E	attaching and effacing
AIDS	acquired immunodeficiency syndrome
amp	ampicillin
ADP	adenosine diphosphate
APS	ammoniumperoxodisulfat
ATP	adenosine triphosphate
BBS	Bardet-Biedl syndrome
BSA	Bovine serum albumin
c	centi-
CA	constitutive active
cDNA	complementary DNA
CDRs	circular dorsal ruffles
cfu	colony forming unit
Da	Dalton
dd	double distilled
DKFZ	German Cancer Research Center
DMEM	Dulbeccos' modified Eagle medium
DMSO	dimethyl sulfoxide
DN	dominant negative
DNA	deoxyribonucleic acid
E	glutamic acid
EDTA	ethylenediaminetetraacetic acid
e.g.	exempli gratia
EHEC	enterohemorrhagic *E.coli*

EPEC	enteropathogenic *E.coli*
EtOH	ethanol
ESCRT	endosomal sorting complexes required for transport
et al.	et alii
F-actin	filamentous actin
FCS	fetal calf serum
g	gram
G	glycine
G-actin	globular actin
GAP	GTPase activating protein
GBD	global burden of disease
GDI	guanosine nucleotide dissociation inhibitors
GDP	guanosine diphosphate
GEF	guanosine nucleotide exchange factor
GFP	green fluorescent protein
GST	glutathione sepharose
GTP	guanosine triphosphate
h	hour(s)
HGF	hepatocyte growth factor
HIV	human immunodeficiency virus
HRP	horseradish peroxidase
Hs	Homo sapience
IF	immunofluorescence microscopy
IFN	Interferon
IFT	intraflagellar transport
Ig	immunglobulin, immunglobulin-domain
Il	interleukin
IP	immunoprecipitation
IPTG	isopropyl β-D-1-thiogalactopyranosid
k	kilo-
kana	kanamycin
KO	knockout
l	liter(s)
L	leucine

LB	Luria Bertani broth
LEE	locus of enterocyte effacement
LPS	lipopolysaccharide
m	milli- or meter(s)
M	molar mass
mc	monoclonal
MBP	maltose binding protein
MEFs	mouse embryonic fibroblast
MEM	minimum Essential Medium Eagle
MHC	major histocompatibility complex
min	minute(s)
Mm	Mus musculus
MVB	multivesicular body
n	nano-
N	Newton or asparagine
No.	number
NPF	nucleation promoting factors
n.s.	not significant
OD_{600}	optical density at 600 nm
p	pico-
PAGE	polyacrylamide gel electrophoresis
PBS	phosphate buffered saline
pc	polyclonal
PCR	polymerase chain reaction
PDGF	platelet-derived growth factor
PDZ	PSD-95/Disk-large/ZO-1 binding motif
PFA	paraformaldehyde
P_i	phosphate
PS	penicillin/streptomycin
PVDF	polyvinylidenfluorid
Q	glutamine
RHPN	rhophilin
rpm	rounds per minute
s	second(s)

SAP	supernatant after pull down
SCV	*Salmonella* containing vacuole
SDS	sodium dodecyl sulfate
Sifs	*Salmonella* induced filaments
SN	supernatant
SS	super-sonication
t	time
T	threonine
T3SS	type 3 secretion system
TAE	tris base, acetic acid and EDTA containing buffer
TBS	tris-buffered saline
TBS/T	tris-buffered saline / Tween 20
TIF	tagged image file format
Tir	translocated intimin receptor
TLR	Toll like receptors
µ	micro-
U	unit
V	volt or valine
v/v	volume per volume
W	tryptophan
w/v	weight per volume
WHO	world health organization
WT	wild type
x	times magnification
x*g*	times gravitation constant
Y2H	yeast two hybrid
YLL	years of life lost

1 Introduction

1.1 Host pathogen interaction

Why should we study host pathogen interactions? To answer this question, a simple look into the latest world health organization (WHO) report on "The Global Burdon of Diseases" (GBD) is sufficient. In 2010 5.3 million or 76 of 100,000 people died on infectious diseases, these are 10 % of all death on diseases. If we take a closer look at diarrhea, caused for example by enteropathogenic *E.coli* (EPEC), *Salmonella* or *Shigella*, which are subject of this thesis, it becomes even more obvious. Diarrhea killed 1.4 million people in 2010, this is the same case number as for HIV/AIDS. Diarrhea is on position four of the global years of life lost (YLLs) ranking, with huge differences between high and low income countries (Figure 1). Every year, 1.25 million (20 % of all death) children under an age of 5 years die of infectious diseases. However, one promising fact from this report is, that in the last twenty years, the number of deaths caused by infectious diseases decreased from 7.8 million in 1990 by 32 %, reflecting the increased efficiency of treatment and technology of this poverty connected disorders (Lozano *et al.*, 2012).

	Global	Western Europe	North America	South America	Australasia	High-income Asia Pacific	Central Asia	South Asia	North Africa	South Africa
Ischaemic heart disease	1	1	1	1	1	2	1	4	1	11
Lower respiratory infections	2	9	11	3	14	5	2	1	3	2
Cerebrovascular disease	3	2	3	2	3	1	3	9	2	7
Diarrhoeal diseases	4	61	54	55	76	57	14	3	7	3
Malaria	5	120	120	122	117	119	116	36	41	14
HIV/AIDS	6	40	26	20	56	65	20	13	38	1

Ranking Legend	1-10	11-21	21-30	31-51	51-90	91-177

Figure 1 Global and regional ranking of leading causes of years of life lost (YLL)

To calculate the YLL the years, lost by early death, till anticipated average life, in certain region or country are counted. With other words this graphic shows which disease "steel" how many years, global and in different regions. Rank one to three ischaemic heart diseases, lower respiratory infections and cerebeovascular diseases respectively have an equally huge influence all over the world, without noticeable effects of income. In other cases it is different, diarrhea for example is concentrated on poor regions and the influence of malaria depends on the distribution of the anopheles mosquito (Lozano et al., 2012).

1.2 The Host

1.2.1 Motion

Motion is an essential feature of life. Cellular motility is tightly connected to the formation of actin driven membrane protrusions, namely lamellipodia, filopodia and ruffles (Small *et al.*, 2002). In 1980 Abercrombie first linked the thin layer of protruding cytoplasm at the cell periphery to motility. Protrusions, parallel to the substrate, were named “leading edge” or “lamellipodium” (Abercrombie *et al.*, 1970a). Abercrombie further noticed a random continuous protrusion and retraction of the lamellipodium, with a net plus on protrusions, pushing the cell forward. In the following thirty years intensive research generated much insight to cell movements, so that today, the events at the leading cell edge are quite well described. The mechanism behind protrusion and retraction of the dynamic structures at the cell front is the assembly and disassembly filamentous actin (F-actin) (see 1.2.1.5). This process is tightly regulated in mammalian cells. Key regulators in this process are the small guanosine triphosphatases (GTPases) of the Rho-family (Hall, 1998). Some pathogens are able to hijack these cellular processes in order to manipulate the hosts actin cytoskeleton resulting in local ruffle formation and lamellipodia extension which trigger the internalization of bacteria into membrane bound vacuoles (Patel *et al.*, 2005, McGhie *et al.*, 2009). In the following passages I attempt to shed light on the different protrusive structures and the established factors involved in their regulation. Furthermore I would like to focus on actin polymerization, the core process behind migration.

1.2.1.1 Lamellipodia and ruffles

There is a lot of knowledge available on the lamellipodium since it has been studied for more than a half decade. Ingram and Abercrombie were among the first who used light microscopy techniques, to systematically analyze the “leading edge” of moving cells (Ingram, 1969, Abercrombie *et al.*, 1970a, Ladwein *et al.*, 2008).

The 0.1-0.2 µm thick and 1-5 µm wide seam (according to the cell type) at the leading edge of the cell consists of a dense meshwork of actin-filaments, pushing their fast growing ends against the plasma membrane (Small *et al*., 1978) (Figure 2). If the lamellipodium detaches from the substrate and curls upwards, we have a special form, called “membrane ruffle” or only ruffles (Abercrombie *et al*., 1970b).

By the injection of fluorescent actin into fibroblasts, it could be shown that the leading edge of the lamellipodium is in fact the primary site of actin incorporation (Glacy, 1983). Embedded in the lamellipodium actin bundles could often be observed. If these bundles stay inside the lamellipodium they are called "microspikes" and if they extend beyond its edge they are referred to as "filopodia" (Small *et al*., 2002). Apart from their functions in cellular migration, lamellipodia fulfill several other important functions. Namely they participate in development of adhesions and are involved (as ruffles) in macropinocytosis as well as in phagocytosis. The exertion of those different functions demand an exact regulation. This regulation mainly occurs by actin polymerization and disassembly. The primary pathway leading to lamellipodia and ruffle formation is via the small Rho GTPase Rac and the actin nucleator Arp2/3 (see 1.2.1.5). The significance of GTPases for the actin cytoskeleton in general and of Rac for the lamellipodium in particular is known since Ridley and colleagues microinjected purified constitutively active Rac into fibroblasts and observed massive lamellipodia and ruffle formation (Ridley *et al*., 1992).

In mice the absence of Rac1 is embryonic lethal at day 6.5, because of incomplete gastrulation (Sugihara *et al*., 1998). Therefore further genetic analysis requires the creation of conditional alleles. This allows embryonic survival followed by tissue specific knockout later in differentiation (Gu *et al*., 2003). Using this method, Vidali and colleagues generated mouse embryonic fibroblasts (MEFs) deleted for Rac1. These cells show a dramatic change in morphology and lack lamellipodia and ruffles. However, their knockout (KO) cells were still able to migrate with help of pseudopodia like protrusions, along a platelet-derived growth factor (PDGF) gradient (Vidali *et al*., 2006).

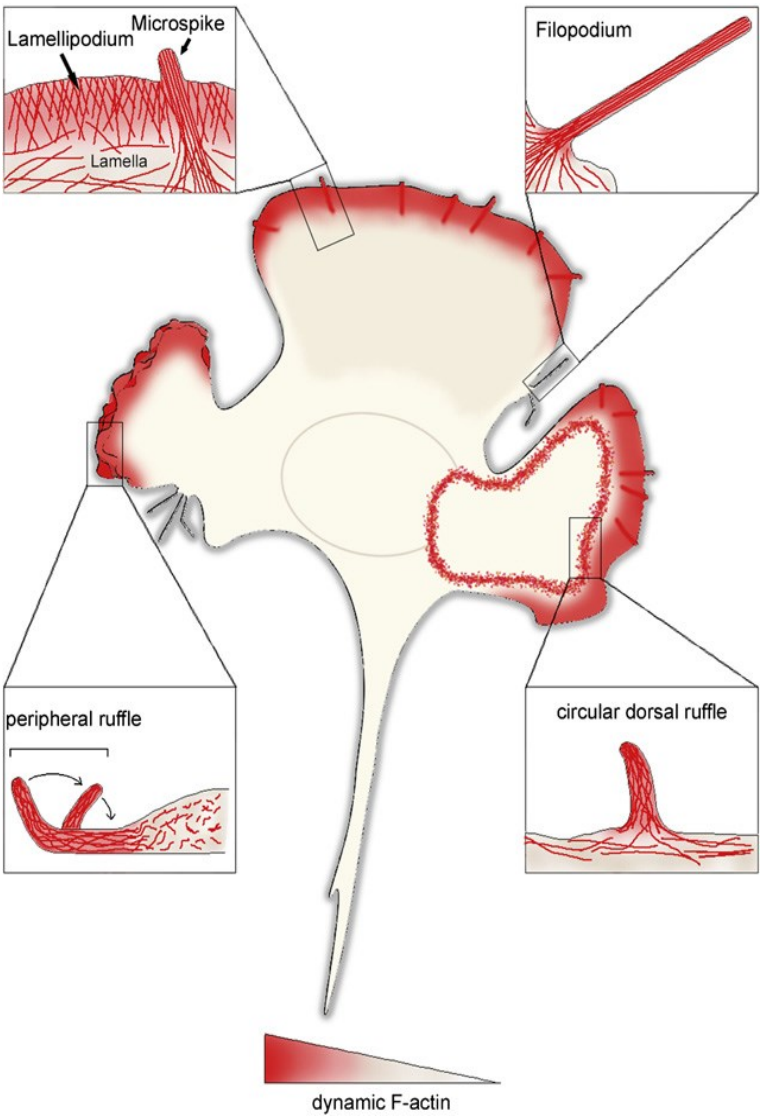

Figure 2 Schematic illustration of protrusive structures at the cell surface

The image illustrates the protrusive membrane structures of a migrating cell. The intensity of the red color symbolizes the grade of actin dynamics. Finally there are four close-ups, which show the different structures in a higher resolution. We have lamellipodia along the leading edge with embedded microspikes. If the membrane curls up, either at the cell periphery or on top of the cell as circular structures, so called ruffles are formed. Furthermore there are rods of parallel actin, protruding beyond the cell borders into the extracellular space, which are termed filopodia (Ladwein *et al.*, 2008).

Besides membrane ruffles at the leading edge of the cell, which were already mentioned, there is a second type of ruffles, the so called circular dorsal ruffles (CDRs) (Figure 2). This highly dynamic structure is rich in F-actin. They can be observed a few minutes after treatment with growth factors such as PDGF (Mellström *et al.*, 1983) or hepatocyte growth factor (HGF) (Dowrick *et al.*, 1993).

The lamellipodium often curls up from the substratum and moves, like small sails, on the cell surface towards the cell center. Alternatively, CDRs can establish directly on the back of the cell in 2D tissue culture. Single membrane ruffles can group together and build circular ruffles, which constrict and close within 5-20 minutes (Mellström *et al.*, 1983). The cup-like structure formed by CDRs goes perfectly with the process termed macropinocytosis and may serve receptor internalization (Swanson, 2008, Hoon *et al.*, 2012). However, the impact of CDRs on macropinocytosis is under discussion. As Suetsugu *et al.* showed, the uptake of fluorescently labeled dextran through macropinocytosis did not occur at places of CDRs (Suetsugu *et al*., 2003). Further research will be necessary to clarify this point.

1.2.1.2 Filopodia and Microspikes

In contrast to the dense meshwork of differently angled actin filaments building the lamellipodium (Köstler *et al*., 2008), filopodia are finger like protrusive structures, regularly embedded in or extending beyond the lamellipodium that contain parallel bundles of actin filaments (Ridley, 2011). Bundles of actin which remain within the lamellipodium and do not protrude further are called microspikes (Small *et al*., 2002). Microspikes also can serve as precursors of filopodia (Svitkina *et al*., 2003). Filopodia participate in many processes, ranging from sensing the environment (Wood *et al.*, 2002b) or chemoattractants (Koleske, 2003), over anchorage of the cell to the extracellular substrate (Wehrle-Haller, 2012, Partridge *et al.*, 2006), to wound healing (Wood *et al.*, 2002a). Furthermore, as already mentioned in the previous paragraph, filopodia can develop independent of lamellipodia and take part in cellular motility, as it was shown e.g. in Rac1 KO cells (Vidali *et al*., 2006) or cells deficient in WAVE complex function (Steffen *et al.*, 2006).

Studies in different cell types revealed that there is huge variation in dynamics and length of filopodia, even positioning of these protrusions differ (Mattila *et al.*, 2008). The dynamics of filopodia, protrusion and retraction results from the balance between actin polymerization at the tip and retrograde flow (Mallavarapu *et al.*, 1999).

Like already described above for lamellipodia, the formation of filopodia is regulated by a member of small Rho GTPase family. In 1995 Hall and others investigated the role of small Rho GTPases by microinjection experiments combined with live time imaging. Co-microinjection of dominant negative Rac1, to abolish lamellipodia and

constitutive active Cdc42 showed, that the formation of filopodia starts after five minutes (Nobes *et al.*, 1995, Kozma *et al.*, 1995). The regulation of filopodia formation by Cdc42 was initially believed to occur via activation of WASP and N-WASP, leading subsequently to induction of the actin nucleator Arp2/3 (Prehoda *et al.*, 2000, Rohatgi *et al.*, 1999). But more recent studies have shown that filopodia can form independent of Arp2/3 and Cdc42 (Steffen *et al.*, 2006, Sigal *et al.*, 2007) and highlighted the role of formins and VASP (Figure 6) as actin nucleator leading to filopodia formation (Faix *et al*., 2009). Nevertheless, contribution of Arp2/3 is still subject of discussion (Rottner *et al.*, 2011, Mattila *et al.*, 2008, Yang *et al.*, 2011).
To concentrate single actin filaments to a stiff actin bundle, so called actin cross-linking proteins are necessary. One member of this group, which localizes to filopodia shafts is fascin, other proteins like fimbrin, α-actinin, espin and villin can cross-link F-actin too, but are not specifically targeted to filopodia (Kureishy *et al.*, 2002, Vignjevic *et al.*, 2006).

1.2.1.3 Stress fibers

The last of the prominent cytoskeletal actin structures are stress fibers, thick bundles of actin filaments which pervade the cell. Each bundle consists of 10-30, in some cases of up to 300 filaments which are themselves composed of actin and non-muscle motor protein myosin II (Cramer *et al.*, 1997, Weber *et al.*, 1974). Bundling is accomplished by α-actinin, maybe in cooperation with other actin cross-linking proteins (Lazarides *et al.*, 1975, Pellegrin *et al.*, 2007). Due to their subcellular localization, stress fibers are grouped into three different classes, ventral and dorsal stress fibers plus transverse arcs (Small *et al*., 1998) (Figure 3). One of the first descriptions of those structures, although not specially named yet, was made by Heath and colleagues (Heath *et al.*, 1978). The most commonly observed are ventral stress fibers which span the cytoplasm along the ventral side of the cell and are linked to focal adhesions at both ends. In contrast, dorsal stress fibers are significant shorter and only attached to adhesions on one side. Finally transverse arcs are situated at the dorsal surface, behind the lamella, and seem not to be connected to any adhesions (Heath *et al.*, 1978). When the loose ends of dorsal stress fibers, or arcs, meet they are able to fuse, resulting in a new ventral stress fiber, so dorsal fibers could be seen as precursors of ventral ones (Hotulainen *et al.*, 2006). The combination of focal adhesions, actin fibers and myosin II suits perfectly to generate

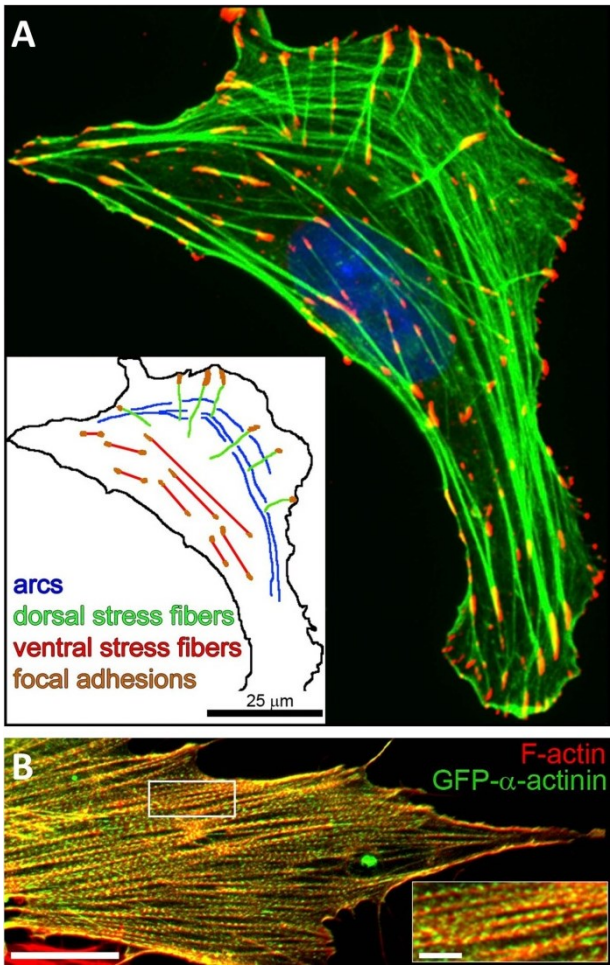

Figure 3 Three types of stress fibers in the cell

In the immunofluorescence image (A) a U2OS human osteosarcoma cell stained for focal adhesions (red) F-actin (green) and the nucleus (blue) is shown. Ventral stress fibers, connecting two adhesions are located in the back part of the cell. Dorsal ones grow from focal contacts at the protruding front. The more filigree arcs could be found right behind the lamella. An overview of the different structures is given in the drawing. In (B) the periodical composition of stress fibers is illustrated by α-actinin (green) and F-actin (red) staining in Swiss 3T3 cells. (Bars: left 25µm; right 10µm) (Burridge *et al.*, 2013).

tension. The result of force measurements revealed, that a constant stress of 5.5 ± 2 nN/µm^{-2} is applied on single adhesions by actomyosin (Balaban *et al.*, 2001). Loss of stress fibers in response to C3 toxin treatment suggested participation of the three Rho members of the small GTPase family in the signalling pathway leading to stress fiber formation (Chardin *et al.*, 1989). The role of RhoA, RhoB and RhoC, all main targets of C3 toxin, was validated by microinjection, which results in massive stress fiber formation and alters the complete cell shape (Paterson *et al.*, 1990). Under physiological conditions RhoA seems to be the major regulator of stress fiber formation, while RhoB and RhoC fulfill a minor role or they are specialists for

particular situations or cell types (Pellegrin *et al.*, 2007). Later two main players downstream of RhoA were discovered, namely the ROCK/ROK protein kinases (Leung *et al.*, 1995) and the diaphanous-related formin, mDia1 (Watanabe *et al.*, 1997). On their own, both proteins are not able to emulate the effect of a RhoA overexpression. Only if ROCK and mDia1 work concurrently, they are able to induce thick and long actin bundles (Watanabe *et al.*, 1999).

1.2.1.4 Small GTPases

It has already become clear in the previous chapter that dealt with protrusive structures, that small GTP-binding proteins have a central role in controlling cellular locomotion. Beyond this, they are key regulators in a lot of cellular processes, including cell polarity, vesicle trafficking and cytokinesis (Heasman *et al.*, 2008). The story of their discovery started in 1982 with the identification of the mutationally activated oncogene *RAS* in human cancer cell lines. In the following decades immense effort has been put into research and a huge superfamily of Ras related small GTPases, which is highly conserved from yeast to mammals, has been discovered (Cox *et al.*, 2010). One member is the Rho GTPase family, which comprise 20 proteins at the moment (Heasman *et al.*, 2008). Among them are Cdc42, Rac1 and RhoA (Figure 4).

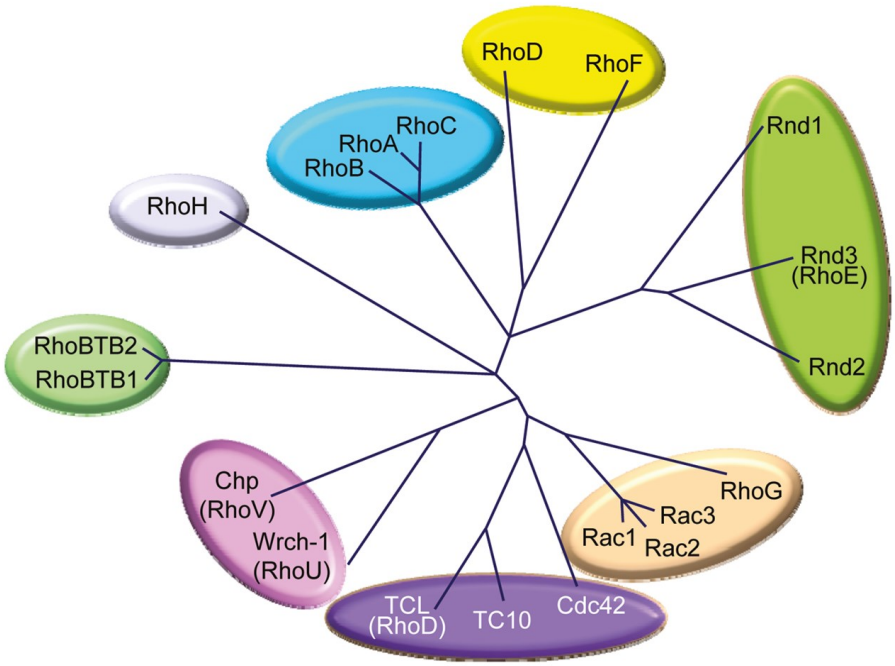

Figure 4 Dendrogram of the small Rho GTPase family

Members of the human Rho GTPases, shown in a Clustal/W dendrogram (Cox *et al.*, 2010)

Most GTPases shuttle between two conformational stages (Figure 5), one is the GTP bound active stage, in which the GTPase is able to interact with its downstream effectors, the other is GDP bound and inactive. The dissociation of GDP and incorporation of GTP is catalyzed by one of over 80 guanine nucleotide exchange factors (GEF). This takes place at the cell membrane, to which the GTPases are associated via an isoprenyl moiety that is post-translationally added to the carboxyl terminus of the protein. The other way round, the hydrolysis of GTP is driven by GTPase activating proteins (GAP), there are more than twenty of them. There is one more regulatory component, the GDIs (guanine dissociation inhibitors), which keep the GTPase inactive (Aktories, 2011, Cherfils *et al.*, 2013) and protect them from degradation (Boulter *et al.*, 2010).

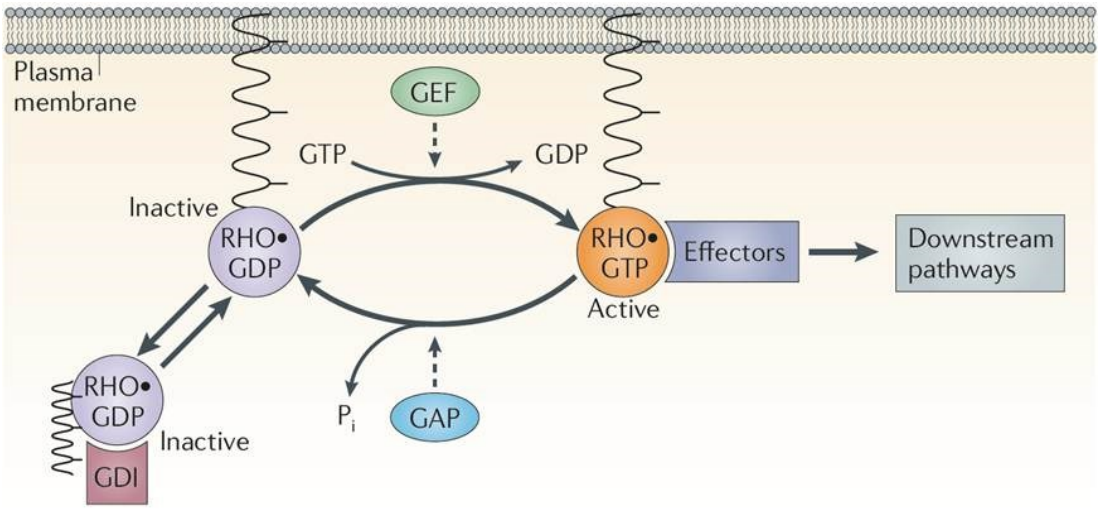

Figure 5 Regulation of the Rho-family GTPase cycle

The activation of Rho-family GTPases is catalyzed by GEFs and takes place at the plasma membrane. In the GTP bound active state, the GTPase is able to interact with its specific effector proteins to affect downstream pathways. GAPs enhance the intrinsic GTPase activity and thereby help to hydrolyze GTP to GDP+P_i. By capping the isoprenyl moiety, GDIs keep the GTPase away from the plasma membrane, resulting in a durable inactivation (Aktories, 2011).

The tight regulation of GTPases by different GEFs, GAPs and GDIs with partially overlapping activities has the advantage that the cell can respond specifically to different signals, guiding them precisely in their target pathways. This level of regulation is a main target of the manipulation by pathogens that have evolved intricate strategies to hijack or block the GTPase activation cycle. On the other side the cycle is prone to interference and manipulation by pathogens. In the following I

will give several examples, to illustrate the variety of possibilities for pathogens, to subvert the GTPase cycle: 1) the two virulence factors of *Salmonella Typhimurium*, SpoE and SopE2, which serves as bacterial GEF for Rac1 and Cdc42 (Hardt *et al.*, 1998); 2) DrrA from *Legionella pneumophila*, which functions in two ways, by stimulating the GTP incorporation and by releasing its target GTPase from GDIs (Murata *et al.*, 2006, Schoebel *et al.*, 2009); 3) *S. Typhimurium* SptP which is able to act as a bacterial GAP facilitating the hydrolysis of GTP (Fu *et al.*, 1999).

1.2.1.5 Actin polymerization

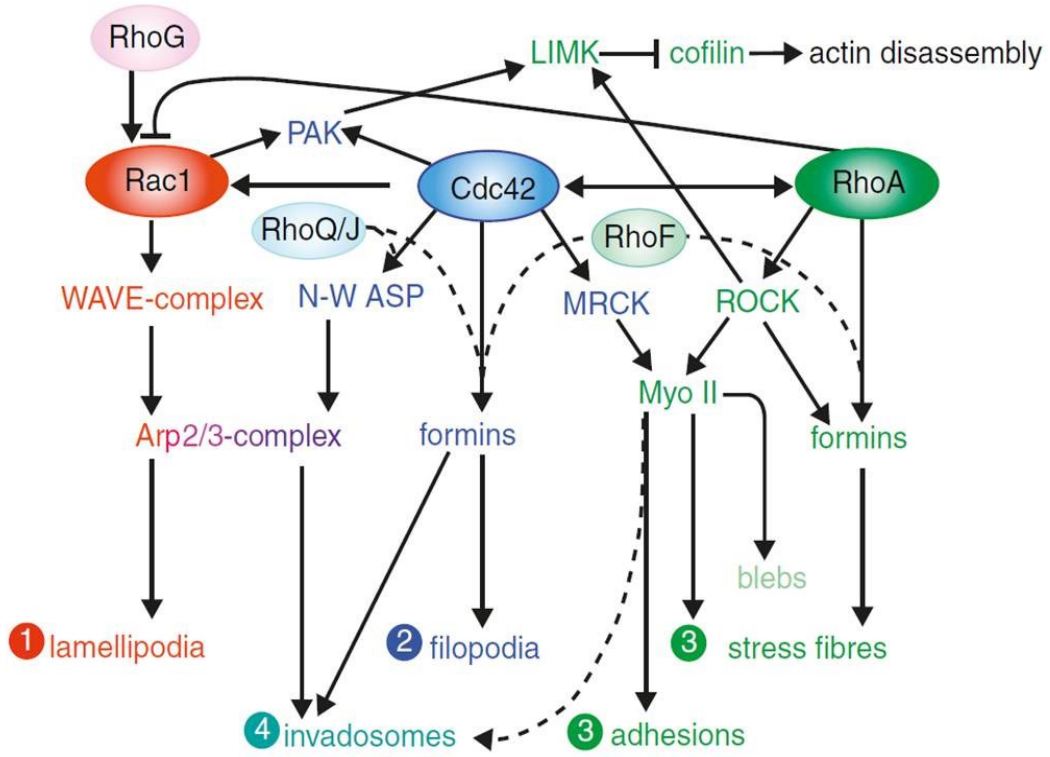

Figure 6 Organization chart of the signaling network leading to actin structures

Cytoskeletal reorganization is mainly mediated via the small GTPases Rac1, Cdc42 and RhoA, leading to lamellipodia, filopodia and stress fibers respectively. An additional level of complexity is added by the fact that the different pathways crosstalk with each other. Cdc42 for instance, is able to influence invasive migration or contractility in addition to and independent of filopodia formation. The main actin-nucleators are Arp2/3 complex and formins. Arp2/3 is activated by NPFs such as N-WASP or WAVE-complex. Actin polymerization via formins is triggered by RhoA (Rottner *et al.*, 2011).

Figure 6 shows the complex network, controlling the formation of actin riche protrusions. In this chapter I would like to focus on the very last step of the cascade, the procedure of actin nucleation.

Actin is one of the most abundant proteins in eukaryotic cells. Two forms of this ATP-binding protein are present in the cell: 1) is the 42 kDa monomeric globular actin (G-actin) and 2) filamentous actin (F-actin) derived from non covalent-self-assembly of monomers. These filaments have two asymmetric ends. The growing barbed end has a high affinity for filamentous (thus favoring polymerization) while the pointed end has a lower affinity for globular actin (thus favoring depolymerization in the equilibrium). The difference between (+) and (-) end results in a slow treadmilling of subunits (Figure 7).

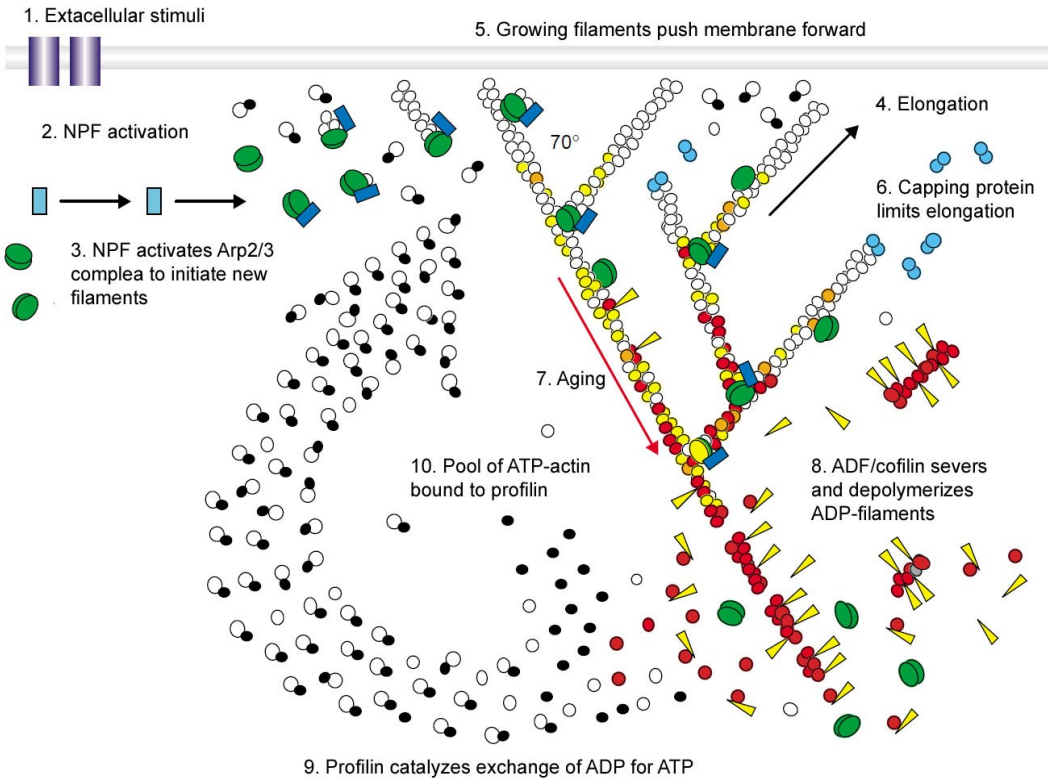

Figure 7 Assembly and recycling of branched actin filament networks

The treadmilling model of actin filament assembly and recycling involves the Arp2/3 complex and several other proteins which posses regulatory influence on the cycle. At the beginning of the cycle an external stimulus (1), signals to cell to move or to alter its shape. The external signal triggers a pathway, which at the end activates a NPF (2), which in turn binds to actin and activates the Arp2/3 complex, a new filament is initiated (3). These filaments are elongated by incorporation of ATP-actin (4), which pushes the membrane forward (5). The elongation stops when capping protein binds to the barbed end, preventing the addition of further actin monomers (6). During maturation of the filaments (7) hydrolysis of ATP-actin and γ-phosphate dissociation takes place. ADF/cofilin promotes dissociation and severs ADP-actin filaments (8). Finally profilin catalyzes the ADP for ATP exchange of G-actin (9), refilling the pool of polymerization-competent actin (10) waiting for the next round of filament nucleation (Pollard *et al.*, 2003).

In case of pure actin filaments, treadmilling results in a forward movement with a velocity of 0.04 µm/min. However, under in vivo conditions filaments can grow much faster with up to 10 µm/min. The velocity is increased by additional factors that facilitate growth. To start a new filament, three monomers have to group together to form a nucleation seed called "nucleus". In principle, the nucleation of F-actin can occur spontaneously but it is highly inefficient, since formation of actin dimers or trimers is kinetically unfavorable. To solve this problem, actin nucleators and so called nucleation promoting factors (NPF) are available in the eukaryotic cell, which catalyze the process to overcome the kinetic barrier. For a long time only one nucleator, Arp2/3 complex and a few NPFs were known. The past decade however, lead to the identification of more NPFs, other nucleators like formins, and further proteins involved in actin polymerization. All this can be found in a variety of reviews on this topic, for example (Campellone *et al.*, 2010, Goley *et al.*, 2006, Pollard *et al.*, 2003, Rotty *et al.*, 2013).

Arp2/3-complex

The Arp2/3-complex was discovered several times independently in the 1990s, for example by affinity chromatography from *Acanthamoeba*, using the G-actin binding protein profiling as affinity matrix (Machesky *et al*., 1994), or as a human factor required for actin-comet tail formation of *Listeria monocytogenes* (Welch *et al*., 1997) and as a essential factor of Cdc42 induced actin filament assembly (Ma *et al*., 1998). The complex consists of seven subunits with two actin related components, the actin related proteins 2 and 3 (Arp2 and Arp3) (Machesky *et al*., 1994). The subunits Arp2 and Arp3 build a dimer and function as a nucleator by imitating the structure of a free (+) end, thus generating a nucleation seed. The complex binds to pre existing filaments and is able to generate new filaments by Y-shaped branching, afterwards Arp2/3 remains at the pointed end of the new filament (Rouiller *et al.*, 2008, Mullins *et al.*, 1998). Due to its structural conformation, Arp2/3 on its own is rather inefficient in nucleating (Campellone *et al.*, 2010). To increase the nucleation efficiency, two things are necessary. The complex has to bind to an existing actin filament and it has to be activated by NPFs, resulting in conformational changes bringing Arp2 and Arp3 in the right conformation (Goley *et al.*, 2004).

Nucleation promoting factors

The first NPF was discovered in 1998 by Welch and colleagues. They could show that the *Listeria* surface protein ActA is able to activate the Arp2/3 complex, resulting in an accelerated actin filament formation. ActA alone was not able to generate filaments. They estimated that this mechanism of Arp2/3 activation may play a role in the cell too (Welch *et al*., 1998), which turned out to be true in the following years. Today we know that there are two subclasses of NPFs (Figure 8), recently reviewed by Rotty and colleagues. All class I NPFs contain a VCA domain, which allows G-actin as well as Arp2/3 binding at the same time. This VCA domain (also known as WH2 = WASP homology 2 domain) consists of 3 modules: the V = verprolin homology, the C = connector and the A = acidic motif. Members of this class are WASP, N-WASP, WAVEs and the more resent discovered WASH, WHAMM and JMY. Class II NPFs include cortactin and Hs1, they lack the VCA domain but nevertheless they are able to bind to Arp2/3 and F-actin instead of G-actin. They are thought to have stabilizing effects on existing filaments. Besides activating cofactors of the Arp2/3 complex, there are also repressive ones, like cofilin or PICK1. Both types of cofactors underlay a tight regulation by various signaling pathways (Rotty *et al*., 2013).

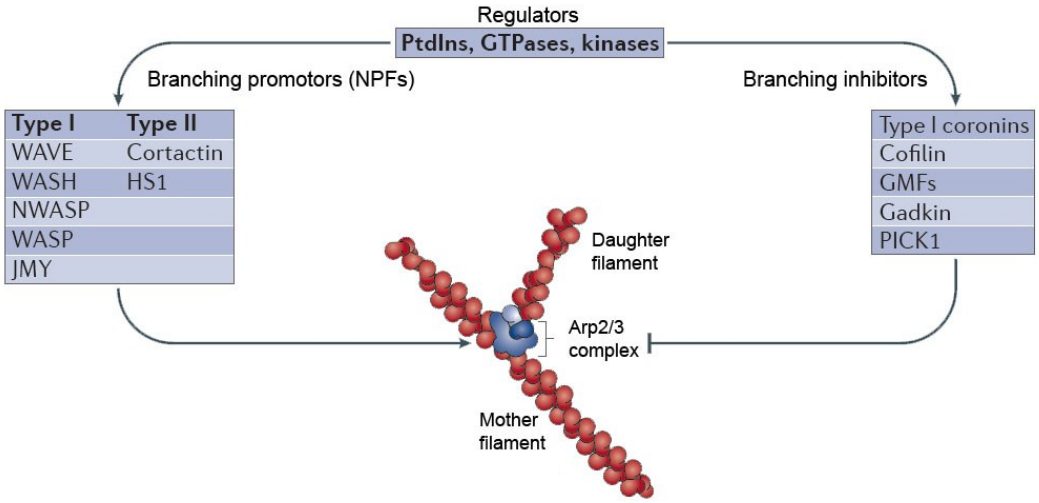

Figure 8 Positive and negative regulation of the Arp2/3 complex

The Arp2/3 complex initiates new filaments from the side of preexisting mother filaments. For this function the complex has to be tightly regulated. The activators, so called nucleation promoting factors are divided into two subclasses, containing either directly activating or stabilizing effects. The inhibitors execute a lot of different functions, among them filament severing or destabilizing. Positive as well as negative cofactors of Arp2/3 underlay the regulation of various signaling pathways (Rotty *et al*., 2013).

1.2.2 Defense mechanisms

Higher organisms are under constant thread of bacteria, viruses and other hazardous organisms or toxins. Only very complex self-defense mechanisms secure survival. In case of animals, this mechanism is the immune system. In mammals, it is divided into two parts, the innate and the adapted immune system. To survive and proliferate within the host, pathogens have either to hide or to escape. The mammalian intestine is a well studied example of how a host defends against intruders, because this niche embodies the zone where the bacteria-containing gut lumen and the sterile body adjoin, separated only by a barrier made of a thin layer of epithelia cells. Indeed, these cells are the first physical and chemical defense line. If pathogens are able to breach this barrier to invade deeper tissues, they face the innate immune system, which is represented by different phagocytic cells.

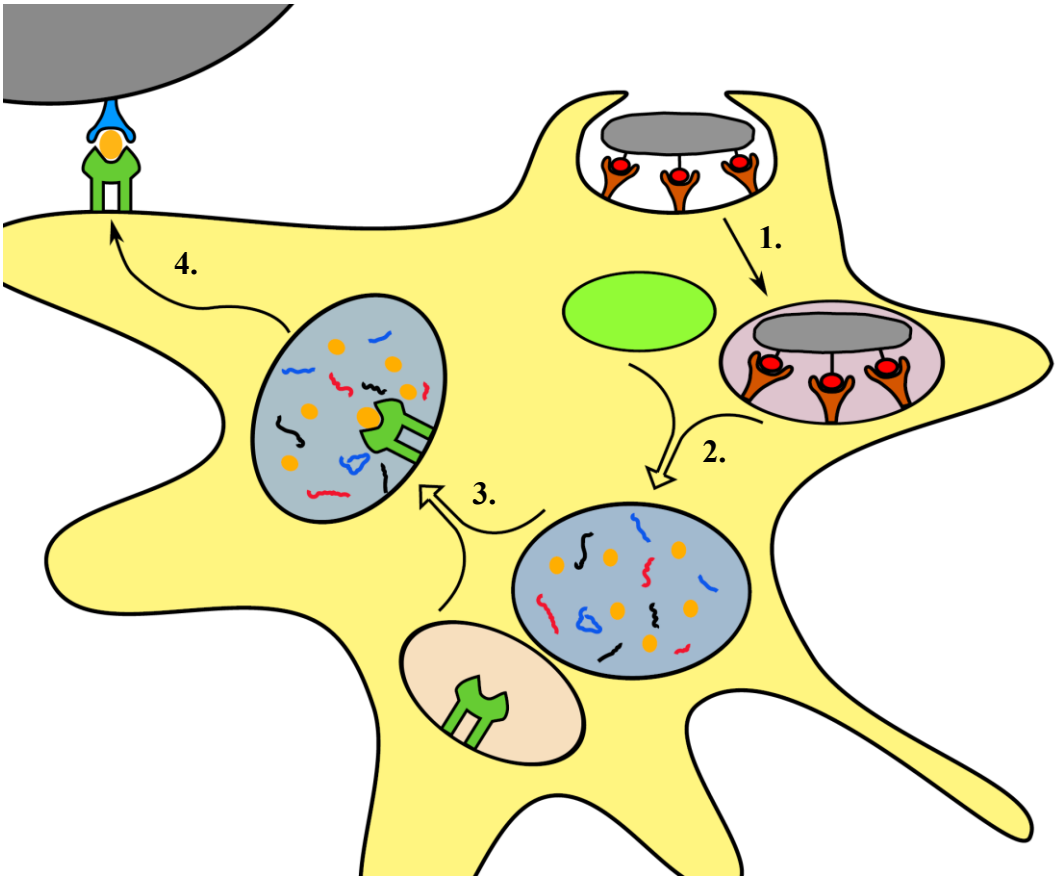

Figure 9 Recognition, phagozytosis and subsequent degradation of pathogens

Specialized cells for phagocytosis like macrophages or dendritic cells carry receptors on their surface that detect certain pathogen related antigens or structures. Upon pathogen recognition, phagocytosis takes place (1.). In the next step, the phagosome fuses with lysosomes and the pathogen is degraded (2.). After fusion with a MHC carrying vesicle, antigens of the pathogen remnants are prepared for antigen presentation (3.). Finally, the loaded MHC is translocated to the cell surface and presents the antigen to naïve T cells (4.).

During phagocytosis specialized cells, like macrophages, neutrophils and dendritic cells, recognize, engulf and digest large particles (Figure 9), for example bacteria (Botelho *et al.*, 2011). For obsonized particles the best characterized pathways go via the FCγ- or the complement receptor (Caron *et al.*, 1998). In case of non-obsonized particles, there are multiple other receptors, including Toll like receptors (TLR) (Shen *et al*., 2010) or the scavenger and mannose receptors (Zhang *et al.*, 2005), that can indicate phagocytosis. Pathogens that invade host cells and escape from the phagosome, face the autophagy system as the next line of host defense (Yuk *et al*., 2012). Although phago- and autophagocytosis belongs to the innate immune system, they are also crucial for the activation of adopted immunity. Pathogen derived peptides from the phagosome are processed for presentation on major histocompatibility complex (MHC). The antigen presenting MHC is translocated to the plasma membrane, where naïve T cells are able to recognize the antigen and induce the adapted immune response (Kagan *et al.*, 2012). In addition, triggering of the TLR or any type of pathogen recognition leads to the activation of inflammatory factors, like NF-κB, AP-1 or various cytokines (Medzhitov, 2009).

1.3 Pathogens

1.3.1 Infection strategies

Depending on the bacterium, there are different strategies to survive the host´s immune response and to establish infection of the host cell. Some bacteria are able to evade phagocytosis, either by encapsulation (*Neisseria, Streptococcus*) or by avoiding recognition by receptors (*Staphylococcus, Streptococcus*). Another possibility to avoid phagocytosis is to manipulate the host cytoskeleton to prevent the formation of the phagosome (*Yersinia*, EPEC, EHEC). Other bacteria follow different strategies: they allow or even promote phagocytosis and then inhibit phagosome maturation (*Salmonella, Legionella*) or actually live in the harsh environment of the mature phagosome (*Mycobacterium*). Finally, there is the possibility to escape from the early phagosome and persist in the cytoplasm (*Listeria, Shigella*) (Sarantis *et al.*, 2012)

1.3.2 EPEC/EHEC

Enteropathogenic and enterohemorrhagic *Escherichia coli* (EPEC and EHEC) are human pathogens of the intestine which share a unique mechanism to colonize the host. They transduce a number of effector proteins via a type III secretion system (T3SS) into the host´s cytoplasm (see 1.3.5). These effectors not only result in the typical attaching and effacing (A/E) lesions leading to disappearance of the microvilli brush border, but also manipulate several other signaling pathways. Both strains belong to the family of diarrhoeagenic pathogenic *Escherichia coli*. EPEC (enteropathogenic *E.coli*) causes gastroenteritis with massive water loss in infants while EHEC (enterohemorrhagic *E.coli*) causes bloody diarrhea. The difference between the two pathogens is that EHEC but not EPEC is able to produce Shiga toxins. Both bacteria carry a genomic pathogenicity island, the locus of enterocyte effacement (LEE) which encodes for the T3SS and several virulence factors, like Tir (translocated intimin receptor), Map (mitochondria associated protein) and EspF (*E.coli* secreted protein F) (Wong *et al.*, 2011a, Robins-Browne *et al.*, 2002).

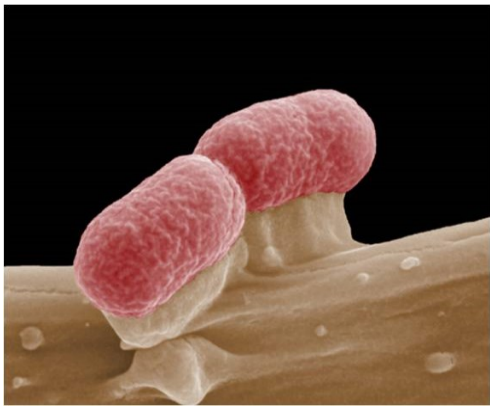

Figure 10 EPEC mounted on pedestals

Pseudocolored electron microscope image of EPEC (red) sitting on actin rich pedestals (Manfred Rhode, HZI Braunschweig)

After the first contact of the A/E-pathogen with the host´s plasma membrane, the T3SS and the first set of secreted proteins like EspA, EspB and EspD assemble a translocation machine (Knutton *et al.*, 1998, Hartland *et al.*, 2000, Ide *et al.*, 2001). This machine allows injection of a variety of effector proteins into the host cytoplasm. Secretion is tightly regulated and follows an exact order (Wong *et al.*, 2011a). One of the first translocated proteins is Tir. Once in the host cytoplasm, Tir becomes phosphorylated and integrates into the plasma membrane. The extracellular part of Tir then binds to the bacterial surface protein intimin (Kenny *et al.*, 1997) leading to a tight connection between the bacterium and the cell. Intimin binding, leads to Tir clustering, what in turn triggers host signaling pathways, which drive actin polymerization, resulting in actin rich pedestals beneath the bacterium (Campellone *et al.*, 2004). Other early translocated

effectors are Map and EspT. Both belong to the WxxxE protein family of virulence factors (see 1.4) and induce actin cytoskeletal rearrangement within the infected cell (Bulgin *et al.*, 2009a, Kenny *et al.*, 2002).

1.3.3 Salmonella

Salmonella represents a group of Gram-negative bacteria which is currently categorized into two species, *S. bongori* and *S. enterica*. *S. bongori* is represented by only one subspecies, while *S. enterica* comprises seven, but only one of them is specific to endotherms. The others are restricted to cold blooded animals like reptiles (Garai *et al*., 2012). Here I would like to concentrate on *Salmonella enterica* serovar Typhi and Typhimurium because they serve as common model organisms to study host pathogen interaction. Both serovars infect the mammalian intestine and cause inflammation and diarrhea. The transmission happens via oral ingestion of contaminated food or water. Due to its adaptive acid tolerance, *Salmonella* is able to survive the low pH of the stomach and reach the gut (Garcia-del Portillo *et al*., 1993a). In the gut, *Salmonella* loosely attaches to epithelia cells, translocates virulence factors and enters the cells. This can occur via two different routes. In case of phagocytes the invasion occurs as described in Figure 9 (Vazquez-Torres *et al*., 1999), but *Salmonella* has also the ability to invade non-phagocytic cells by bacterial-mediated endocytosis (Francis *et al.*, 1992).

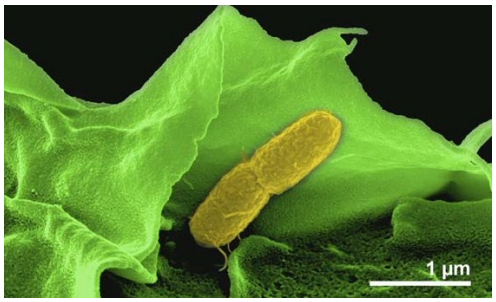

Figure 11 *Salmonella* invades Cos7 cell

Pseudocolored scanning electron microscopy image of *Salmonella* (yellow) invading the host cell (green) by induction of membrane ruffling (Rottner *et al*., 2005)

To achieve being endocytosed by non-phagocytic cells, *Salmonella* injects via T3SS (see 1.3.5) a cocktail of virulence factors, including SopE, SopE2 and SopB (Zhou *et al.*, 2001, Friebel *et al.*, 2001) resulting in massive membrane ruffling on the host cell surface, and subsequent internalization of the bacterium. This mechanism is referred to as the "trigger" mode of entry, the uptake is very rapid and occurs normally within minutes after the first stable contact between bacterium and host membrane (Cossart *et al.*, 2004). After internalization *Salmonella* prevents endosomal maturation at stage of the late

endosome and stays in the so called *Salmonella* containing vacuole (SCV), establishing a unique niche for replication (Haraga *et al*., 2007). At these later stages of infection a second T3SS and another set of virulence factors enter the scene. This T3SS II secretes effectors like SifA, SseF and SseJ, which play a role in maintenance of the SCV, movement of the SCV towards the perinuclear region and in the formation of *Salmonella* induced filaments (Sifs) (Srikanth *et al.*, 2011, Haraga *et al.*, 2007). These are long tubular structures, derived from the SCV, spreading throughout the whole cell. Sifs are important for SCV positioning, bacterial replication and *Salmonella* pathogenesis in general (Srikanth *et al.*, 2011, Garcia-del Portillo *et al.*, 1993b).

1.3.4 Shigella

The group of *Shigella* is a genus of gram-negative bacteria which contains four serovars. These bacteria infect human and primates via the fecal oral route. They cause an acute intestinal infection, with abdominal cramps and severe diarrhea, called shigellosis. By rehydration and antibiotic treatment it comes to a rapid resolution of the infection. However, in immunocompromised patients or in absents of proper healthcare the disease becomes live-threatening (Schroeder *et al.*, 2008).

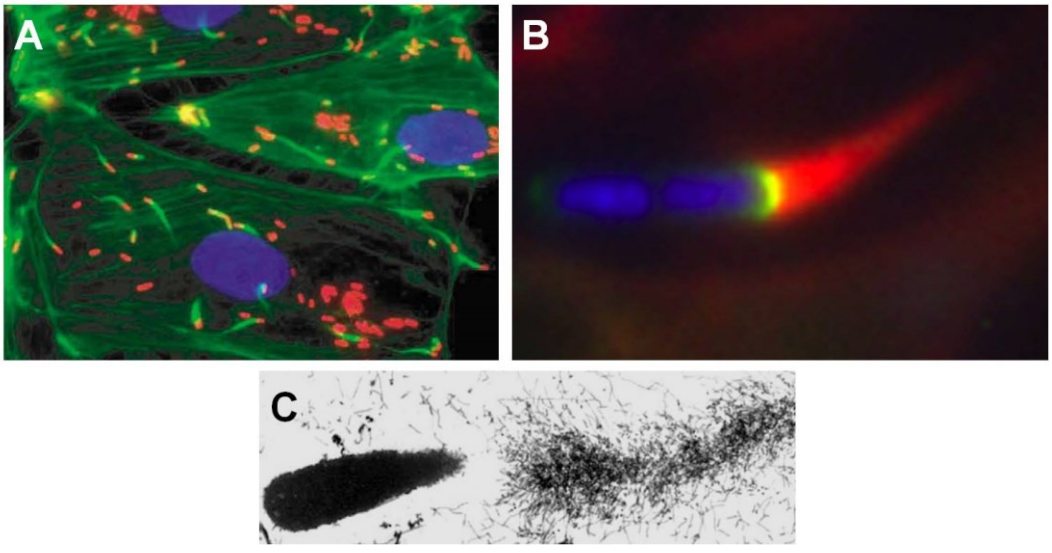

Figure 12 Actin driven bacterial movement within the host cell.

In (A) a *Listeria* infected cell, stained for F-actin in green and for *Listeria* in red, is shown. The bacteria are propelled by actin-comet tails (Gouin *et al*., 2005). In (B) a close-up of *Shigella* with comet tail is shown, bacteria in blue, N-WASP in green and actin in red (from the homepage of Goldmann Lab, Massachusetts). A *Shigella* actin-comet tail taken with an electron microscope is shown in (C) (Gouin *et al.*, 2005).

After arrival in the gut, *Shigella* passes the epithelial barrier via microfold cells, immediately followed by macrophage phagocytosis. Within macrophages *Shigella* escapes from degradation by disrupting the phagosomal membrane. In the cytoplasm bacteria rapidly multiply and cause cell death. After release from dead macrophages, they can enter surrounding enterocytes from the basolateral side by induction of ruffling and macropinocytosis (Ogawa *et al*., 2008). Here *Shigella* escapes again from its membrane envelop and starts replicating in the cytoplasm. To manipulate the host cell, *Shigella* secrets a variety of virulence factors which then target regulatory nods of the host. As already mentioned earlier for EPEC and *Salmonella*, also *Shigella* carries a T3SS allowing secretion of virulence factors directly into the cytoplasm of the host (Mattoo *et al*., 2007). Among those factors are IpgB1 and its homologue IpgB2, both target host GTPases and provoke rearrangements of the actin cytoskeleton in the early stage of a *Shigella* infection (Hachani *et al*., 2007). Another secreted factor is IcsA (also known as VirA), this one recruits the actin polymerization machinery of the host and induces, like in *Listeria*, actin-comet tails (Figure 12), which propel *Shigella* forward (Bernardini *et al.*, 1989, Goldberg *et al.*, 1995, Gouin *et al.*, 2005).

1.3.5 T3SS

Secretion in general is the process of transduction or release of a chemical substance, from a cell or bacterium into the surrounding medium. In Gram-negative bacteria there are six different types of secretion systems (Henderson *et al.*, 2004, Pukatzki *et al.*, 2006). In this thesis I would like to concentrate on the T3SS which was already mentioned in previous paragraphs. The T3SS, also called injectisome, is a needle like structure, which is used by pathogenic bacteria to secrete virulence factors into the host´s cytoplasm (reviewed in Cornelis 2006). There are seven subfamilies of the injectisome. Analysis of their evolution revealed no similarities to development of the bacteria, indicating, that T3SS spread by horizontal gene transfer among the respective bacteria. Early genetic studies revealed significant similarities to flagella. This evidence was later supported by comparison of electron microscope studies of *Salmonella* needle complex and flagella. The architecture of the different injectisome subfamilies is more or less the same. Every secretion system consists of a cylindrical basal part, called needle complex with an inner and an outer ring that anchors the T3SS to the bacterial membrane. On the extracellular side, a needle with a tip

complex is formed (Figure 13). Inside the bacterium, a ring of ATPases is associated beneath the needle complex. The ATPases are required to deliver the energy for secretion. Blocker *et al.* were able to show, that there is a tunnel of 2-3 nm spanning the whole structure from end to end. This core structure is built by nine different proteins and a multiplicity of scaffolding proteins facilitating assembly. After the injectisome is constructed and connected to the host cell three proteins (IpaB, C and D in case of *Shigella*) are immediately secreted and insert into the host membrane to build a pore, the final and essential component of the system. To ensure that secretion only occurs into hosts and not spontaneously, this process is strictly regulated. Normally secretion is blocked by an inhibiting complex, until a specific signal is trigged. Upon signal recipe, which is thought to be the contact with the host membrane, expression of effector proteins is boosted, the inhibitor complex falls apart and translocation starts (Cornelis, 2006).

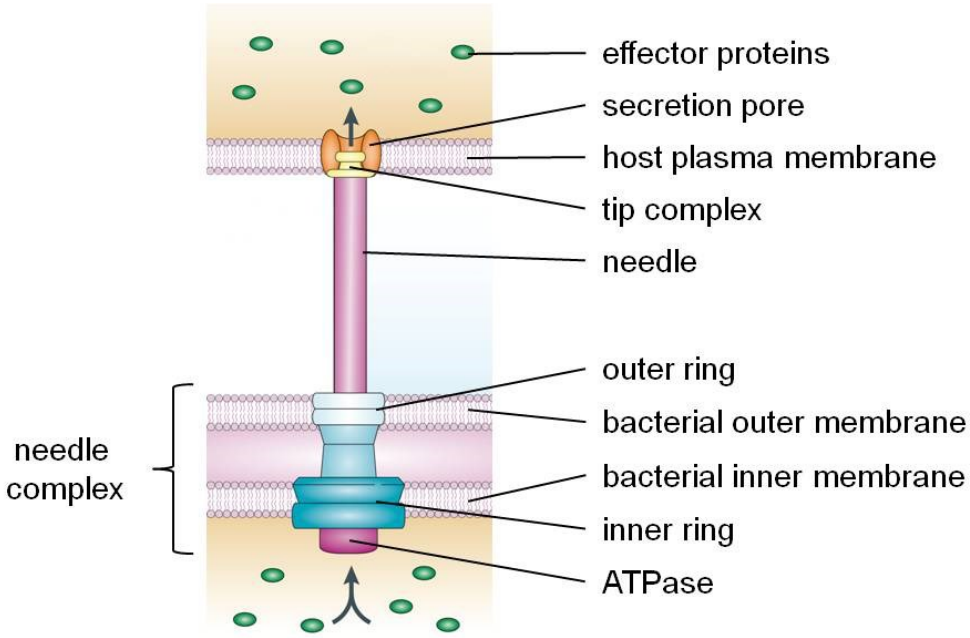

Figure 13 Schematic overview of the T3SS

The T3SS consists of two basic parts. The first is the needle complex, anchoring the whole structure with the inner and outer ring to the bacterial membrane. Furthermore it is connected to a ring of ATPases which supply the energy for the effector translocation. The extracellular part includes the needle, which bridge the distance between bacterium and host cell, the tip complex and the pore, which opens the door into the host cytoplasm. Together, this complex machinery allows to translocate effector proteins through three membranes and the extracellular space, from the bacterial into the host cytoplasm (Cornelis, 2006).

1.4 WxxxE

Many pathogenic bacteria use a T3SS to deliver a variety of virulence factors into the host cytoplasm. Here they act as potent regulators and allow the bacteria to directly access crucial signaling pathways. In 2006 Alto and his colleagues grouped a new family of effector proteins. They recognized a common sequence motive and a shared function among several virulence factors from different pathogenic bacteria, including *Salmonella*, *Shigella* and enteropathogenic *E.coli*. Using the BLAST algorithm for a database search for EPEC Map homologues, they identified several proteins, mostly of the A/E group, that shares a Trp-x-x-x-Glu (WxxxE) sequence motive. Assuming that this motive contributes to a common function, the authors extend the data analysis for WxxxE containing proteins. They came up with 24 different proteins from pathogenic bacteria. For three of those proteins (Map from EPEC and its homologues from *Shigella* IpgB1 and IpgB2) they could identify a common function, leading to characteristic cytoskeleton rearrangements of the host cells. Alto came to the conclusion, that all this proteins are, despite any sequence similarities, functional mimics of small Rho family-GTPases (Alto *et al*., 2006). Today we know, that this conclusion does not hold true. A database based on the structure of SifA identified SopE, an already known bacterial GEF mimic *(Hardt et al*., 1998), as the closest known structural relative of SifA.

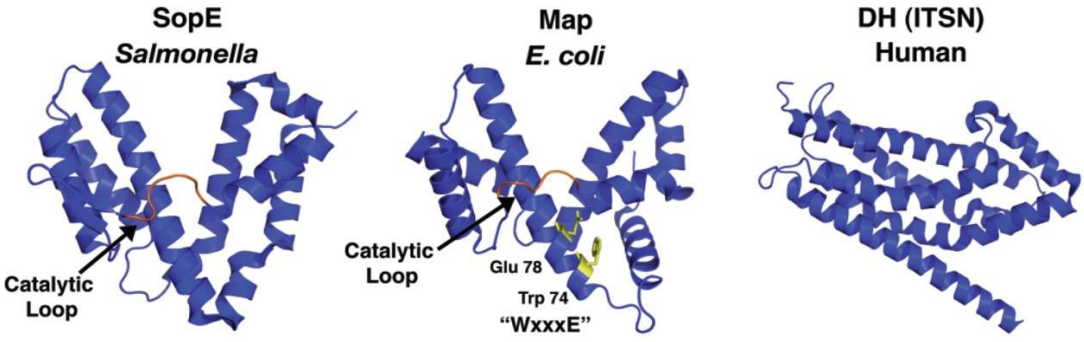

Figure 14 Structural comparison of bacterial and human GEFs

The fold of the two bacterial GEFs SopE from Salmonella and Map from pathogenic E.coli is in large parts superposable. Although there is no sequence similarity, especially the catalytic loops (orange) are closely related. In case of Map, the Trp and Glu residues of the WxxxE motive are highlighted in yellow. As a representative for human GEFs ITSN is depicted on the right side. Its folding differs completely from SopE and Map (Orchard *et al.*, 2012a).

This finding and the fact that SifA binds to GDP- and not to GTP-bound RhoA only allows to conclude, that WxxxE family members do not function, as GTPase mimics but as bacterial GEFs (Ohlson *et al.*, 2008). Interestingly there is no similarity in sequence or fold between SifA and SopE or any known eukaryotic GEF.

In 2009 Huang and his co-workers could for the first time show in 2.3-Å resolution, that the EPEC effector Map forms selectively a complex with Cdc42. Furthermore they could show in vitro that Map function as a potent guanine nucleotide exchange factor for Cdc42 (Huang *et al.*, 2009). However, these results still left open the mechanism, of how members of the WxxxE family are able to catalyze the GDP-GTP exchange in GTPases. This last gap was closed when Klink and fellows where able to solve the crystal structure of every single step of the nucleotide exchange for the IpgB2-RhoA complex (Klink *et al.*, 2010). Although the knowledge gained in the last years on the WxxxE family is enormous (Bulgin *et al.*, 2010, Aktories, 2011, Orchard *et al.*, 2012a), there are still lots of open questions. Especially the regulatory influence of host proteins on the virulence factors is largely unknown. In the following paragraphs I would like to introduce some of the WxxxE family members which are subject to this study, in more detail.

1.4.1 Map

One WxxxE member is the type three secreted virulence factor Map. It is present in bacteria of the A/E group, like EPEC, EHEC and *C.rodentium* and was first identified as a mitochondria associated protein, involved in the disruption of membrane potential (Kenny *et al.*, 2000). Two years later, it was reported that Map is sufficient to induce filopodia during the early stages of EPEC infection, independent of Tir (Kenny *et al.*, 2002). Later it was shown, that Map selectively targets and activates Cdc42 to induce filopodia formation. Furthermore the binding of Map to ezrin/radixin/moesin (ERM)-binding phosphoprotein 50 (EBP50), also known as Na+/H+exchanger regulatory factor 1 (NHERF1) was described to be important to stabilize Map-induced filopodia (Berger *et al.*, 2009). Map binds to EBP50 via its carboxy-terminal PSD-95/Disk-large/ZO-1 (PDZ)-binding motif (Simpson *et al.*, 2006).

In this study we follow results from an initial yeast two hybrid (Y2H) screen indicating that Map might interact with the human RhoA binding protein rophillin1 (RHPN1). Only little is known about rhophilins, which comprise 2 members,

RHPN1 and RHPN2 in mammals. Both proteins were reported to target RhoA GTPases in order to regulate actin cytoskeleton organization (Watanabe *et al.*, 1996, Peck *et al.*, 2002). According to SMART protein domain prediction web tool, the two homologues contain a HR1 domain, which is known to mediate interactions with small GTPases. Furthermore both rhophilins possess a Bro domain which is implicated to be involved in endosomal targeting. This domain is quite interesting, because it gives room to speculations about a potential involvement of the ESCRT III complex in EPEC infection. Since it was reported that enveloped viruses are able to recruit the ESCRT III machinery by targeting the human Bro domain containing protein Alix, to facilitate virus budding (Strack *et al.*, 2003, Morita *et al.*, 2011, Boonyaratanakornkit *et al.*, 2013, Popov *et al.*, 2009). Finally, both RHPN isoforms comprise a PDZ domain, which could serve as the interaction surface between RHPN and Map.

1.4.2 EspT

Another, but very rare T3SS effector of A/E pathogens is EspT. According to surveys on clinical isolates of EPEC and EHEC, only 2 % of the EPEC strains contain EspT (Arbeloa *et al.*, 2009). In 2009 it was identified by Bulgin and colleagues, as a novel member of the WxxxE protein family. They reported that ectopic expression of EspT from *C.rodentium* results in lamellipodia or ruffle formation, depending on the tested cell type. These rearrangements of actin were interpreted to result from ELMO- and Dock180-independent targeting of Rac and Cdc42 (Bulgin *et al.*, 2009b). During EPEC infection the effector is able to provoke membrane ruffling on the host surface, resulting in the invasion of non-phagocytic cells (Bulgin *et al.*, 2009a). In this study the internalized bacteria resided in the phagosome where they induce intracellular pedestals. Another study revealed a role of EspT in the regulation of immune mediator production. Via extracellular signal-regulated kinases (Erk), c-Jun N-terminal kinases (JNK) and NF-kB it stimulates the secretion of Il-1β, Il-8 and PGE2 (Raymond *et al.*, 2011).

In our previous mentioned Y2H screen we got several hints for putative interaction partners from the host side. We decided to focus on the interaction with Arf6, because it is a small GTPase that might be regulated by this GEF mimic. Furthermore Arf6 was described to be involved in reorganization of the actin cytoskeleton and in membrane trafficking, facilitating phagocytosis (Donaldson,

2003, D'Souza-Schorey *et al.*, 2006). Both are functions which could be of interest for pathogens.

1.4.3 SifA/B

SifA and SifB from *Salmonella* are two of the originally identified WxxxE family members (Alto *et al.*, 2006) but different from the other family members, in that they seem to be not involved in actin dynamics (Bulgin *et al.*, 2010). SifA is secreted via the second T3SS, localizes at the phagosome and is required for its tabulation (Stein *et al.*, 1996). While SifA is necessary to deploy full virulence in macrophages and mice (Beuzon *et al.*, 2000), the role of SifB during pathogenicity remains still unknown and is under ongoing research. Finally, SifA and –B display a long N-terminal extension that is essential to the phagosome function. Ohlson *et al.* were able to show that SifA consists of two domains, one binding to the host protein SKIP, an interaction essential for the maintenance of the SCV (Boucrot *et al.*, 2005), and the other containing the WxxxE motive (Ohlson *et al.*, 2008). Although SifA shares a common fold with other bacterial GEFs like Map or SopE (Ohlson *et al.*, 2008), no GEF function could be demonstrated for SifA yet (Orchard *et al.*, 2012a).
In our Y2H screen we got only five putative interaction partners for SifB, including Cdc42 and Rac1. In case of SifA we got more than 30 predicted interactions, among them the Rap GTPase interactor RADIL, the adapter protein of the Toll-like and IL-1 receptor signaling pathway ECSIT, or SPIRE1, a protein involved in actin organization (see result section 2.1 and 2.2.4).

1.4.4 IpgB1/2

The two *Shigella* effector proteins IpgB1 and IpgB2 are encoded on the *Shigella* virulence plasmid (Parsot, 2005). Both of them belong to the type three secreted virulence factor WxxxE family (Alto *et al.*, 2006). Ectopic expression of IpgB2 was reported to induce stress fibers, while IpgB1 stimulates the formation of lamellipodia and ruffles (Ohya *et al.*, 2005, Alto *et al.*, 2006). Later it was shown that IpgB1 promotes bacterial entry by triggering ruffle formation and activating Rac1 via the ELMO-Dock-180 pathway (Handa *et al.*, 2007). Infection studies, using deletion mutants for IpgB1 and IpgB2, revealed different effects on pathogenicity of those proteins with respect to the infected cell line or organism (Hachani *et al.*, 2008).

More recent studies show that IpgB1 function as a GEF for Rac1 and Cdc42, while IpgB2 is able to catalyze the nucleotide exchange on RhoA (Huang *et al.*, 2009, Klink *et al.*, 2010).
In our Y2H screen we found no interactions of IpgB1 together with any host protein. In case of IpgB2 this was different here we got hits for BBS4 and TRAPPC6A. BBS4 is a component of the BBSome, a multiprotein complex located at the primary cilium and at centriolar satellites (Loktev *et al.*, 2008, Nachury *et al.*, 2007). TRAPPC6A is also a multiprotein complex subunit, the TRAPP I complex is involved in vesicular transport at the endoplasmic reticulum (Sacher *et al.*, 2008).

1.5 Aim

The research of the last decade accumulates more and more knowledge about the very complex molecular processes, on the bacterial side, leading to infectious diseases. One landmark in the understanding host-pathogen-interactions was the discovery of the WxxxE family of bacterial virulence factors. Their function as bacterial GEFs allows pathogens not only to target single proteins, but total signaling cascades and thereby the direct control on multiple cellular functions from endocytosis over motility till apoptosis. Since the regulation of mammalian GEFs is quite tight and the number of translocated virulence factors is rather low, it is most likely that host adapter- or scaffolding proteins are involved in the regulation of bacterial GEFs. It is the right time to find out what these proteins are and how they participate in regulation during infection. To tackle this question we started this study with a large scale Y2H screen to identify so far unknown interaction partners of WxxxE family members. Subsequently we here try to verify these potential hits by using biochemical and microscopic methods.

2 Results

2.1 Y2H screen

At the start of this study, we initiated a large scale Y2H screen to identify novel host targets of different bacterial virulence factors. The screening was performed in collaboration with Manfred Kögl and Frank Schwarz from the German Cancer Research Center in Heidelberg. As bait proteins we used full length, or truncated and mutated versions of *Salmonella enterica* serovar Typhimurium SifA, SifB, SopB, SopE and SopE2. Furthermore, we included IpgB1 and IpgB2 from *Shigella flexneri*, as well as Map and EspT from EPEC and *Citerobacter rodentium*. A human cDNA-based protein library served as prey. Each result was categorized in one of four groups: certain interactions, if a specific bait prey interaction occurs more frequently; uncertain interactions, if a specific bait prey interaction occurs only once; likely false positives, based on empirical data, if a prey is "sticky", and thus frequently found in different screenings (prey promiscuity) and finally false positives, if the prey protein contains UTR elements. For more detailed information on data evaluation see (Albers *et al.*, 2005). The output of the screen was diverse: when grouping the certain and uncertain hits for all different variants of one bait protein, the numbers differed from 68 hits (e.g. SifA) to zero (SopE or IpgB1). Interestingly, among the 40 certain and uncertain hits for EspT from *C. rodentium* and EPEC only four could be found for EspT of both bacteria. With its appearance in three different approaches the transcription factor HOXA1 was the most frequently found among the certain hits. Only the transposable element TIGD1 and the zinc finger protein 343 were more frequently isolated (both four times) but they belong to the likely false positive group. Out of all 185 potential interaction partners we pre-selected those which possess known functions in processes like migration, endocytosis, or cellular transport (Table 1).

Table 1 Pre-selected list of Y2H results

Bait	Prey	No. of Isolations	Prey promiscuity	Prey function
Map	NHERF-2	8	2	Scaffolding protein
	RHPN1	2	2	RhoA interactor
	Spire1	1	4	WH2 protein involved in actin organization
EspT	Arf6	2	3	Small GTPase
	Appl1	2	2	Adapter protein involved in cell proliferation
	Cep70	2	5	Organization of the mitotic spindle
IpgB2	BBS4	2	1	Cilia formation; microtubule-related transport
	TRAPPC6A	2	4	Trafficking protein particle complex subunit
SifA	ECSIT	4	2	Signaling intermediate
	RADIL	2	1	Effector of Rap in migration and adhesion
	Spire1	1	4	WH2 protein involved in actin organization
	Cep70	1	5	Organization of the mitotic spindle
SifB	Cdc42	60	3	Small GTPase
	Rac1	1	3	Small GTPase
SopB	HGS	45	7	Recycling of membrane receptors
	ATP6V1E1	12	3	Subunit of the ATPase
	SNX6	3	3	Intracellular trafficking
	Rab11A	1	7	Small GTPase

2.2 Recombinant proteins and subsequent pull down assays

In order to prepare recombinant proteins, a plasmid carrying the gene encoding for the protein of interest was transformed into the *E.coli* protein expression strain BL21. The purification protocol varied depending on the used protein tag and on the properties of the specific protein. After purification, the samples were loaded and ran on a SDS-PAGE and subsequently stained with Coomassie Brilliant Blue to determine efficiency of expression, purity and concentration. When available, known interactors were used as positive controls in pull down assays, before the other experiments were started.

2.2.1 EspT and its putative interactors

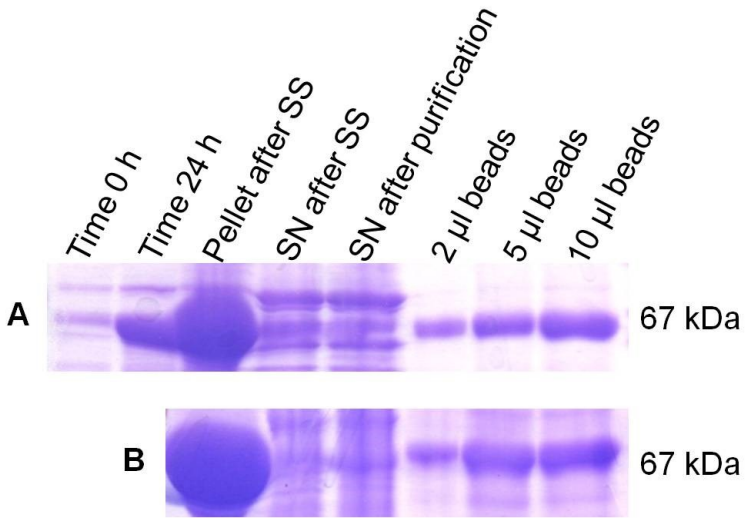

Figure 15 Coomassie stained SDS-PAGE of EspT protein purification

EspT (with tag 67 kDa) from *C.rodentium* (A) and EPEC (B) were both expressed from the pETM-41 His-MBP vector. Induction was performed overnight using 0.5 mM IPTG at 20°C. Huge amounts of the proteins after super-sonication (SS) and centrifugation were found in the pellet (insoluble fraction) and only traces could be found in the supernatant (SN). Nonetheless, the bands in the bead lanes are pure and robust.

After disintegration of the cells by sonication and subsequent centrifugation, the majority of the EspT protein remained in the insoluble fraction and could be found in the pellet (Figure 15). Nevertheless, the preparation of EspT beads from both bacteria *C.rodentium* (Figure 15 A) and EPEC (Figure 15 B) revealed enough pure protein. For later pull down experiments 30 µl of bead material were used.

One of the putative interaction partners for EspT from *Citerobacter* was the small GTPase Arf6. This member of the Ras-superfamily has been reported to be involved in several cellular processes, including reorganization of the actin cytoskeleton and endocytosis (Donaldson, 2003, D'Souza-Schorey *et al.*, 2006)

To confirm this interaction, we performed pull down assays using a constitutive active and different dominant negative mutants as well as the wild type version of C-terminal GFP tagged Arf6 (Figure 16). Furthermore, it was described that Rac1 and Cdc42 are substrates of EspT, but a direct interaction has not been shown so far (Bulgin *et al.*, 2009b, Orchard *et al.*, 2012a). Therefore, we performed also pull downs with these GTPases (Figure 17).

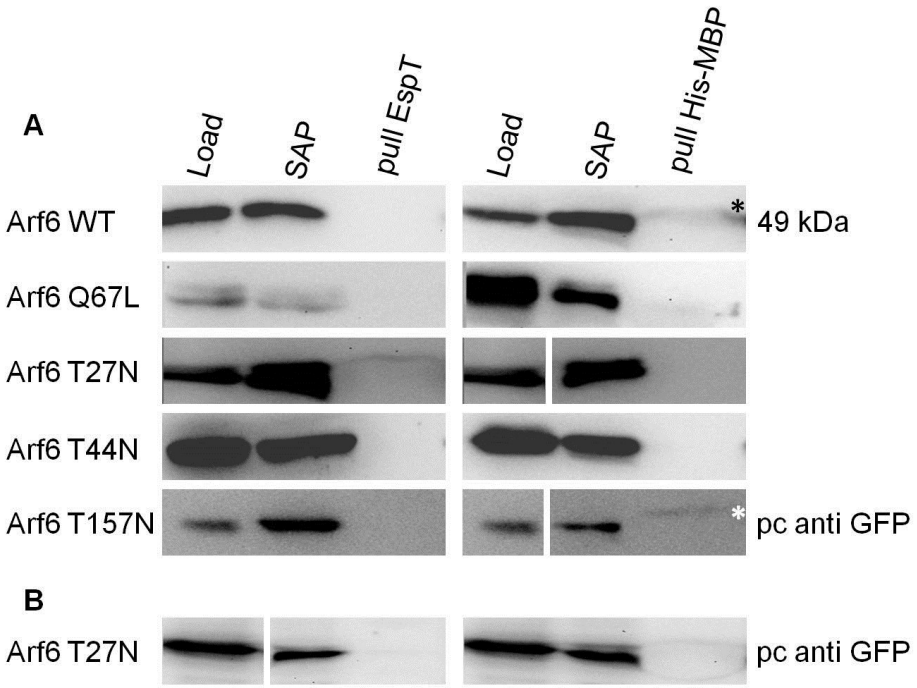

Figure 16 No interaction between Arf6 and EspT in pull down experiments

Western blot analysis after pull down assay using wild type (WT), constitutive active (mutation QL) and different dominant negative (mutation TN) versions of Arf6 are shown. The experiments were performed using EspT from *C.rodentium* (left) and non-fused His-MBP (right). The proteins were detected by a polyclonal GFP antibody. There are robust signals in the load controls and in supernatant after pull down (SAP). The respective pull down lanes are empty. In (A) the standard triton X-100 containing washing buffer was used, in (B) no triton was used. Asterisks indicate weak interactions.

The pull down experiments were performed using the constitutive active Arf6 Q67L mutant, or the dominant negative variants T27N, T44N, T157N and WT. To exclude interactions between His-MBP and the GTPases, the immobilized tag was used for control pull down assays. Each approach was run in triplicates and in every case, no direct interaction could be detected. Sometimes very weak bands, like seen in the T157N pull down of Figure 16 A (right), were observed. To ensure, that no interaction was washed away by triton X-100, one stet of pull down assays was performed, using a washing buffer lacking triton. The result of these experiments did not differ from the experiments including triton. Exemplarily the Arf6 T27N pull down without use of triton is shown in Figure 16 B. An attempt with EspT beads from EPEC showed the same result.

To address the question whether Rho GTPases can interact with EspT directly, pull down assays with EspT from *Citerobacter* against WT, CA and DN versions of Rac1 and Cdc42 were performed. This set of experiments included also WT RhoG from mouse, human RhoG G12V/T17N and CA and DN RhoA (Figure 17).

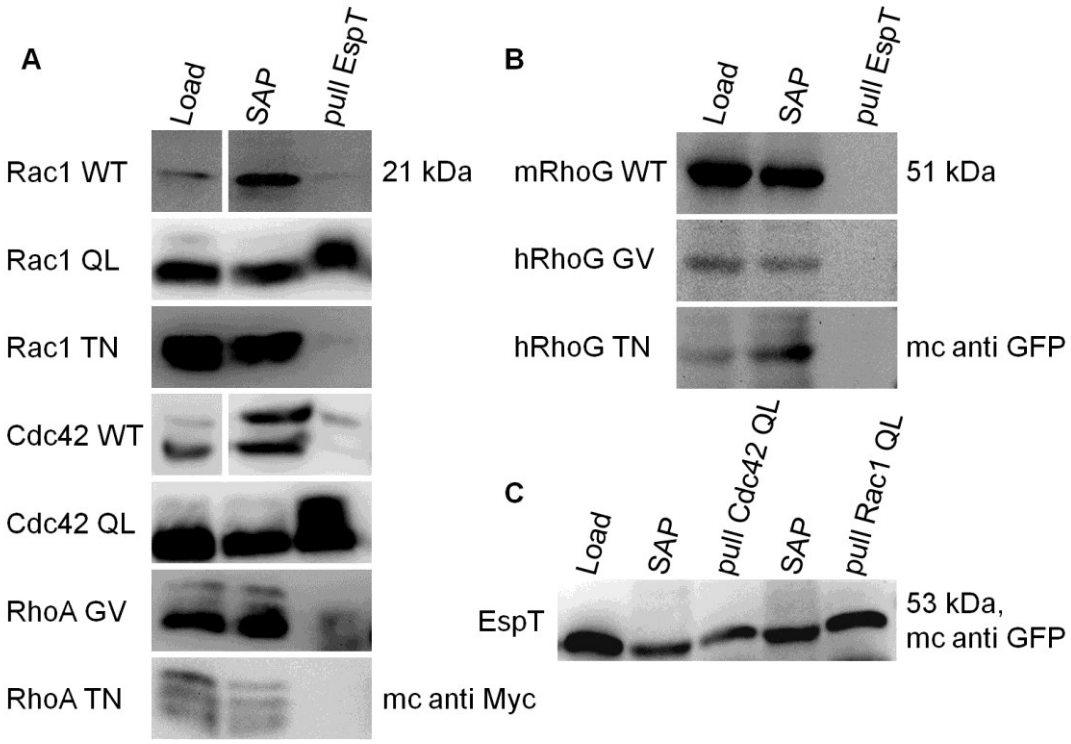

Figure 17 EspT interacts with constitutive active Rac1 and Cdc42

Immobilized EspT from *Citerobacter rodentium* was used in pull down assays against different versions of Myc-tagged (A) and GFP-tagged (B) GTPases. The clearly positive interactions with Cdc42 QL and Rac1 QL were double checked in a vice versa experiment (C), which gave the same result.

In pull down experiments with constitutive active versions of Rac1 and Cdc42, regardless whether EspT or one of the GTPases was used as bait or pray protein, always a strong interaction between the tested proteins was observed (Figure 17 A+C). The result was different in case of other GTPase variants. Interestingly, no interaction between EspT and dominant negative versions of Cdc42 and Rac1 could be observed. This was a surprise, because EspT as potential GEF mimic which provokes reorganization of the actin cytoskeleton in the host cell was expected to interact especially with dominant negative GDP loaded GTPases. In an attempt using Myc-tagged WT versions of Rac1 and Cdc42, both showed only weak interactions with EspT. The experiments concerning CA RhoA showed a weak or no interaction

with EspT, the DN version no interaction. Also using RhoG revealed no interaction with EspT, no matter which version was tested (Figure 17 B). However, the RhoA and RhoG experiments were not yet performed in triplicates, further pull down assays have to be done.

2.2.2 SopB and its putative interactors

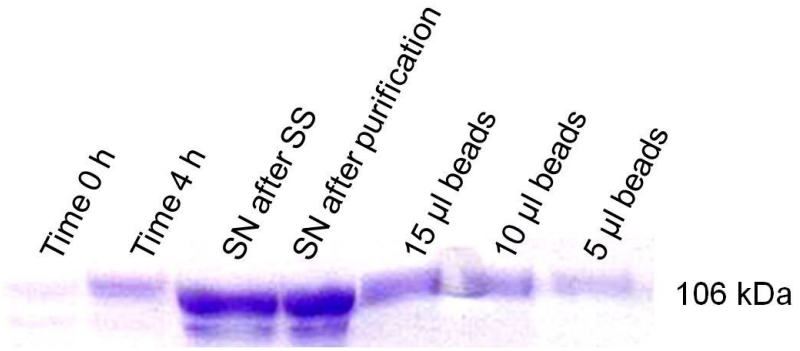

Figure 18 Coomassie stained SDS-PAGE of SopB protein purification

SopB (with tag 106 kDa) from *Salmonella enterica* was expressed in the pETM-41 vector and purified in *E.coli* BL21 after 4 h induction at 37°C. After sonication and incubation with the bead material, huge amounts of the protein could be found in the supernatant. However, the SopB concentration on the beads seems to be sufficient.

The efficiency of the SopB purification was rather low, after the incubation with the bead material, still high amounts of the protein remained in the supernatant. Nevertheless, SopB concentration on the beads was sufficient (Figure 18) and for subsequent experiments 30 µl of the beads were used.

Based upon our Y2H screening the subunit ATP6V1E1 of the V-ATPase is a potential interactor of SopB. However, in pull down experiments a direct interaction between these two proteins could not be detected (Figure 19).

To test whether there is truly no interaction between both proteins or if there might be an experimental problem, such as misfolding of SopB, we tried to reproduce the known interaction between SopB and Cdc42 (Rodriguez-Escudero *et al.*, 2011, Burkinshaw *et al.*, 2012)

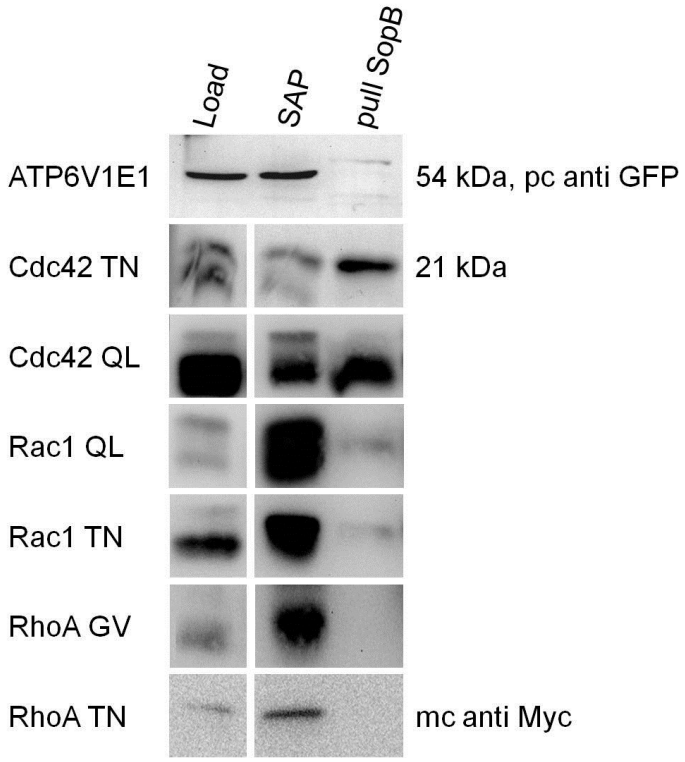

Figure 19 No interaction between the V-ATPase subunit and SopB

The pull down experiments revealed no interaction of SopB with the GFP-tagged V-ATPase subunit. In contrast the interaction with Myc-tagged Cdc42 is strong, while there is almost no interaction with Rac1 and RhoA.

Our SopB beads show strong interactions with constitutive active as well as dominant negative Cdc42, as shown before in yeast (Rodriguez-Escudero *et al*., 2011). Furthermore the same experiments were performed with the Rho GTPases Rac1 and RhoA. Again, as shown in yeast, in these cases almost no interaction could be detected (Rodriguez-Escudero *et al*., 2011).

2.2.3 IpgB1/2 and its putative interactors

After successful purification of IpgB1 and IpgB2 (Figure 20), 30 µl and 10 µl of the beads were used in pull down experiments, respectively. Since there was no result for a possible IpgB1 interactor in our Y2H screen, we only tested these beads against the already published interactors Rac1 and Cdc42 (Huang *et al.*, 2009). However, in our hands, after five independent experiments, using dominant negative mutants, no interaction could be detected (Figure 21). The same was true for using constitutive active mutants. We found the same negative result for RhoA and RhoG.

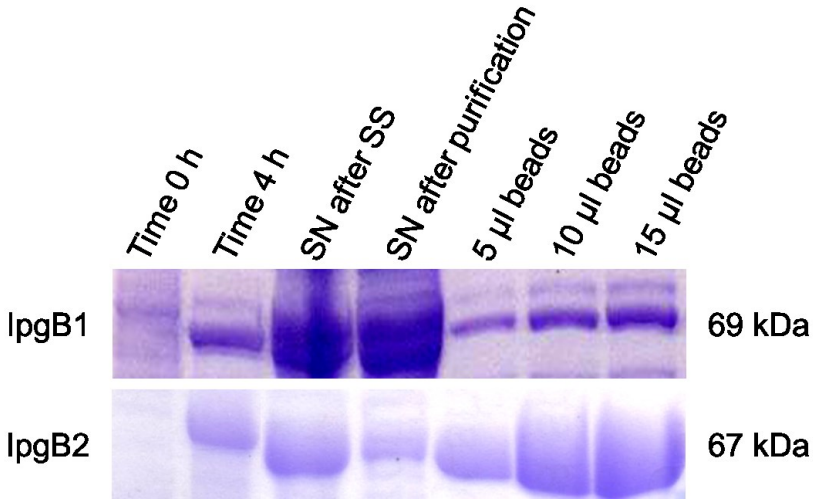

Figure 20 Coomassie stained SDS-PAGE of IpgB1 and IpgB2 protein purification

Both proteins (around 70 kDa with tag) are equally well expressed after 4 h IPTG induction at 37°C. However, under the used conditions, IpgB2 seems to bind more efficient to the beads compared to IpgB1.

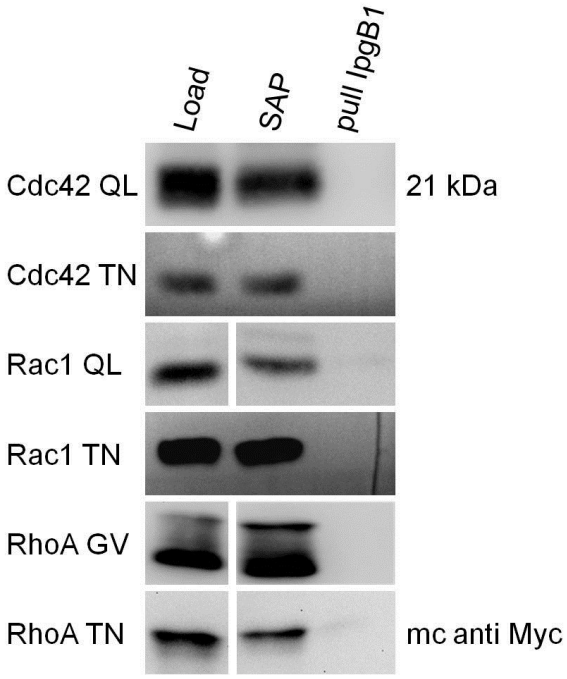

Figure 21 No interaction between Cdc42, Rac1 or RhoA and IpgB1

The pull down experiments between IpgB1 on the one hand and Cdc42, Rac1 and RhoA on the other hand did not reveal any interaction.

In contrast to IpgB1, we identified the putative interaction partners BBS4 and TRAPPC6A for IpgB2 in the Y2H screen. Recombinant IpgB2 was successfully expressed before (Klink *et al.*, 2010) in our group. In an initial experiment, GFP-tagged BBS4 was tested to be pulled down by recombinant IpgB2, however, no interaction could be found (Figure 22 A, upper panel) However, when recombinant BBS4 linked to beads was used in pull downs against IpgB2-GFP (Figure 22 B), we were able to show a clear interaction. We were not able to confirm the second Y2H hit of an IpgB2/TRAPPC6A interaction (Figure 22 A, upper panel). The positive control, dominant negative RhoA (Klink *et al.*, 2010) did interact with the virulence factor (Figure 22 A, lower panel).

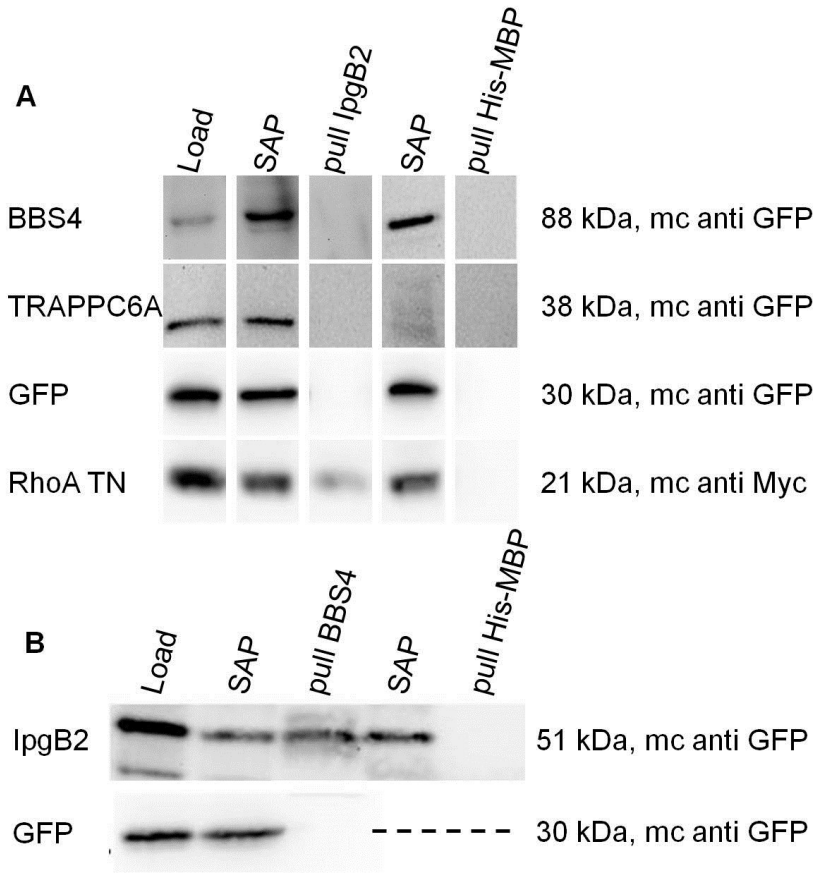

Figure 22 BBS4 and IpgB2 interact in pull down assays if IpgB2 is the bait

(A) The pull down experiments between His-MBP tagged IpgB2 and GFP tagged BBS4 as well as GFP tagged TRAPPC6A showed no interaction. The positive control, using immobilized RhoA T17N was positive. (B) If His-MBP bound BBS4 was used to pull down IpgB2, a clear interaction could be observed.

2.2.4 SifA/B and its putative interactors

The yield of recombinant SifA was rather high, the protein was well expressed, soluble under our buffer conditions and bound with high affinity to the Ni-NTA-beads. For SifB this was totally different. Under other conditions the whole protein could be detected after sonication and centrifugation only in the pellet. Finally, we identified conditions, where a small amount of protein remained soluble and was capable of binding to the beads (Figure 23, lower panel).

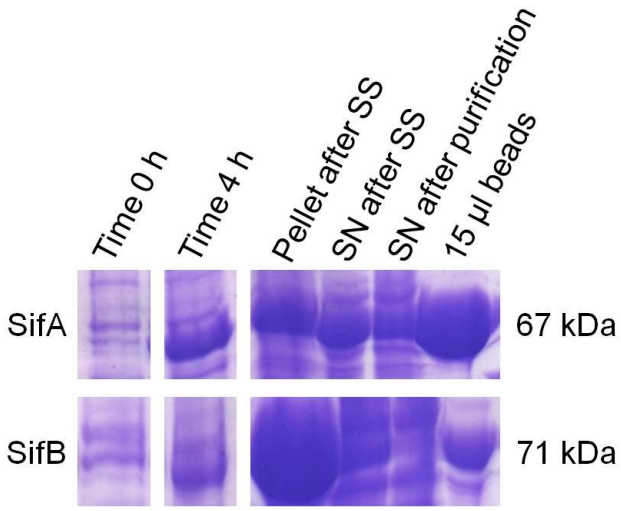

Figure 23 Coomassie stained SDS-PAGE of SifA and SifB protein purification

Both His-MBP tagged proteins (around 70 kDa with tag) are equally well expressed after 4 h IPTG induction at 20°C. However, under the used conditions, SifA seems to bind more efficient to the beads while lots of SifB is bound in the insoluble fraction.

Since the only published interactor of the putative GEF-domain of SifA is the GDP-loaded small GTPase RhoA and even none is known for SifB (Ohlson *et al.*, 2008, Orchard *et al.*, 2012a), we tested both virulence factors for interactions with the small Rho GTPases Cdc42, Rac1 and RhoA (Figure 24). This was supported by the Y2H hit for a putative interaction between SifB and Cdc42. However, no interactions were detected for SifB and only weak interactions (marked with asterisks) were observed for SifA in combination with CA and DN Rac1.

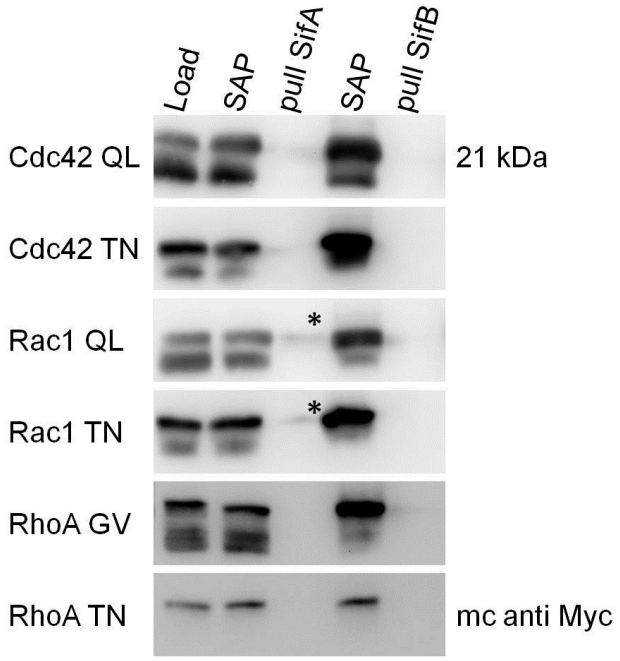

Figure 24 Neither SifA nor SifB interact with any form of Cdc42, Rac1 or RhoA

In pull down assays using immobilized SifA or SifB against dominant negative or constitutive active versions of Cdc42, Rac1 and RhoA, we could not observe any interactions. Asterisks indicate weak interactions.

Furthermore we attempted to detect interactions between SifA and SifB together with different members of the Rab GTPase family in pull down assays. This was of interest since the Rab proteins are involved in vesicular trafficking and so consequently participated in the maturation of the SCV. Moreover the formation of Sifs is dependent on Rab7 and Rab9 (Brumell *et al.*, 2007) and since the same is true for SifA, an interaction on protein level could be possible.

We were not able to show an interaction of any of the tested Rab GTPases with SifB. In case of SifA pull downs, we observed that Rab9a bound to SifA, at least in several of the experiments. Additionally we could exclude interactions with Rab4a, Rab5a and Rab7a. Data concerning Rab11a were not reproducibly positive or negative and thus did not allow a reliable conclusion (Figure 25).

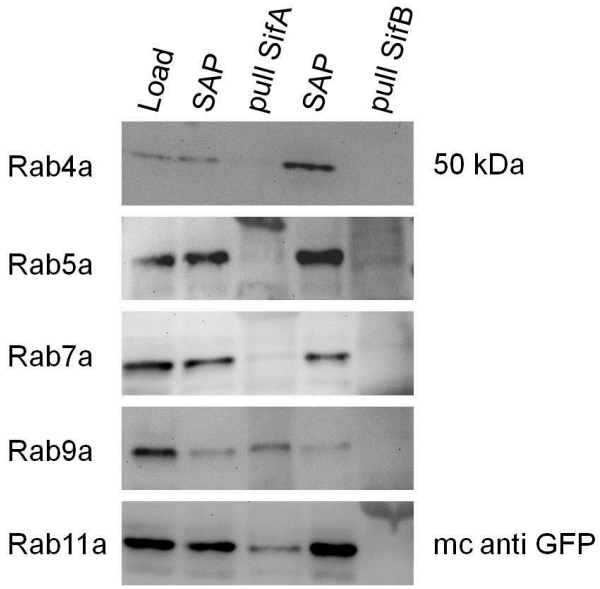

Figure 25 Pull down experiments of different Rab GTPases versus SifA and SifB

In pull down assays using immobilized His-MBP tagged SifA and SifB against GFP fused WT Rab GTPases, SifB did not interact with any of the five tested Rabs. The same was true for SifA in pull downs with Rab4a, 5a, and 7a. Only Rab9a shows frequently interactions with SifA. Results of Rab11a were not consistent enough to allow a reliable conclusion

2.2.5 Map and its putative interactors

From the list of potential interactors of Map, RHPN1 was chosen not at least due to the fact that it harbors a PDZ-domain (Peck *et al*., 2002), while Map possess a PDZ binding motif (Alto *et al.*, 2006) To analyze the putative interaction between Map and RHPN1, both proteins were expressed in *E.coli* BL21 as recombinant fusion proteins (Figure 26). While Map was linked to a His-MBP tag and purified by Ni-NTA sepharose, the human RHPN1 protein was expressed and purified as a GST fusion protein. The availability of both proteins in an immobilized way allowed doing the experiments in vise versa approaches, which increased the reliability of the results.

Beside the putative interaction with RHPN1 we tested also the ability of Map to interact with the small GTPase Cdc42, which should serve as a positive control, since its interaction with the virulence factor has already been described (Huang *et al.*, 2009).

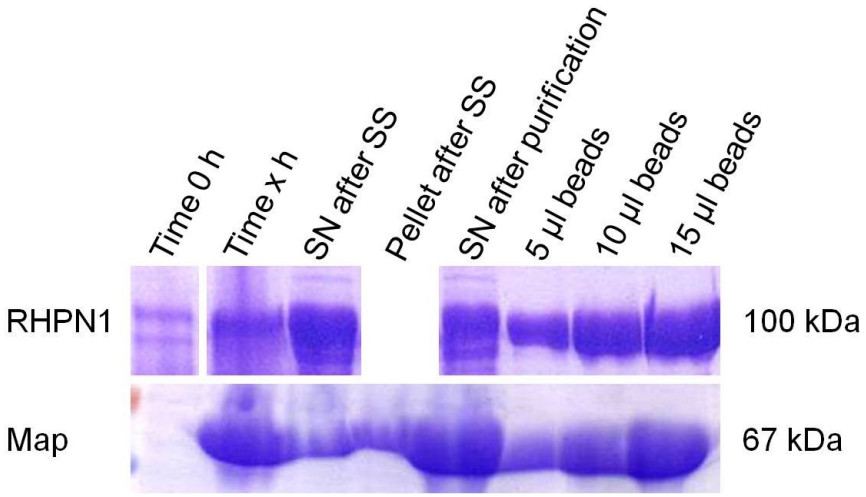

Figure 26 Coomassie stained SDS-PAGE of human RHMN1 and Map protein purification

E.coli BL21 bacteria, expressing the RHPN1-GST fusion protein (100 kDa with tag), were lysed 6 h after IPTG induction at 20°C. After cell breakup, the lysate was incubated with glutathione sepharose to allow GST binding. The resulting protein concentration is shown in the last three lanes. The Map His-MBP fusion protein needed an IPTG induction time of 20 h at 20°C to achieve appropriate amounts of the protein. Under the chosen conditions Map is highly soluble and bound with high affinity to the bead material.

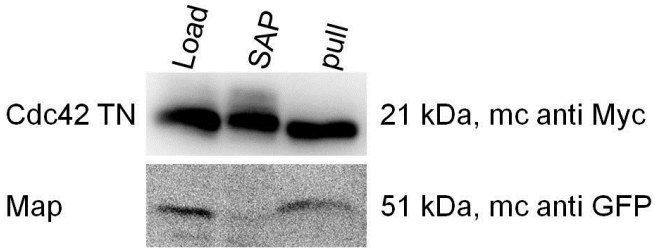

Figure 27 Map interacts with Cdc42 in pull down experiments

In the upper row, Myc tagged Cdc42 T17N expressing B16 cells were lysed and a pull down experiment against immobilized His-MBP tagged Map performed. The Western blot revealed a clear interaction between both proteins. In the row below, the vice versa experiment is shown. Here, a Map-GFP containing lysate was pulled against immobilized dominant negative GST tagged Cdc42. Again an interaction could be detected in the Western blot.

We showed that the positive control between Map and Cdc42 worked (Figure 27) in more than 50 % of all experiments, while the negative controls using GFP alone against Cdc42 beads or immobilized His-MBP against Myc tagged Cdc42 were always negative. Since it is known, that RHPN1 is a downstream effector of the small GTPase RhoA (Watanabe *et al*., 1996), we used RhoA in pull down

experiments as a positive control. Concurrently we tested against Cdc42 and Rac1 for interactions. Beside the expected interaction of RHPN1 and RhoA, we found an unexpected strong interaction with constitutive active Rac1 (Figure 28 A+B) as well as a weaker interaction with constitutive active Cdc42 and dominant negative Rac1.

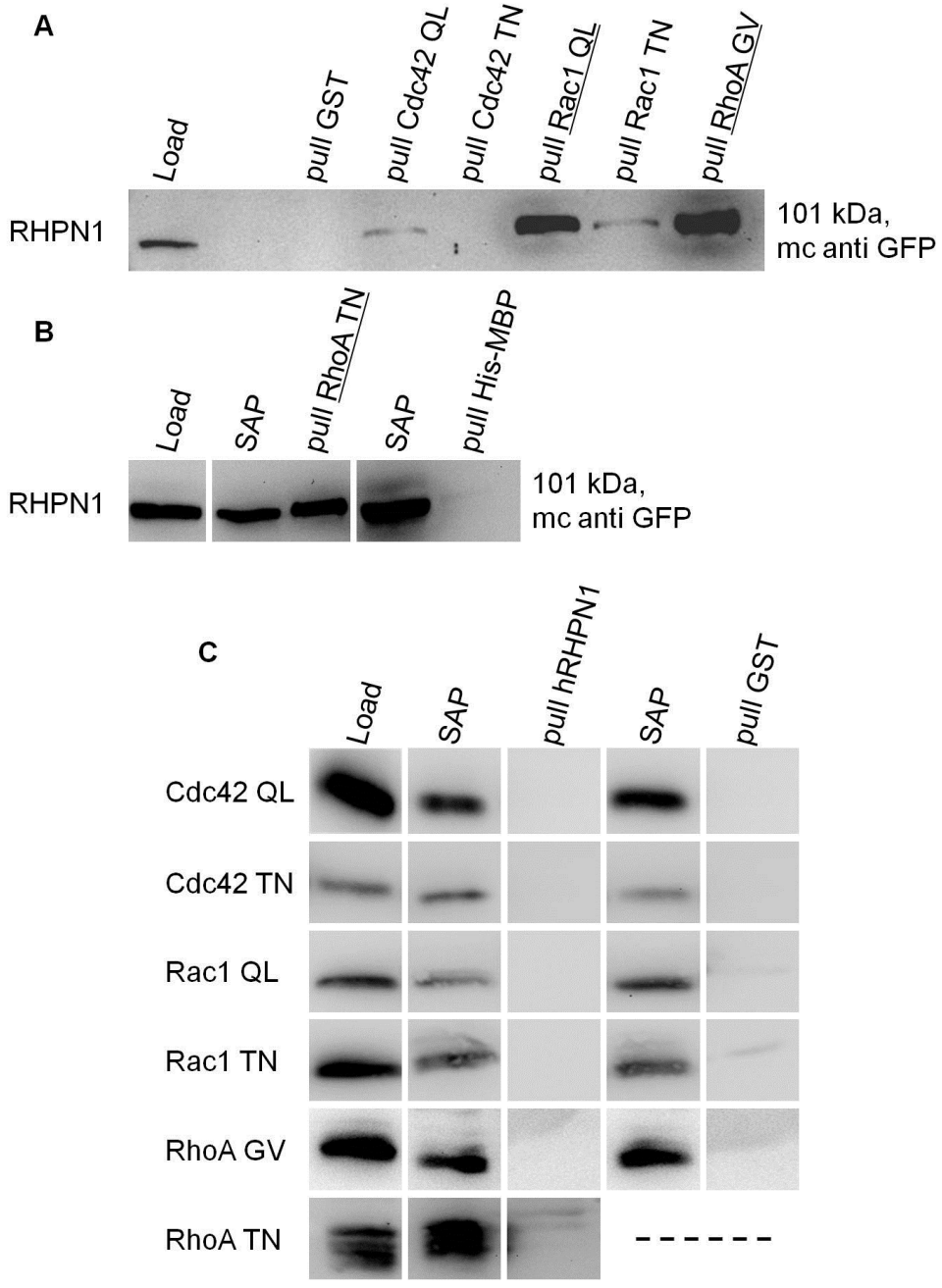

Figure 28 RHPN1 interacts with RhoA and Rac1 in pull down experiments

In pull down assays using GFP tagged RHPN1 against different small Rho GTPases the Western blot revealed strong interactions with constitutive active Rac1 and both, CA and DN RhoA (A+B). The vise versa experiment, using Myc-tagged GTPases, showed no interactions (C).

Only the pull downs with dominant negative Cdc42 and the GST negative control revealed no interaction in the Western blot. Interestingly these results arise from experiments using immobilized GTPases. In cases if RHPN1 was bound to beads, no interaction to any GTPase could be observed (Figure 28 C), maybe because recombinant RHPN1 is not properly folded in bacteria, at least its GTPase binding domain HR1 is possibly not functional.

We next tried to verify the putative interaction between Map and RHPN1 in pull down experiments. As before in the Map-Cdc42 experiment, again vice versa approaches were performed.

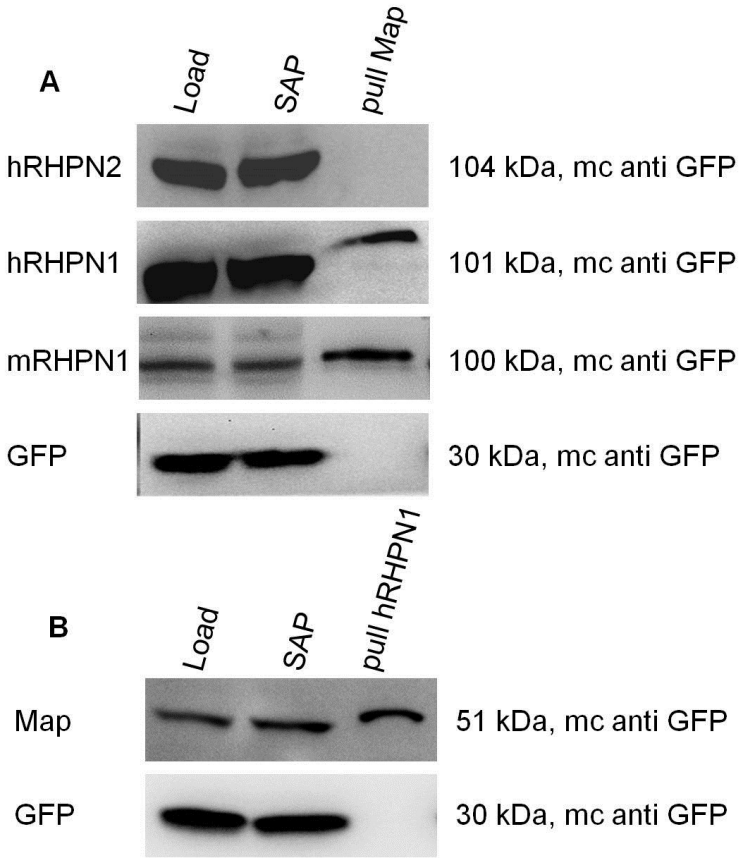

Figure 29 Map and RHPN1 are able to interact in pull down experiments

In (A), lysates of cells expressing GFP labeled human RHPN1, human RHPN2 or mouse RHPN1 were used for pull down experiments against immobilized His-MBP tagged Map. The Western blot revealed that Map clearly interacts with RHPN1, but not with RHPN2. Also an interaction with mouse RHPN1 was observed. The control pull down using GFP alone, stayed clear. Below in (B), a GFP tagged Map containing lysate was pulled against immobilized GST tagged RHPN1. The result was the same as in the vice versa approach above.

By using cell lysates of B16 cells transfected with GFP tagged RHPN1 for pull down experiments against immobilized His-MBP tagged Map, in all of the five independently performed approaches the Western blot revealed a clear interaction between both proteins. Additionally, also a clear interaction between mouse RHPN1 and Map was observed (Figure 29 A). In case of the vice versa experiment, GFP tagged Map against immobilized GST-RHPN1, more than half of all pull down revealed an interaction (Figure 29 B). Pull down assays against the second human rhophilin RHPN2, did not show any interactions between Map and RHPN2. Again, the proper folding of the recombinant full length RHPN1 may be causative of these negative results.

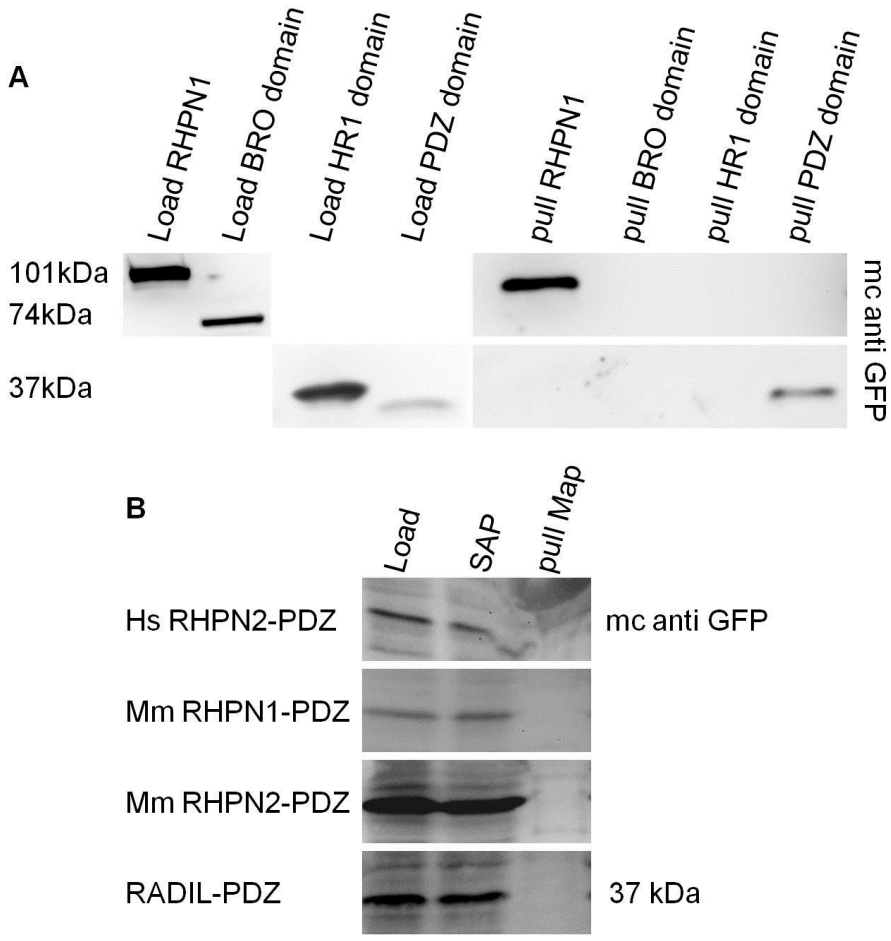

Figure 30 The PDZ domain of human RHPN1 binds exclusively to Map

In (A), again the interaction of GFP tagged RHPN1 to immobilized His-MBP tagged Map is shown. Furthermore you could see pull downs of the RHPN1 domains BRO, HR1 and PDZ against Map. The Western blot revealed that only the PDZ domain is able to bind to the virulence factor. The pull down experiments shown in figure (B) could not detect interactions of His-MBP tagged Map to further GFP-PDZ domains. However, the functionality of the single PDZ domains was not tested.

After verifying the interaction between the virulence factor Map and the human RhoA interactor RHPN1, we turned to the identification of the interaction surface between both proteins. Therefore GFP tagged domain constructs of human RHPN1 were designed and tested in pull downs against immobilized recombinant Map. Western blot analyses showed, that the RHPN1-PDZ domain was the only isolated protein domain, which was able to interact with Map (Figure 30 A).

The exclusiveness of this interaction was highlighted by the negative results of pull down experiments against other PDZ domains from human RHPN2, mouse RHPN2 or the PDZ domain of RADIL, which has been tested as a rhophilin unrelated control (Figure 30 B). Surprisingly, also mouse RHPN1 showed a negative result in pull down assays against Map, although we observed interactions with the full length protein (Figure 29 A). Since no interactor of these PDZ domains was known or available, therefore the functionality could not be tested. Experimental insufficiencies like miss folded recombinant proteins could not be excluded.

2.2.6 Rhophilin CHMP4b interaction

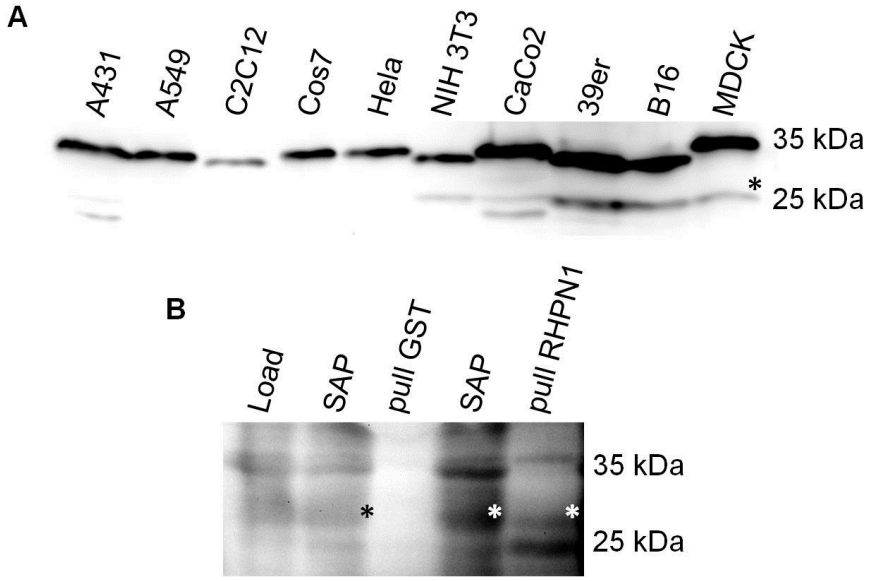

Figure 31 CHMP4b antibody test

In order to test the efficiency of the abcam® CHMP4b antibody, we run a SDS-PAGE with lysates of the indicated cell lines and performed the Western blot. Subsequent antibody detection (A) revealed a strong unidentified band at 35 kDa and one or two weak bands around 25 kDa. CHMP4b is expected to migrate at 27 kDa. The band marked with an asterisk is assumed to correspond to CHMP4. Pull down assays (B) of B16 cell lysates against immobilized human RHPN1 revealed no clear result, because of the high background signal. Potentially a weak interaction is present.

To analyze the potential link between Map, RHPN1 and the ESCRT III complex, we tested two CHMP4b specific antibodies, sc-134946 (Santa Cruz) and ab105767 (abcam®). CHMP4b is one subunit of the ESCRT III complex, which is able to interact with Bro domain containing proteins (Boonyaratanakornkit *et al*., 2013). First, we tested the antibodies against lysates of different cell lines. Results of the abcam® antibody are exemplarily in Figure 31 A.

According to the expected size of 27 kDa for CHMP4b, lysates of 39er or B16 cells seemed to be most suitable to perform pull down assays against human RHPN1. Pull down assays using B16 cell lysates against immobilized human RHPN1 revealed no convincing result, because the antibody detection repeatedly produced high background signals (Figure 31 B). In our hands, both antibodies did not work satisfactory in biochemical experiments. Further experiments are needed to clarify this issue.

2.3 Co-immunoprecipitations

To further support the results of the pull down experiments between Map and RHPN1, we decided to perform co-IPs. Therefore we used Myc tagged Map and GFP tagged human RHPN1. After co-transfection into B16 cells and subsequent cell lysis, we either used 5 µg of GFP antibody to link RHPN1 to bead material, or 200 µl of an anti Myc supernatant or directly beads, coated with Myc antibody to immobilize Map. The control blots of each IP showed that at least in two of three cases the antibody recruitment of the bait protein to the beads was successful.

After GFP detection of the GFP IP, we saw a strong signal for the RHPN1-GFP protein around 100 kDa. Also the Myc staining of the Myc-bead IP revealed a weak but clear band. Only in case of the Myc antibody IP we were not able to show precipitation of RHPN1. Since it was repeatedly hard to detect any bands (also load or SAP control) in these experiments, there had to be a general technical problem. When, using the Myc coated beats, at least 50 % of the experiments resulted in a clear RHPN1 precipitation (Figure 32). When we were performing the experiment with immobilized RHPN1, we always got a strong 25 kDa signal in the IP lane. Unfortunately, the antibody light chain is migrating at the same height and the specificity of our Myc antibody is not focused enough. Because of this we could never be totally sure if we were looking at a Map precipitation, or a cross-reaction.

Subcloning of RHPN1 in Myc- or HA-vectors and the usage of Map-GFP will solve this issue in the future.

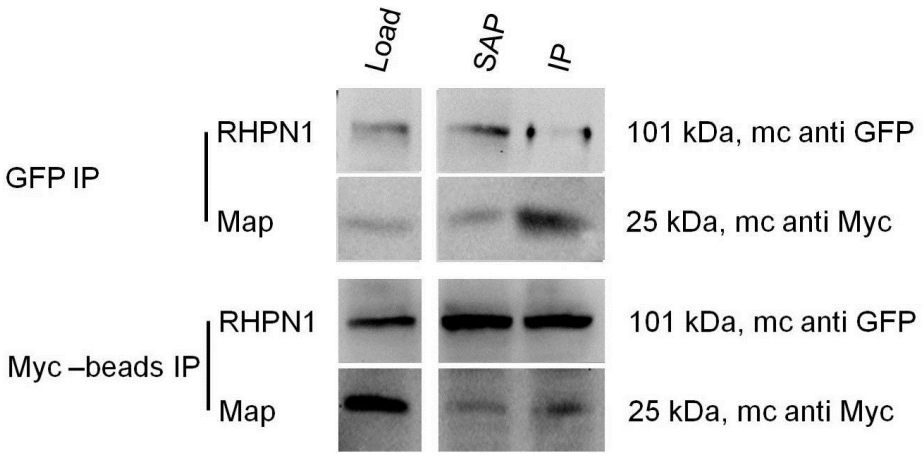

Figure 32 Co-IP experiments between RHPN1 and Map supported our pull down results

Two IPs, realized with anti GFP antibody, or with anti Myc coated beads (from top to bottom).

2.4 Microscopy

2.4.1 Influence of WxxxE proteins on the actin cytoskeleton

Since many members of the WxxxE virulence factor family are known to function as bacterial GEF mimics and because of this function being tightly knotted to GTPases, it is mandatory to understand the host cell morphology subsequent to virulence factor and GTPase transfection.

To compare the effect to continuous activity of Rho family GTPases on the morphology of the cell, overexpression of constitutive active Rac1, Cdc42 or RhoA mutants in Hela cells followed by subsequent phalloidin staining of the actin cytoskeleton was performed (Figure 33). In all following microscopy panels, DAPI staining is only shown in the merge, except for some infection assays. The overexpression of CA Rac1 resulted in the typical wide spread cells, with large fan-shaped lamellipodia at the cell periphery. The ectopic long term expression of CA Cdc42 induced a phenotype similar to that of Rac1 expressing cells, due to the crosstalk in the GTPase pathways and numerous fine stress fibers. Finally, the overexpression of CA RhoA results in an enhanced formation of thicker stress fibers.

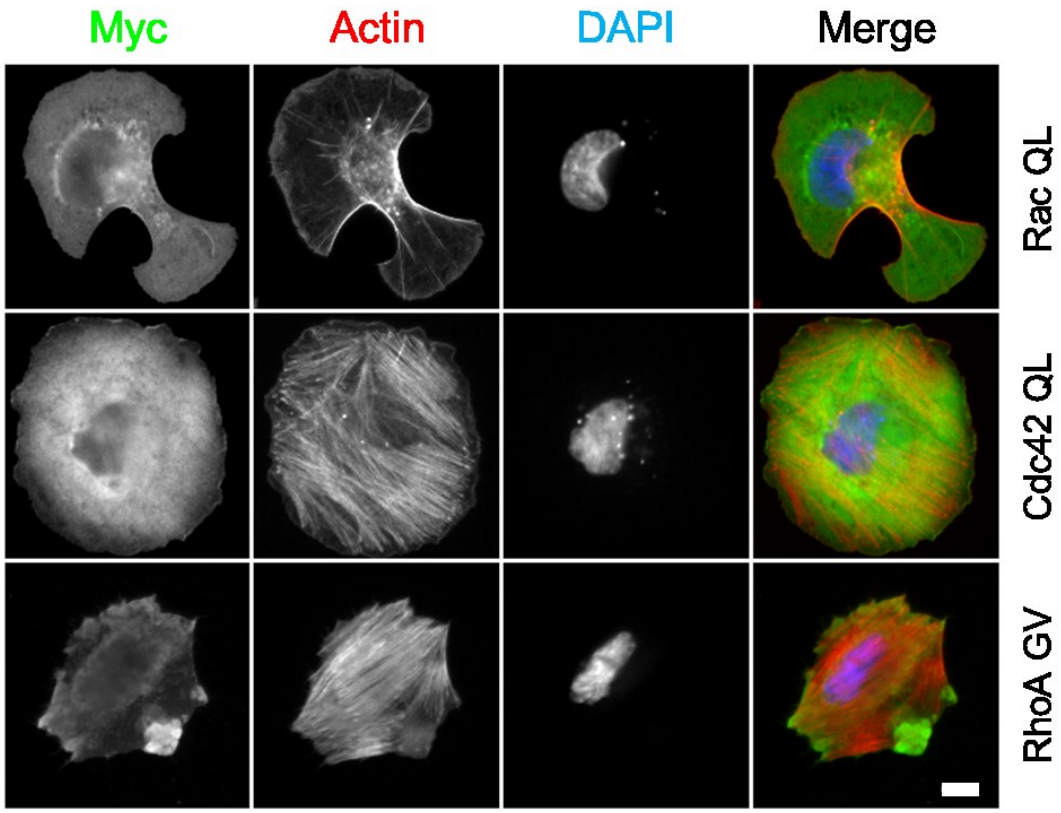

Figure 33 Hela cells, ectopically expressing constitutive active Rac1, Cdc42 and RhoA

Hela cells were transiently transfected with Myc tagged Rac1 Q61L, Cdc42 Q61L or RhoA G14V. After fixation, transfected cells were identified using antibody staining (green). Red labeled phalloidin was used to stain the actin cytoskeleton and DAPI for the nucleus. The cells were imaged at a 60 x resolution and the scale bar represents 10 µm.

As described above for the small Rho GTPases, all the virulence factors of this study were transiently transfected into Hela cells, followed by fixation, phalloidin staining and DAPI staining. Also cells transfected with GFP alone were analyzed (Figure 34, upper panel), to ensure that the tag had no effect. Overexpression of EspT (Figure 34, middle) resulted in a Rac1-like phenotype, wide spread cells, with prominent lamellipodia at the cell front. This observation was virtually identical with either EspT from EPEC or from *C.rodentium*. The only difference between both proteins was, that EspT from EPEC was more equally distributed throughout the cytoplasm, while the *Citerobacter* protein was frequently observed to localize in smaller spots close to the nucleus (Figure 34, middle).

In case of SopB it is difficult to describe the cell morphology upon transfection, because this protein seems to be highly toxic to the cells. The standard transfection protocol, used for all the other virulence factors was not applicable. Indeed, the

transfection efficiency was very high, more than 80 %, but nearly every transfected cell was dead before the microscopy started. Toxicity of SopB has been described before (Aleman *et al*., 2005).

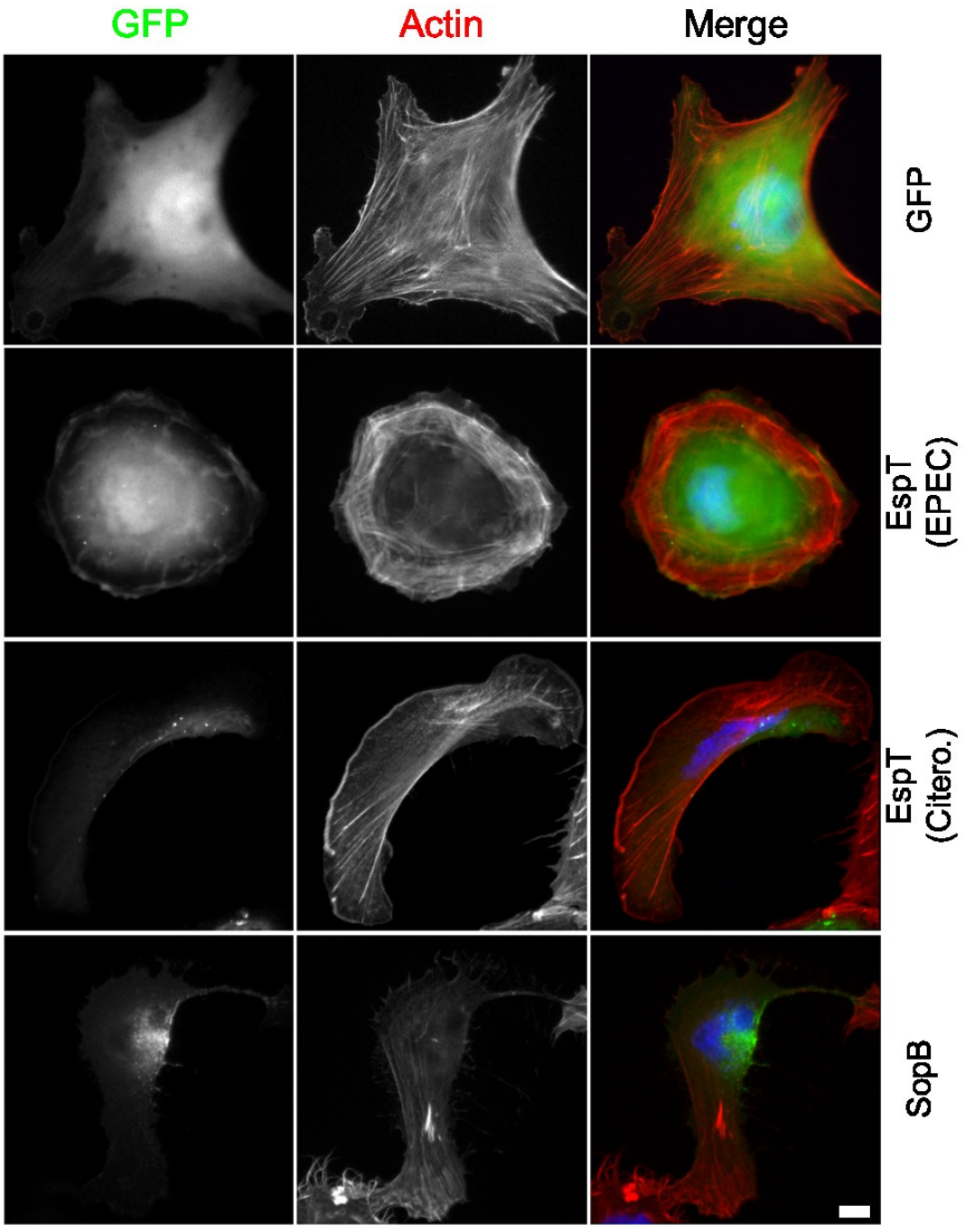

Figure 34 Transient transfection of different bacteria virulence factors in Hela cells (part I)

Hela cells were transient transfected with GFP as a control or GFP tagged full length constructs of EspT (either from EPEC or from *Citerobacter rodentium*), or SopB. The actin cytoskeleton was stained with red labeled phalloidin, the nucleus with DAPI. The cells were imaged at a 60 x resolution and the scale bar represents 10 µm.

Only when little amounts of DNA (4 times less than other transfections) were used for transfection combined with a rescue treatment by medium exchange two hours post transfection, the cells survived long enough to be imaged, but still most of them looked troubled. The few transfected and "healthy looking" cells displayed an uneven, ragged edge with numerous, long filopodia. In those cells, SopB was frequently seen in clusters which concentrate in the nuclear region (Figure 34, lower panel), vaguely reminiscent of what was described before.

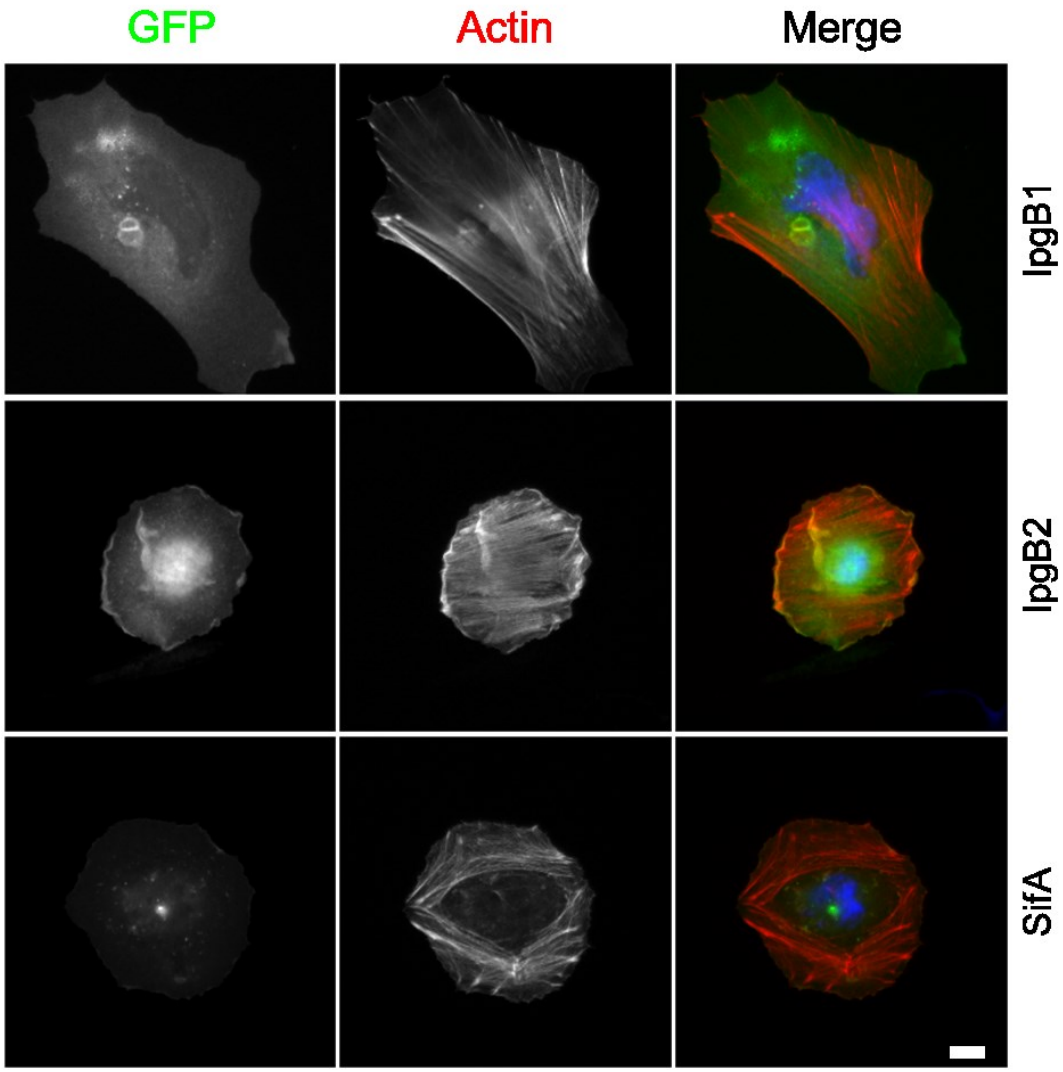

Figure 35 Transient transfection of different bacteria virulence factors in Hela cells (part II)

Hela cells were transient transfected with GFP tagged full length constructs of IpgB1, IpgB2 or SifA. The actin cytoskeleton was stained with red labeled phalloidin, the nucleus with DAPI. The cells were imaged at a 60 x resolution and the scale bar represents 10 µm.

The ectopic expression of the *Shigella* virulence factor IpgB1 resulted in an ambivalent morphology (Figure 35, upper panel). We observed cells, displaying a Rac1-like lamellipodial phenotype, as well as cells producing lots of filopodia, in a Cdc42-like fashion. The protein itself was mostly distributed throughout the cytoplasm. In contrast, the IpgB2 overexpression resulted in a clear cell morphology. We mainly observed small rounded cells with a dense stress fiber network within the cell and frequently increased ruffling. This lead in some cases to huge membrane ruffles, spanning the whole dorsal surface of the cell. Therefore, RhoA activation via IpgB2 does not seem to suppress Rac1 activation, at least not in these cells. IpgB2 was, always found to be equally distributed throughout the cytoplasm (Figure 35, middle).

Finally, the transient expression of the *S.enterica* virulence factor SifA resulted in wide spread, often rounded cells without polarity. These cells only displayed small or even no lamellipodia. Instead, we frequently observed cells producing short filopodia. However, these changes were quite subtle for the diverse shape Hela cells can show. Again, the protein was mainly equally distributed throughout the cytoplasm, with some concentration in the nuclear region (Figure 35, lower panel).

2.4.2 Map provokes a Rac1 like phenotype, RHPN1 induces mild stress fibers

Before studying putative co-localization of Map and human RHPN1 the effects of the single proteins on cell morphology were investigated. For this purpose, Hela cells were transfected with GFP labeled Map, RHPN1 full length or RHPN1 domain constructs. After fixation of the transfected cells, the actin cytoskeleton was stained using red labeled phalloidin and DAPI for the nucleus.

As shown in Figure 36, Map transfected cells, in contrast to the GFP control, display a wide spread, round shape. Furthermore, we observed a dense rim of actin along the cell periphery. Both effects are typical for pronounced Rac1 activity. Cdc42 is known to induce downstream Rac activation (Nobes *et al.*, 1995). Map itself, is distributed throughout the whole cytoplasm. Sometimes, we observed green clusters of Map at variable positions. A clear recruitment of Map, for example to actin dense lamellipodia or to mitochondria was never seen. This came as a surprise, since Map was first described as “Mitochondria associated protein” (Kenny *et al.*, 2000). However, in that study an anti Map polyclonal antibody was used and not a GFP tagged expression construct.

After transfection of human RHPN1 or transfection of the domain construct, we made, despite the uniform distribution of the proteins throughout the cytoplasm, a different observation. The morphology of these cells was similar to the controls and not round. Notably, compared to the control RHPN1 transfected cells display a mild increase of stress fibers.

Map, human RHPN1, human RHPN2 and murine RHPN1 were also ectopically expressed in Cos7 cells. In this case, the dot like localization of Map was strongly increased. The human RHPN1 was also found in clusters within Cos7 cells, but not as prominent as Map was. Only human RHPN2 and mouse RHPN1 were usually found equally distributed throughout the cytoplasm.

Apart from the enhanced expression, the effects on the actin cytoskeleton were not that strong in Cos7 cells (data not shown). In brief, Map transfection slightly rounded the cells and the RhoA-like effect of RHPN1 expression was present, but milder than in case of Hela cells. This raised the question whether the localization of Map and rhophilin is random, or if they are targeted to a specific cellular compartment. Since it has been reported that recruitment of Map to mitochondria occurs during later stages of an EPEC infection (Kenny *et al.*, 2000), we decided to perform a co-staining with MitoTracker®, to determine whether Map and RHPN1 locate at mitochondria (see 2.4.5).

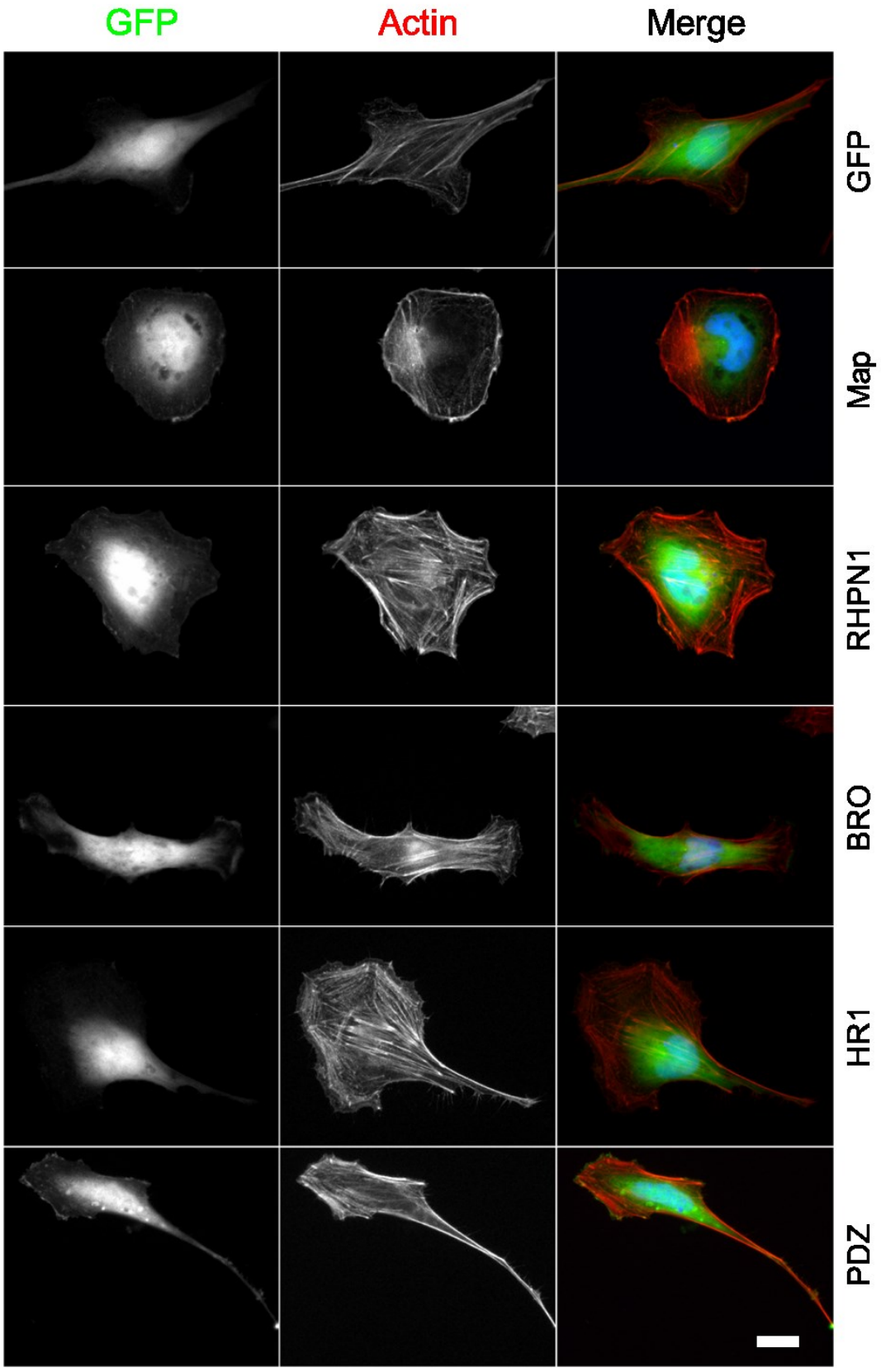

Figure 36 Localization of Map, RHPN1 and its domains after transfection in Hela cells

Hela cells were transfected with either GFP alone or GFP-Map, -RHPN1, -RHPN1 BRO domain, -RHPN1 HR1 domain, -RHPN1 PDZ domain (from top to bottom). Subsequently these cells were co stained with red labeled phalloidin and DAPI (blue), to visualize the actin cytoskeleton and the nucleus respectively. The cells were imaged at a 63 x resolution and the scale bar represents

2.4.3 Map and RHPN1 can co-localize

Because of the positive interaction between Map and human RHPN1 in pull down assays, we decided to study their subcellular level of co-localization. Therefore co-transfections were performed using GFP and RFP labeled versions of RHPN1 and Map, respectively.

After transfection of both constructs into Hela cells, we observed a dramatic change in the protein distribution pattern compared to single transfections. In almost every cell expressing both proteins, red/green aggregates were observed, these signals co-localized perfectly (Figure 37). These aggregates were frequently localized in the proximity of the nucleus (A). If not clustered in the cell center, RHPN1-GFP and Map-RFP protein aggregates were spread throughout the cell (B). Interestingly, the wide spread cell shape, observed after single transfection of Map, was either reduced or sometimes even absent in the additional presents of RHPN1.

In rare cases (about 17 %), transfected cells displayed ruffle formation. In that case no aggregates could be found within the cell. Instead, we observed both proteins to localize in membrane ruffles near the cell surface (C).

Finally, we explored the co-localization characteristics of Map together with the GFP tagged PDZ domain of RHPN1, which embodies the interaction surface for Map. When examining co-transfection of RHPN1-PDZ together with Map, we saw a similar distribution pattern as observed for the full length RHPN1-Map co-transfections. In other words, both proteins co-localized around the nucleus (D) and in rare cases in ruffles near the cell surface (not shown). Noteworthy, the protein spots seemed to be smaller and closer to each other (D). In contrast, and as expected, the HR1 and BRO domain did not co-localize with Map (not shown).

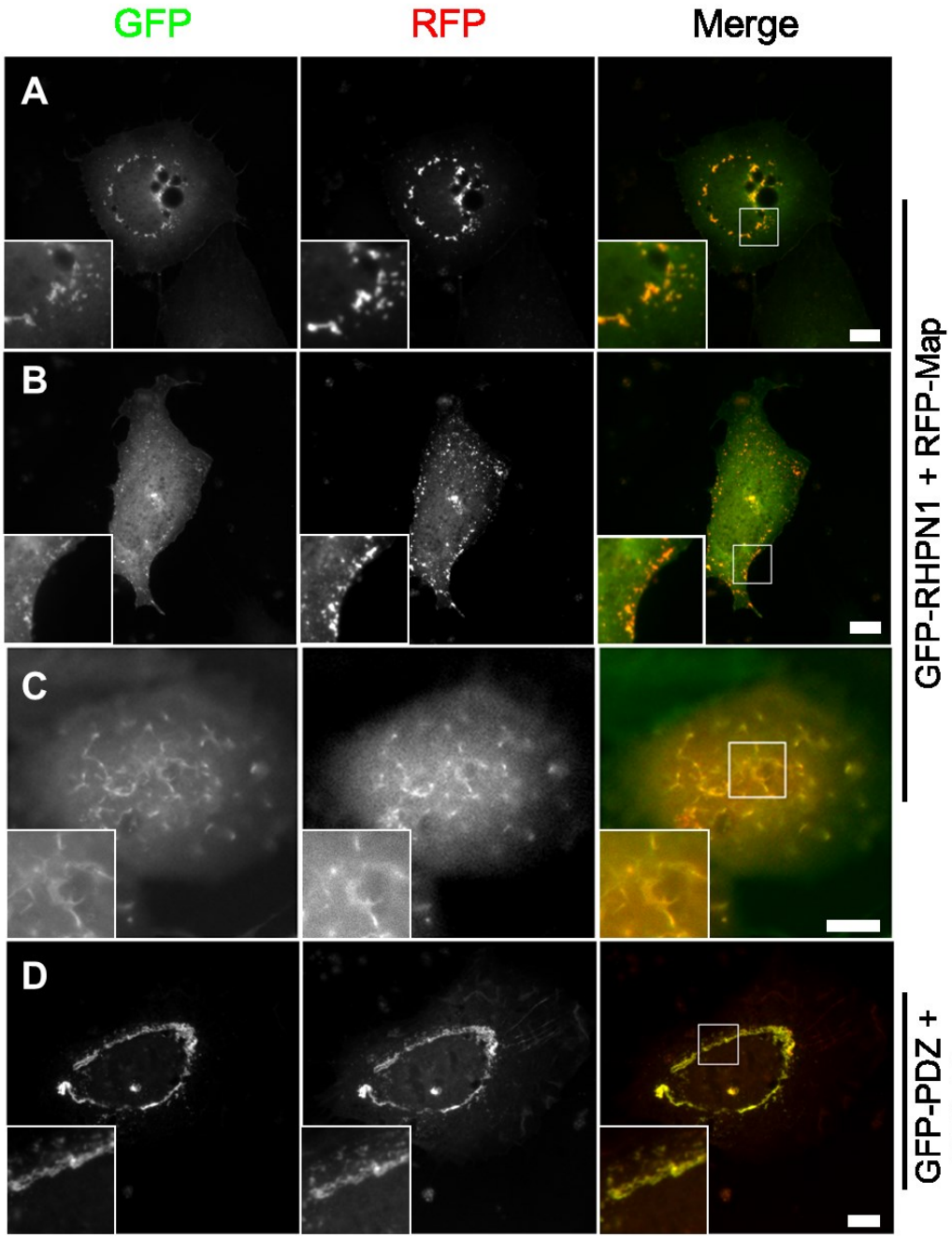

Figure 37 RHPN1 and Map co-localize in Hela cells after co-transfection

Hela cells were transfected with RFP-Map, either together with GFP-RHPN1 (A-C) or the GFP tagged RHPN1 PDZ domain (D). After fixation, cells were imaged at a 63 x resolution. The color merge clearly show the strong co-localization of Map and its partner. The scale bar represents 10 µm

2.4.4 Co-transfection of small GTPases does not affect the RHPN1-Map interaction

Map and RHPN1 are both able to interact with small GTPases. Map interacts with Cdc42 and RHPN1 with RhoA. This rose the question, whether small GTPases are able to alter the interaction between Map and RHPN1. To answer this question, Hela cells were co-transfected with GFP-RHPN1, RFP-Map and Myc tagged GTPases. It was hard to find cells, which were positive for all of the three proteins. In cells, in which all three proteins were expressed, no effect of dominant negative Cdc42 or of dominant negative RhoA on the RHPN1-Map interaction could be observed and also no GTPase recruitment to RHPN1-Map positive sites. In fact, the distribution pattern of RHPN1 and Map in this experiment was similar to the distribution found in double transfections without the small GTPases. However, the morphology of the cells was affected. For example, Cdc42 co-transfection induced or restored the wide spread cell shape and sometimes provoked filopodia formation, even though the dominant negative variant of Cdc42 was used. In contrast, RhoA co-transfection resulted in more contracted cells, only in rare cases wide spread cells were detected.

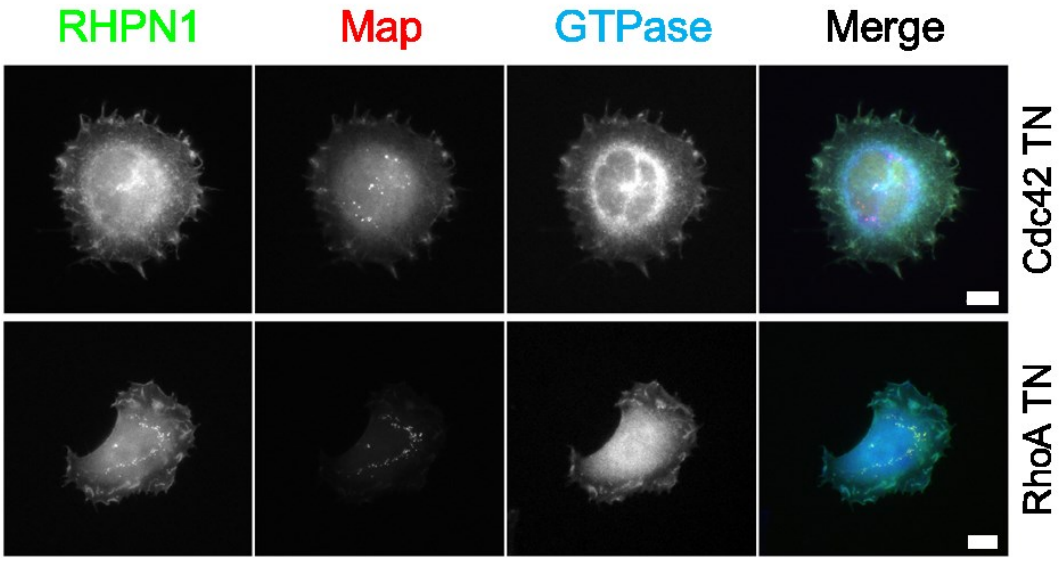

Figure 38 No influence of GTPases on RHPN1-Map co-localization

Hela cells were triple-transfected with GFP-RHPN1, RFP-Map and Myc-Cdc42 TN or Myc-RhoA TN. Subsequently, cells were fixed and the Myc tag was visualized by using appropriate antibodies. Neither the overexpression of Cdc42 TN, nor of RhoA TN alters the localization of RHPN1 and Map. The scale bar represents 10 µm

2.4.5 MitoTracker staining revealed co-localization between human RHPN1 and mitochondria

The localization of Map and human RHPN1 in Hela and Cos7 cells, made us assume that mitochondria could be the cellular compartment where these proteins localize. Moreover Map has been described earlier to localize to mitochondria (Kenny *et al.*, 2000). In order to examine whether Map and human RHPN1 are enriched at mitochondria, we used MitoTracker® to visualize the mitochondria in transfected cells.

We found the mitochondria as a tubular network, spreading from the nucleus towards the cell periphery. In all experiments, independent of the transfected plasmids, this tubular network looked similar.

In case of the GFP control (Figure 39 A), the ectopically expressed protein was evenly spread throughout the cytoplasm and no co-localization between mitochondria and the proteins was observed.

When Map, human RHPN1 or its PDZ domain were expressed, we could clearly detect the protein accumulations described before. No relevant overlap between ectopically expressed Map and mitochondria was observed (Figure 39 B). In case of hRHPN1 or PDZ transfected cells the result was different. In these cells we indeed could observe co-localizations of the overexpressed proteins with mitochondria, as indicated by arrowheads in the respective blow ups of Figure 39 (C+D).

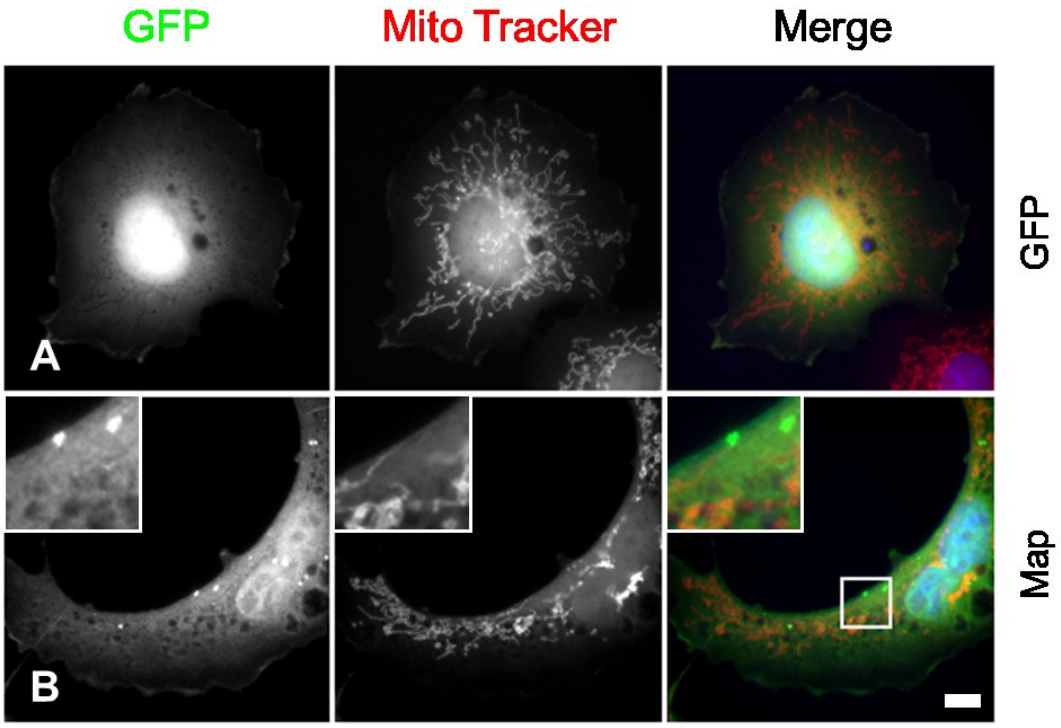

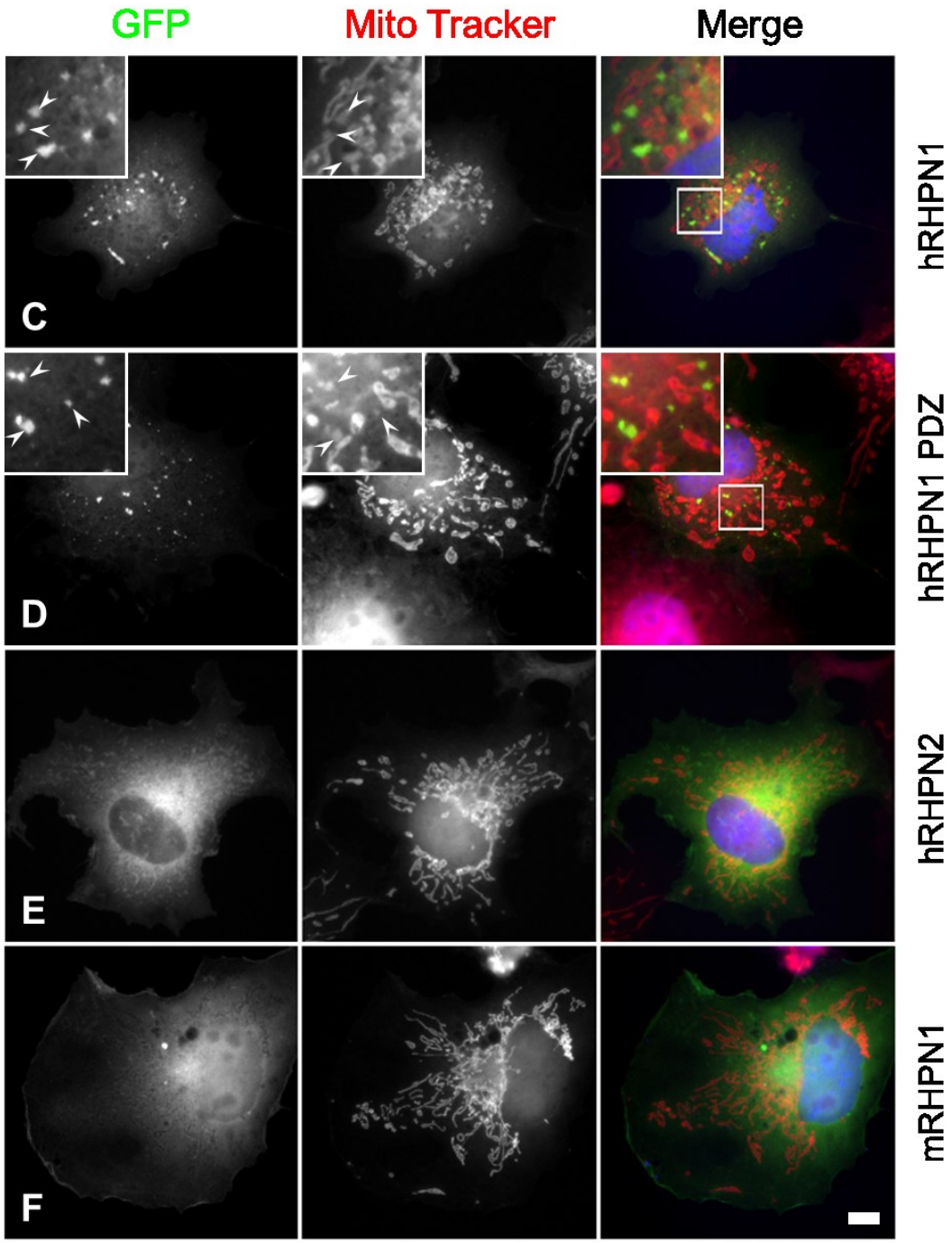

Figure 39 Map did not localize to mitochondria but human RHPN1

Cos7 cells were transfected with the indicated GFP constructs and treated with MitoTracker® according to the manufactures manual. Microscopic analysis revealed at least partial localizations of hRHPN1 and hRHPN1-PDZ to mitochondria, as indicated by arrowheads. The scale bar represents 10 µm.

The observed overlap was not complete but partial, since there were still some green hRHPN1 or PDZ dots without MitoTracker® signal and many mitochondria without RHPN1. Upon transfection of human RHPN2 (Figure 39 E) and mouse RHPN1

(Figure 39 F), no localization of those proteins at mitochondria was observed. Together, it will require further experiments with exchanged colors to pinpoint where and when RHPN1 and mitochondria come together.

2.5 Infection assay

In order to determine whether and how RHPN1 is involved in EPEC infection, we performed infection assays. To do so, Cos7 cells were transfected with GFP tagged human RHPN1, human RHPN2, mouse RHPN1, Map or the PDZ domain of human RHPN1. Next, the transfected cells were infected with the EPEC strain E2348/69, washed and fixed at different time points (30 min, 60 min and 180 min post infection). The cells were stained with DAPI to detect the bacteria attached to the cell surface and phalloidin to visualize the actin cytoskeleton, in particular the actin rich pedestal below the bacteria. At 30 min post infection, no bacteria were found to be attached to the cell surface, therefore only images after 60 and 180 min are depicted here (Figure 40).

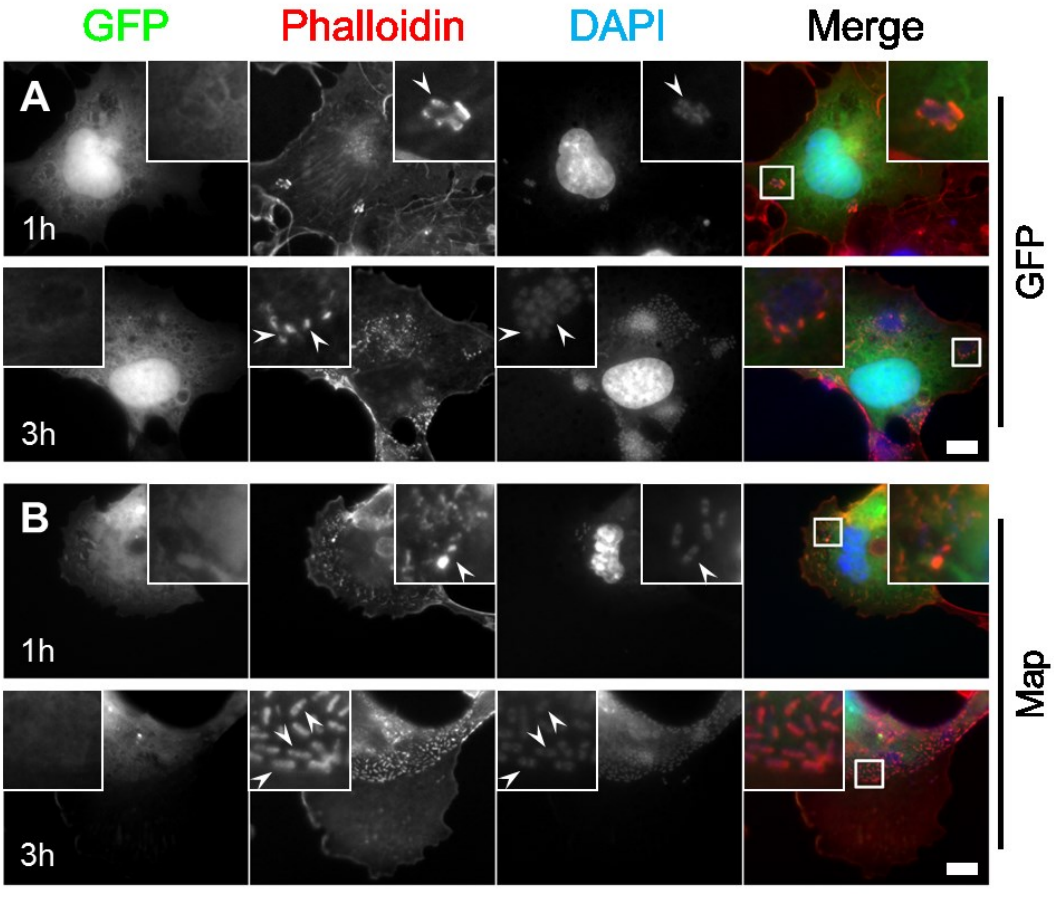

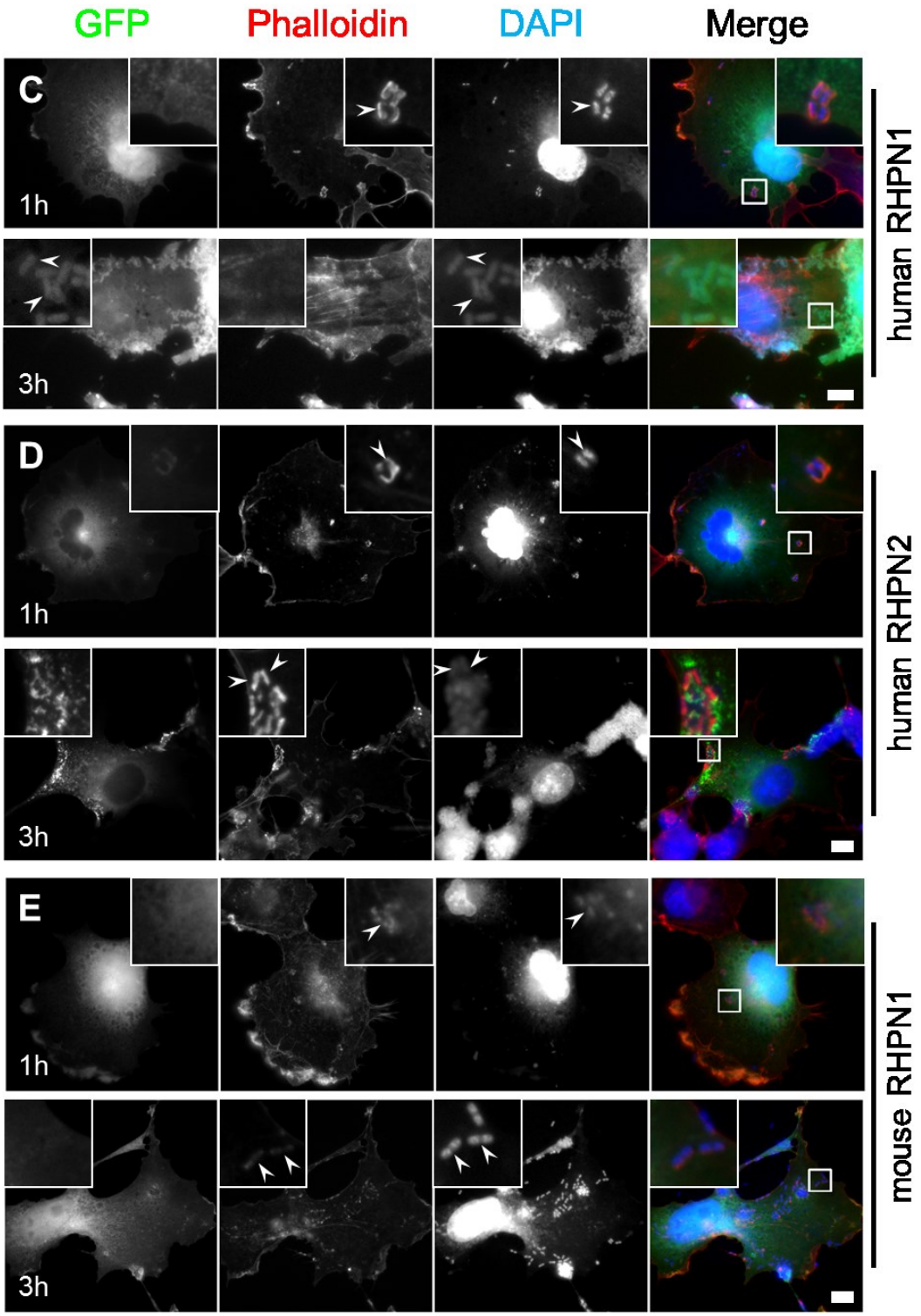
GFP
Phalloidin
DAPI
Merge
C
1h
3h
human RHPN1
D
1h
3h
human RHPN2
E
1h
3h
mouse RHPN1

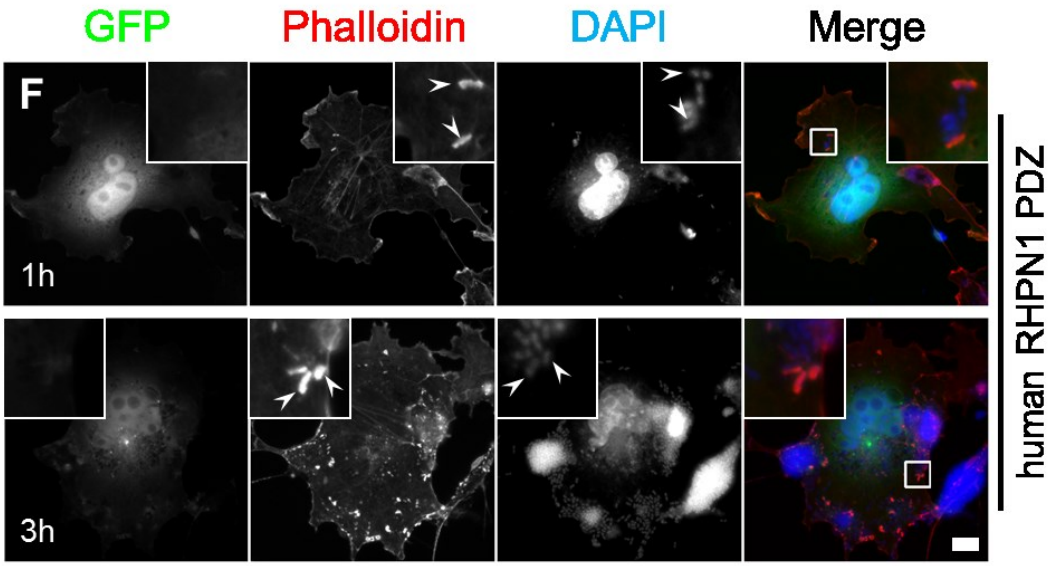

Figure 40 Pedestal formation beneath attached bacteria at different time points after infection

Cos7 cells, transfected as named on the right side of each set of images, were infected with EPEC and subsequently fixed after 1 h or 3 h infection. Later the cells were stained with red labeled phalloidin in order to visualize the actin cytoskeleton and stained with DAPI, to highlight the bacteria which are attached to the cell surface. Arrowheads indicate infection sides. The scale bars represent always 10 µm.

In general, 1 h after infection, we found 3 to 10 bacteria, or clusters of bacteria attached to the cell surface. This number was consistent, independent from the transfected plasmid. Two hours later, although the cells were washed every hour to reduce the amount of bacteria, the number of bacteria attached to single cells increased to very high numbers. For this reason, only the images of the 1 hour time point were used for statistical analysis. The bacteria attached to each transfected cell were counted, as well as the number of corresponding pedestals (Figure 41), the results of this statistics will be analyzed together with the microscopy images in the following paragraph.

The negative control, Cos7 cells transfected with GFP alone (Figure 40 A) revealed a normal cell shape and in addition some pedestals after 1 h and many more after 3 h. Out of 48 analyzed images, we found 220 bacteria or bacteria clusters attached to the transfected cells. Only 141 of them were attached to pedestals. Consequently, 64 % of the bacteria attached to GFP positive cells provoked the formation of pedestals within one hour of infection (Figure 41). Interestingly, at the 3 h time point, the

pedestals are smaller and less proper in shape, compared to after 1 h. Furthermore it seemed that the amount of pedestal positive bacteria had decreased. This may be explained by the increased numbers, leading to actin consumption and cell stress.

In case of Map expression (Figure 40 B), the amount of pedestal positive bacteria, 1 h after infection, in 46 analyzed images was increased by approximately 14 % to 78 % compared to the GFP control (Figure 41). After 3 h the pedestals are still equal in shape and size and it seems, as if every bacterium has its own pedestal. The number of pedestals built up below these attached bacteria, however, was not statistically evaluated. Thus, the presents of Map may reduce cell stress and/or mobilize actin to help establish the infection.

In contrast, when expressing human RHPN1 the number of pedestal positive bacteria 1 h after infection was decreased by 12 % down to 52 % (Figure 41). Two hours later, although the number of bacteria was apparently similar to that in the other experiments, it was hard to find any pedestals at all (Figure 40 C). Instead the bacteria showed up in the GFP channel (Figure 40 C, lower panel). We saw this

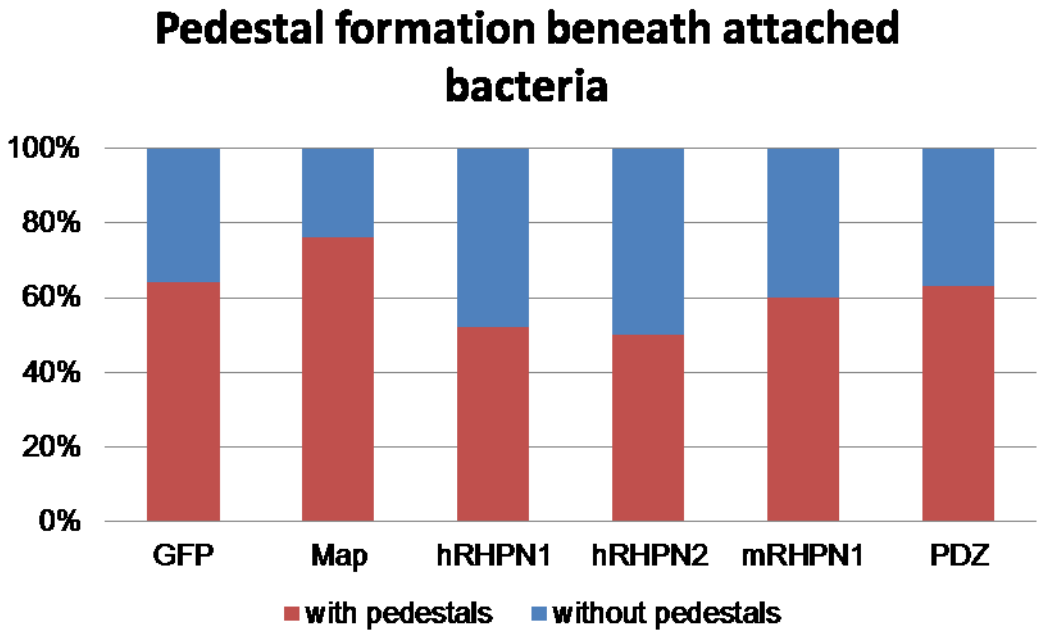

Figure 41 Pedestal formation efficiency differs with respect to the transfected plasmid

The images taken from the infection assays at time point 1 h were analyzed on the one hand for the number of bacteria, attached to transfected cells and on the other hand for the corresponding pedestals beneath each bacterium. Clusters of two or more bacteria were counted as one. The same is true for the belonging pedestals, even though, if not every bacterium within a cluster had its own pedestal.

phenomenon in about 50 % of all transfected cells. The GFP signal perfectly co-localized with the bacteria in the DAPI channel, indicating the recruitment of RHPN1 to the infection side. However, the complete absence of F-actin made it impossible to judge on the exact status of infection. The GFP signal also did not accumulate beneath the bacteria in a characteristic pattern, making it possible that we look at bacterial invasion and subsequent recruitment of the GFP labeled protein to internalized bacteria. To address the possibility of bacterial internalization, we performed a gentamycin protection assay (see 2.6). With this assay, the number of intracellular living bacteria can be exactly determined.

Human RHPN2 also reduces pedestal formation after 1 h, similar to hRHPN1. However, 3 h post infection pedestals were still present, albeit impaired, and the GFP signal had accumulated close to the bacteria but did not label them like hRHPN1 did (Figure 40 D). The pedestal formation efficiency at time point 1 h was lower (50 %) as compared to control (Figure 41).

In mouse RHPN1 expressing cells the portion of bacteria which were able to provoke pedestals (60 %), was almost at control levels (Figure 41). Also after 3 h of infection, the pedestal formation seemed to be unaffected (Figure 40 E).

Finally we tested the influence of the human RHPN1 PDZ domain under infectious conditions. The result was virtually identical to the GFP control

2.6 Gentamycin protection assay

In order to examine the potentially increased invasiveness of EPEC in human RHPN1 transfected cells (Figure 40 C, lower panel), we decided to perform a gentamycin protection assay. Cos7 cells were transfected with GFP or with one of the three GFP RHPN constructs. Next, these cells were either treated with EPEC, or as a negative control with *E.coli* C600. After 3 hours, all extracellular bacteria were killed by applying the non cell permeable antibiotic gentamycin. Subsequently the cells were lysed and plated in appropriate dilutions on LB-agar plates. The next day, the colonies were counted. Each colony represents one living intracellular bacterium. The results of three independent sets of experiments were grouped and analyzed (Figure 42).

In case of *E.coli* C600, usually around 300 colonies were found. The GFP and the human RHPN1 attempt resulted both in 345 colonies. The number of colonies gained

from cells which expressed the other two rhophilins was not statistically significantly different from the control.

In case of EPEC, there was clearly a higher number of colonies, on average 100 times more colonies compared to the *E.coli* control. In this experiment, the highest number of colonies was derived from lysates of cells transfected with GFP alone. The transfection of human RHPN1 did not result in a statistically significant change of colony numbers.

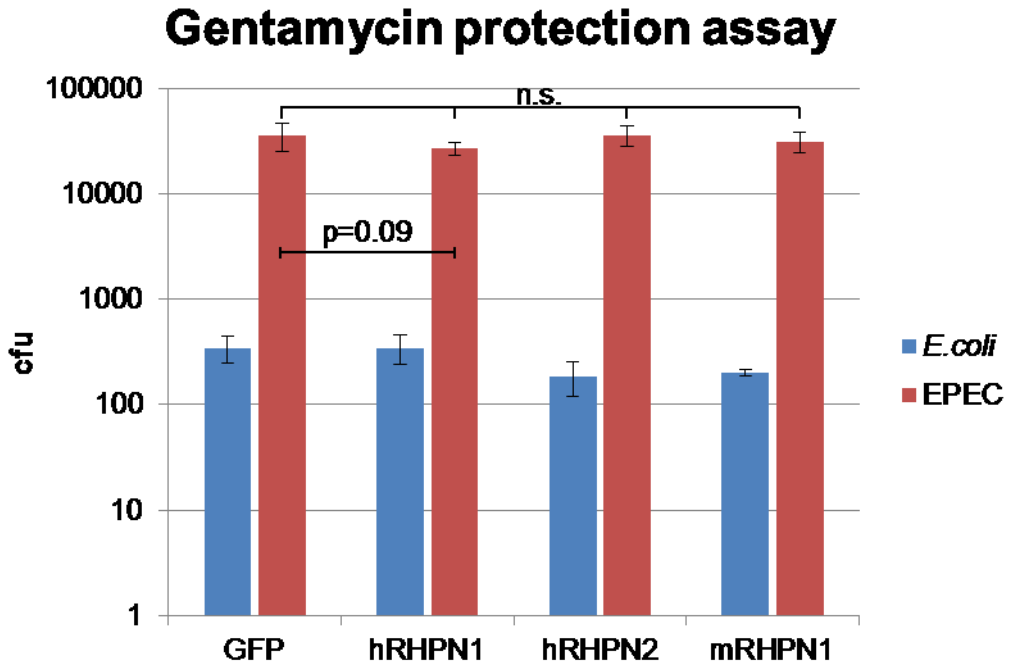

Figure 42 The gentamycin protection assay revealed no rhophilin mediated EPEC invasion

The numbers from counting the colonies grown from bacteria which survived the gentamycin show, that neither human RHPN1 transfection, nor any other tested rhophilin result in an increased invasiveness of *E.coli* (blue) or EPEC (red). The small variations are without statistical relevance.

We next reasoned that the bacteria labeled with GFP-RHPN1 could potentially be intracellular but dead and therefore absent from the gentamycin protection assay, that evaluates only living bacteria. Therefore, we employed an additional approach to specifically stain intra- versus extracellular bacteria. In this experiment we aimed to find out if the green rods, observed in cells transfected with human RHPN1, are internalized dead bacteria or a result of protein recruitment beneath extracellular bacteria. To do so, an anti *E.coli* antibody was used. This antibody from Novus Biologicals specifically recognizes the J5 lipopolysaccharide (LPS) in the bacterial cell wall of all *E.coli*, such as C600 or EPEC.

We repeated the infection assay described in 2.5 using Cos7 cells transfected with human RHPN1 or mouse RHPN1. Three hours after EPEC infection, the cells were fixed and stained with the anti LPS antibody without any permeabilization step. Additionally a DAPI staining was performed. The idea was that the LPS antibody should not be able to permeate the cell and thus, only stain bacteria on the cell surface, while DAPI stains also internalized bacteria. In other words, internalized bacteria should only be stained in blue. When analyzing the fixed cells by fluorescent microscopy, we observed after transfection of GFP, no rod like structures and only small numbers of weak LPS positive structures (Figure 43 A). However, upon transfection of hRHPN1 again in about 50 % of all hRHPN1-GFP positive cells, we noticed rod shaped structures in the GFP channel (Figure 43 B+C). Only very sporadically, single co-localizations with blue labeled bacteria in absence of red were observed (Figure 43 C). More frequently we saw deformed, weak LPS positive structures, which co-localizes with green and blue accumulations (Figure 43 B). In case of mouse RHPN1 transfected cells, sometimes also protein accumulations were observed in the green channel. However, these accumulations were, in contrast to human RHPN1 transfected cells, not co-localized with DAPI or LPS signals but rather diffuse (Figure 43 D).

The weak LPS positive structures could be remnants of phagocytosed bacteria. Also the experimental protocol may lead to staining via small amounts of the anti LPS antibody, which were able to pass the membrane. Further experiments are necessary to unambiguously clarify this. Taken together, the gentamycin result and the high amount of weak LPS positive structures within cells upon human RHPN1 transfection allow to speculate that RHPN1 induces phagocytosis of EPEC probably throughout autophagy of plasma membrane. At the time point of cell fixation, the bacteria are most likely already dead and therefore cannot count positive in the gentamycin protection assay.

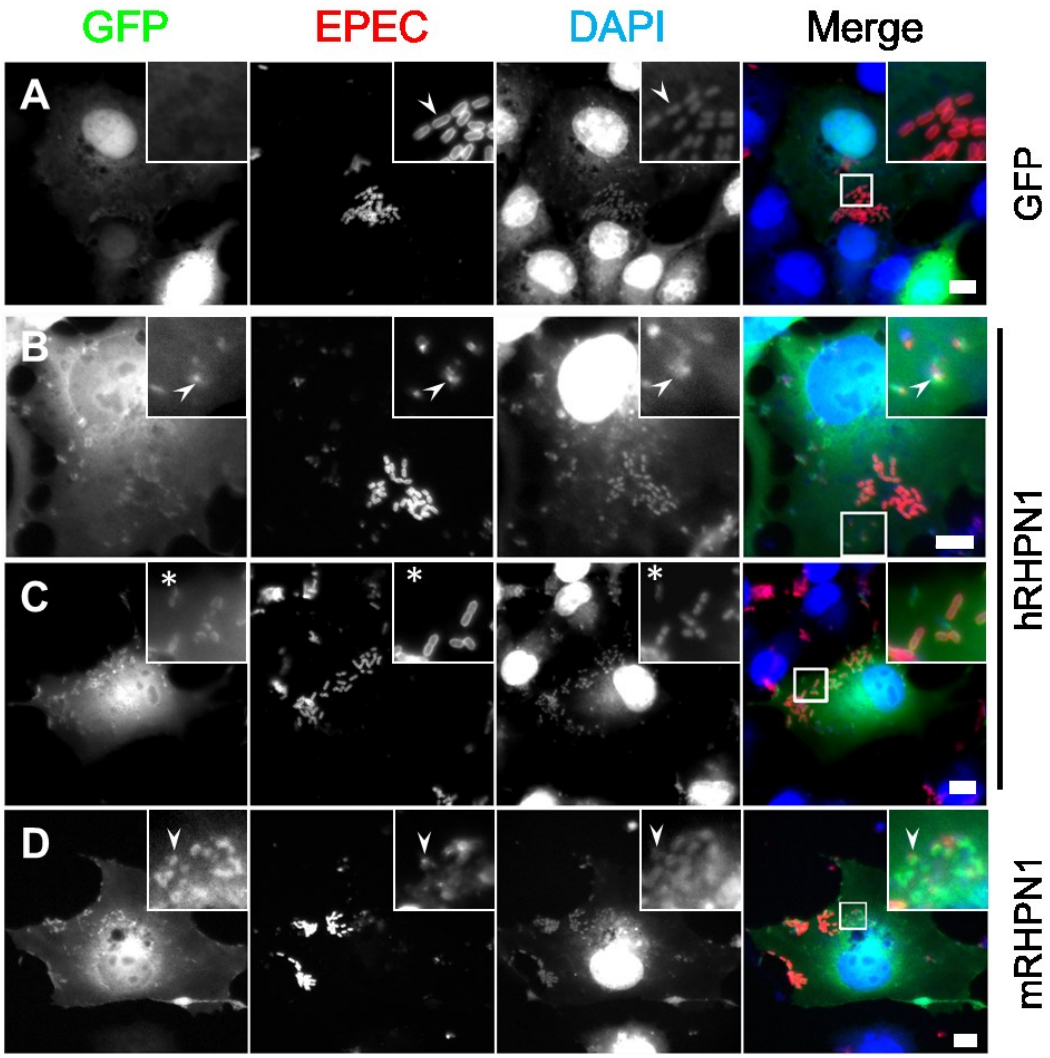

Figure 43 Staining of bacteria with an anti LPS antibody after infection assay

Cos7 cells transfected with either GFP alone, human RHPN1-GFP or mouse RHPN1-GFP were infected for 3 h with EPEC. Subsequently, the cells were fixed and stained with DAPI and an anti LPS antibody without performing a permeabilization step. Arrowheads indicate structures, observable in the red and blue channel, while asterisks highlight structures visible only in the green and blue channel. The scale bar represents 10 µm.

2.7 RHPN1 CHMP4b interaction

The potential autophagy described in the previous chapter may involve the ESCRT III complex, which is known to participate in different membrane associated processes like bending, or fission. Although we were not able to show an interaction between the ESCRT III subunit CHMP4b and human RHPN1 in pull down assays, we tested the abcam® antibody for immunofluorescence microscopy (Figure 44).
No matter if RHPN1 was expressed alone, or together with Map in Hela cells, we were not able to observe a recruitment of CHMP4b towards RHPN1 or RHPN1/Map positive structures.

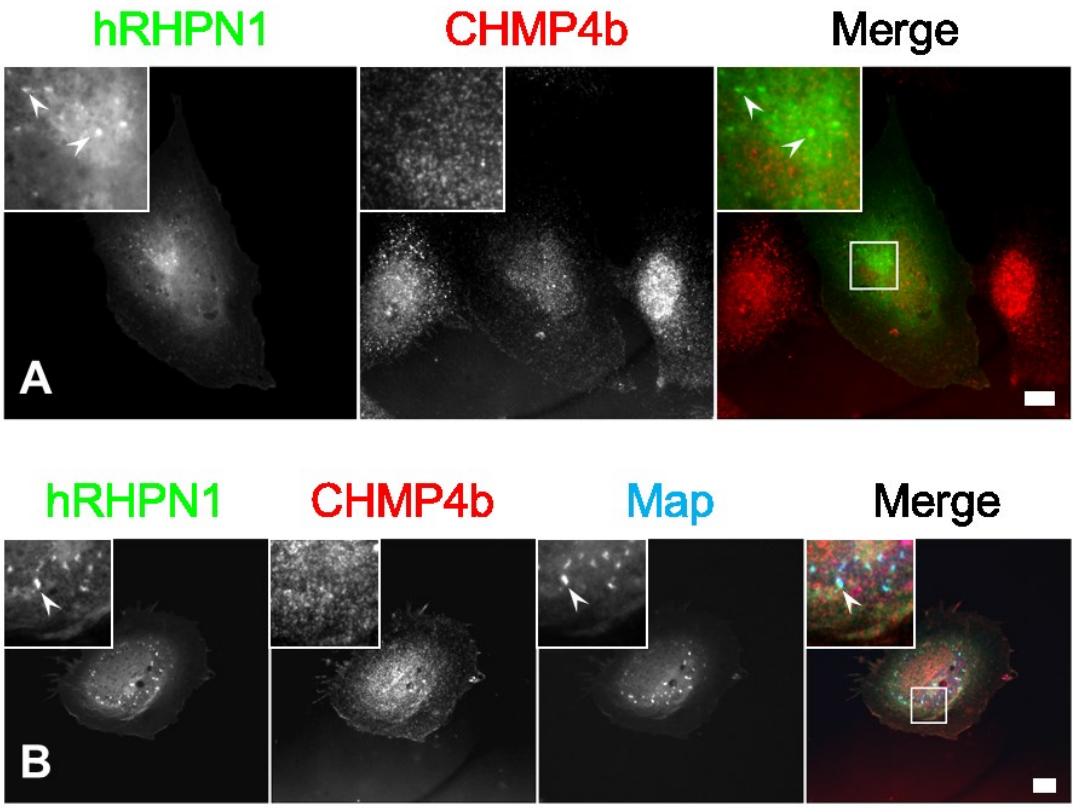

Figure 44 No recruitment of CHMP4b towards RHPN1 and/or Map positive structures

In (A) Hela cells were transfected with GFP tagged human RHPN1 and subsequently stained with abcam® anti CHMP4b antibody. In (B), the cells were additionally co-transfected with Myc tagged Map. Arrowheads indicate spots of protein accumulations. The scale bars represent 10 µm.

3 Discussion

The aim of this work was to identify so far unknown interaction partners of bacterial virulence factors on the host side. To get an idea where we had to start searching, we performed a large Y2H screen which comprised several variants of 10 bacterial proteins as baits and a genome wide human cDNA derived protein collection as preys. This screen resulted in over 150 hits, some of them, being more and some of them, being less likely. This was estimated based on their behavior in more than 100 previous screens performed by our cooperation partners at the DKFZ in Heidelberg.

Out of the pool of likely protein interactions, which was still numerous, we have chosen those involved in processes that might play a role in pathogenicity and as GTPases, their interactors and proteins involved in trafficking or migration. Furthermore we decided to follow some additional hints since they seemed promising.

To verify the selected Y2H interactions, we first utilized biochemical methods. To do so, we purified recombinant virulence factors, as well as their putative interactors from bacteria and immobilized them to appropriate sepharose beads. Subsequently these proteins were used in pull down experiments against lysates of mammalian cells ectopically expressing the putative partner. All pull downs were performed until a statistical relevant conclusion was possible, but at least three times. The experiments always included suitable negative and if available also positive controls. In case that a pull down was repeatedly negative, we put the respective hit aside and focused on the next. We cannot exclude that these hits are relevant since the negative result can come from experimental conditions. However, we decided to test the large number of hits in a straight forward standard procedure, keeping potential overseen interactions in mind. If a pull down experiment was convincingly positive, at the best also in vice versa approaches, we strengthened the result by further methods, namely co-immunoprecipitation, and/or immunofluorescence microscopy.

Finally we tested our findings in infection assays, trying to create a model that puts our results into the whole infection context and explain the biological relevance of this process.

3.1 EspT does not interact with Arf6

The first interaction, which we tested was the one between EspT and Arf6. We considered this pair as potential relevant because Arf6, as a small GTPase involved in reorganization of the actin cytoskeleton and in endocytosis (Donaldson, 2003, D'Souza-Schorey *et al.*, 2006), is very likely active during infection. Although the formal prove of an interaction was still missing, it has been reported that the small Rho GTPases Rac1 and Cdc42 were activated by EspT (Bulgin *et al.*, 2009b, Orchard *et al.*, 2012a). Thus it was attractive to test if EspT is a direct activator of Rac1 and/or Cdc42 or indirect, for instance via Arf6. A direct link between Rac and Arf6 activation has been described before (Radhakrishna *et al.*, 1999, D'Souza-Schorey *et al.*, 1997).

When inspecting the pull down assays between EspT and different versions of Arf6 (Figure 16), it became obvious that no interaction between both proteins was detected. In contrast, strong interactions were observed between recombinant EspT and the constitutive active (CA) versions of Rac1 and Cdc42, also in the vice versa approach using recombinant Rac1 and Cdc42 both activated GTP-loaded GTPases interacted with EspT (Figure 17). As a member of the WxxxE family with predicted GEF activity (Ohlson *et al.*, 2008), we had expected that EspT interacts with the dominant negative GDP-loaded versions. One hand this showed that our experimental procedure is working, on the other hand they raised different new questions. First, if EspT interacts with GTP loaded Rac1 and Cdc42, how is the published GTPase activation accomplished? This is an important question, since also in our hands, EspT overexpression resulted in a typical Rac1/Cdc42 hyper activation phenotype of the cell morphology (Figure 34). Second, if EspT possesses GEF activity and neither the tested Rho GTPases nor Arf6 is the substrate, what is the real target? Finally, the binding to CA GTPases implicates a function as a downstream effector of Cdc42 and Rac1, leading to the question in which pathway EspT might be integrated. Therefore, in the future we will revisit EspT using other assay. Also a crystal structure, that in the case of IpgB2 and RhoA clearly revealed the GEF-activity, may teach us a lot about EspT/Rac1 or EspT/Cdc42.

3.2 SopB does not interact with the V-ATPase subunit ATP6V1E1

In contrast to the other virulence factors mentioned in this thesis, SopB belongs to a different protein class. SopB is not a member of the WxxxE protein family and is not a bacterial GEF. Yet, it is one of the *Salmonella* type III secreted virulence factors (Zhou *et al.*, 2001) and plays an important role in invasiveness and later in infection (Hänisch *et al.*, 2011, Roppenser *et al.*, 2012). The SopB protein comprises two known functions. First a phosphoinositide phosphatase activity (residues 357-561) (Norris *et al.*, 1998) and second a GTPase binding capacity (residues 117-168) (Rodriguez-Escudero *et al.*, 2011), which are both involved in the stimulation of cytoskeletal rearrangements and perpetuation of the SCV.

In our Y2H, SopB interacted with the ATP6V1E1 subunit of the V-ATPase. This ATPase is a evolutionary highly conserved machinery among eukaryotes and play an essential role in acidification of cellular organelles by pumping protons across membranes (Perez-Sayans *et al.*, 2012).

Upon *Salmonella* invasion, several host proteins are targeted to the SCV membrane, among them the V-ATPase (Martinez-Lorenzo *et al.*, 2001). Having a look at other pathogenic bacteria, for example *Streptococcus pyogenes* or *Mycobacterium tuberculosis*, one can see that there are cases, in which the ATPase is a targeted to prevent acidification of the phagosome (Nordenfelt *et al.*, 2012, Wong *et al.*, 2011b). Due to its adaptive acid tolerance (Garcia-del Portillo *et al.*, 1993a) *Salmonella* is not fully dependent on prevention of acidification of the SCV, however an interference with the ATPase could still be advantageous.

Our pull down assay results of SopB and different small GTPases of the Rho family, revealed a strong interaction with dominant negative and constitutive active Cdc42 (Figure 19). This fitted perfectly to the literature (Rodriguez-Escudero *et al.*, 2011) and confirmed that our recombinant SopB is, at least in part, properly folded. The interaction to ATP6V1E1 however, was in three independent experiments always negative.

Besides the possibility that there really is no interaction between the V-ATPase subunit and SopB, we cannot exclude technical reasons for this, since we have no control on the folding of the PiPase region. Moreover the interaction may require membrane or additional proteins. Finally the GFP tag may have blocked an interaction and recloning may solve this problem. We currently plan different additional approaches to clarify this issue.

3.3 IpgB2 interacts with BBS4

IpgB1 and IpgB2 are two related *Shigella* virulence factors. They are further members of the WxxxE family and should stimulate the formation of lamellipodia, ruffles and stress fibers in the host cell upon transfection, respectively (Alto *et al.*, 2006, Klink *et al.*, 2010). Upon transient transfection of IpgB1 into Hela cells, we observed a diverse morphology. In different attempts, we saw IpgB1 positive cells, displaying a Rac1- or Cdc42-like phenotype. Sometimes also a mixture of both phenotypes was seen (Figure 35). This fits to the report, that IpgB1 is able to accelerate the Rac1 activation 32-fold and the Cdc42 activation at least 6-fold (Huang *et al*., 2009), exerting GEF activity on those GTPases.

In our hands however, we were not able to reproduce the interaction of IpgB1 and Rac1 or Cdc42 in pull down experiments (Figure 21), which were described by Huang and colleagues. Since we had no hit in the Y2H and our pull down assays between Rac1 or Cdc42 and IpgB1 were negative, too, it might be possible that the interaction is weak and transient in an "kiss and run" style. Maybe it would have been possible to finally reproduce the interaction, by the preparation of new recombinant IpgB1 or by changes in our experimental procedure. But since the Y2H screen has provided no potential interaction partners, we decided continue on IpgB2.

The ectopic expression of IpgB2 was reported to provoke a RhoA like stress fiber response in HEK293A cells (Alto *et al.*, 2006, Klink *et al.*, 2010). In our experiments, we used Hela and Cos7 cells to analyze the results of transient transfections. We frequently observed rounded cells, often lined with lamellipodia. Cell surface spanning ruffles were also found usually. However, the RhoA effect described by Alto and colleagues was not that strong in these cell types. Indeed, our cells were filled with a dense stress fiber network, but the single fibers were rather thin (Figure 35). One explanation for the difference between the observed cytoskeletal phenotypes could be the usage of different cell types.

For IpgB2 it has been shown on crystal structure level that the virulence factor specifically interacts with GDP-loaded RhoA and catalyses the nucleotide exchange (Klink *et al*., 2010). The authors also showed in the same article, that IpgB2 accelerates the exchange ~10^4-fold compared to the intrinsic rate. This is more than one order of magnitude above the efficiency of mammalian GEFs of RhoA.

In our pull down experiments immobilized IpgB2 clearly interacts with dominant negative Myc-tagged RhoA (Figure 22 A). With this successful positive control we started to analyze the potential interactions with BBS4 and TRAPPC6A.

BBS4 is one of eight proteins, forming the core of a multiprotein complex called BBSome, which is located to non-membranous centriolar satellites and to the primary cilium (Nachury *et al.*, 2007, Loktev *et al.*, 2008). The 52 kDa protein was first described as one of 12 potential mutants, causing the Bardet-Biedl syndrome, a ciliopathic human genetic disorder (Mykytyn *et al*., 2001).

The second protein TRAPPC6A is one, of the six component TRAPP I complex. This complex is involved in vesicular transport at the endoplasmic reticulum (Sacher *et al*., 2008).

In our pull down assays using immobilized IpgB2, we were not able to validate the interaction with TRPPC6A (Figure 22 A). In case of BBS4 we could adjust the experimental conditions, and detect a clear and reproducible interaction between IpgB2 and BBS4 (Figure 22 B).

This experiment demonstrates perfectly, how important it is to modify the experimental setup when an interaction appears negative in a first attempt. Subcloning BBS4 into a protein expression vector, was crucial for showing the IpgB2 BBS4 interaction.

Since nothing is known about an interaction between IpgB2 or any other virulence factor and BBS4, the question rises, how does *Shigella* benefit from targeting BBS4? We already know, that BBS4 as part of the BBSome localizes at the primary cilium. These organelles are found in a broad range of vertebrate cells and are involved in many signaling events, like the wnt signaling or the hedgehog signaling pathway (Gerdes *et al.*, 2009). Furthermore, it was reported that depletion of BBS4 in mice, does not affect the formation cilia (Mykytyn *et al.*, 2004), but might play a role in the intraflagellar transport (IFT) (Wei *et al.*, 2012). Primary cilia are typical for the G_0 phase and are disassembled in all other phases of the cell cycle (Kim *et al.*, 2011). Additionally, BBS4 is a component of centriolar satellites (Loktev *et al.*, 2008). These structures are required for primary cilium formation but may also serve physical checkpoint function since they contain CDK1 and cylinB2 (Spalluto *et al.*, 2013).

But why should IpgB2 target BBS4? One potential connection is the small GTPase RhoA, which was found to be substrate to IpgB2 (Klink *et al*., 2010), involved in

cilia formation (Pan *et al*., 2007) and significantly increased in BBS4 knockout cells (Hernandez-Hernandez *et al.*, 2013). RhoA possibly connects both proteins.
A first experiment to test the influence of IpgB2 in the cilia context might be co-localization studies between the virulence factor, BBS4 and cilia, to see if BBS4 recruitment or cilia formation is altered or even impaired. A current master thesis (Eric Meinhardt) is following this interaction.

3.4 The SifA – Rab9 interaction

The Salmonella virulence factors SifA and SifB were among the first described WxxxE family members (Alto *et al.*, 2006). SifA seems to be absolutely necessary for the formation of Salmonella induced filaments (Stein *et al.*, 1996). It is also known that SifA binds to a host protein termed SifA kinesin interacting protein (SKIP), which is capable to connect to the plus-end directed microtubule motor kinesin. Disturbing this interaction results in impaired tubulation (Boucrot *et al*., 2005). Together with a second effector protein, SseJ, SifA also contributes in the maintenance of the phagosome (Ruiz-Albert *et al*., 2002). In contrast to other WxxxE proteins, SifA and SifB do not appear to affect actin dynamics (Bulgin *et al*., 2010). This largely agrees with our microscopic SifA overexpression studies. We neither observed large lamellipodia or massive filopodia formation, nor did we observe an increase in stress fibers or adhesions. Only the cell shape was slightly altered compared with control transfected cells, as it was more rounded and appeared more widely spread (Figure 35). Up to now there is only one report by Ohlson and colleagues, postulating that SifA may function as a GEF of RhoA. However, they were not able to show GEF activity for purified SifA and the pull down experiments, (with an overexposed load-control, no supernatant-control and a weak signal in the pull down lane), was not very convincing (Ohlson *et al.*, 2008). Consequently, in our experimental setup, which is quite stringent, we were not able to detect an interaction with RhoA (Figure 24).
Alternative to Rho-GTPases we followed hints that SifA might interact with Rab GTPases. In mammalian cells Rab GTPases are involved in multiple vesicle trafficking pathways. Here they organize transport and recycling by marking different vesicle populations (Zerial *et al.*, 2001). In the context of *Salmonella* infection, Rab4 and Rab5 were reported to be recruited to the early phagosome in the

first 60 min after infection, indicative of interactions with early endosomes (Smith *et al.*, 2005). Subsequently, Rab7 and Rab9, late endosomal markers, are recruited to the SCV and were reported to be essential for the Sif formation (Smith *et al.*, 2007, Brumell *et al.*, 2007). In this context, it is remarkable that in cells SKIP interacts with Rab9 and this interaction is disturbed by SifA (Jackson *et al.*, 2008).

In our study, we were able to detect a direct interaction between SifA and Rab9a in pull down experiments. Additionally, a weak interaction with Rab11a was observed, however, not consistent enough and thus requires further experiments. Other Rab GTPases, like Rab4a, Rab5a and Rab7a displayed no direct interactions under these conditions (Figure 25).

In contrast to SifA, only little is known about SifB. SifB is translocated via the second *Salmonella* T3SS and localizes to the SCV, but depletion of the effector protein has no noticeable effect on the SCV integrity or Sif formation (Freeman *et al*., 2003). On these grounds, the authors speculate about a function of SifB in later stages, or special situations of the infection. Interestingly, from our Y2H screen we have a potential interaction with the Rap-GTPase interactor RADIL that is in play in cell adhesion. This hit is currently followed in an independent work together with two other potential hits.

For SifB in our Y2H screen the most significant hit was Cdc42. Thus, we tested the virulence factor against a selection of Rho- and Rab GTPases in parallel to SifA. However, we never got a positive interaction (Figure 24 and Figure 25). At this point we have to consider that for the Y2H screen with SifB and in the biochemical experiments only a truncated version, lacking the first 98 aa, was used. Revisiting SifB interactions with the full length protein is planned for the future.

3.5 The interaction between Map and human RHPN1

The virulence factor Map, present in the A/E group of pathogenic bacteria, is also a member of the WxxxE effector protein family (Alto *et al*., 2006) and was reported to function as a Cdc42 GEF mimic (Huang *et al*., 2009). Upon intimate contact between EPEC and the host cell, Map is translocated via the T3SS and targets Cdc42 in order to remodel the GTPase signaling (Huang *et al.*, 2009, Kenny *et al.*, 2002, Alto *et al.*, 2006). To accomplish the alteration of Cdc42 signaling, the interaction with a second

host protein, the EBP50, via the Map PDZ-domain binding motif, is mandatory (Berger *et al.*, 2009, Simpson *et al.*, 2006).

Targeting Cdc42 by Map results in the formation of Cdc42 dependent filopodia at the infection side (Berger *et al.*, 2009, Kenny *et al.*, 2002, Orchard *et al.*, 2012b) and also ectopic Map expression provokes filopodia formation (Bulgin *et al.*, 2010). In our experiments we observed filopodia formation, too. More frequently, however, we recognized a wide spread cell shape, with protruding lamellipodia (Figure 36). This effect is most likely due to Cdc42 induced Rac1 activation, because of signaling crosstalk between these GTPases (Hall, 1998).

The two most significant hits from the Y2H screen for Map were the EBP50 paralog NHERF2 and rhophilin1 (RHPN1). First, we tested our recombinant Map in pull down assays against Cdc42 and were able to reproduce this direct interaction (Figure 27). Subsequently, we started to examine the predicted interaction partner human RHPN1.

The human RHPN1 was identified as an interactor of GTP bound RhoA (Watanabe *et al*., 1996). Later, Peck and colleagues characterized a structurally related protein (40 % aa similarity), RHPN2, in humans. Both proteins are thought to act as scaffolds downstream of RhoA. Contrary to Watanabe, Peck reported RhoA binding in the GTP as well as in the GDP bound conformation (Peck *et al*., 2002). In our pull down assays, we were able to support Peck by detecting interactions of RHPN1 together with immobilized CA and DN RhoA. Moreover we observed strong interactions with CA Rac1 as well as weak interactions between RHPN1 and DN Rac1 or CA Cdc42 (Figure 28 A+B). Unfortunately, we were not able to detect any interactions in the vise versa approach, using immobilized RHPN1 (Figure 28 C). Possibly the GST tag used in these experiments somehow blocks the N-terminal HR1 domain and prevents an interaction with the GTPases. Allternatively, full length rhophilin might not be properly folded. Therefore we will repeat these experiments with GST-HR1. To address this point, recloning is considered. To test, if RhoB might be a further candidate to interact with human RHPN1, we cloned WT and CA RhoB. Interestingly RhoB binding to human RHPN2 was already described (Peck *et al*., 2002).

The ectopic expression of RHPN2 was described to cause a loss of stress fibers, while RHPN1 expression had no noticeable effect on the cytoskeleton (Peck *et al.*, 2002). Here we also observed no effect of RHPN1 upon transfection (Figure 36) and

indeed, the expression of human RHPN2 resulted in a decrease of stress fibers, however, not in a total loss.

Both proteins share the same domain composition: A N-terminal HR1 domain, which mediates the RhoA binding, a C-terminal PDZ domain, known to be involved in the formation of protein complexes (Jelen *et al*., 2003) and finally a central Bro1 domain, named after its homolog from budding yeast (Nickas *et al.*, 1996). The PDZ domain was promising, since Map contains a PDZ binding motive, too (Alto *et al.*, 2006). In pull down assay we were able to prove a direct interaction between Map and human RHPN1. The specificity of this interaction was emphasized by the fact that Map was shown to interact with mouse RHPN1, but not with human RHPN2 (Figure 29). Subsequently, we mapped the interaction surface. To do so, we designed constructs of the human RHPN1 domains HR1, PDZ and Bro1 and utilized them in pull down assays to probe for Map and vice versa. Western blot analysis revealed a clear interaction between the recombinant protein and the PDZ domain (Figure 30 A). Surprisingly, when running pull down assays with other PDZ domains, including human RHPN2 and mouse RHPN1 PDZ, we detected no interactions, although the full length mouse RHPN1 interacted with Map (Figure 30 B). The reasons for this inconsistency may be found in the design of the PDZ construct, although bioinformatical protein domain predictions were performed before. Another problem could be the position of the GFP tag, a change from the N- to the C-terminus might lead to different results.

To support our results concerning the Map human RHPN1 interaction, we decided to perform co-IPs (Figure 32). We co-transfected GFP tagged RHPN1 and Myc tagged Map in B16 cells and performed the precipitation by using anti GFP or anti Myc antibodies. We used pre-conjugated anti Myc-bead material, which lead to repeatedly positive results. Since Myc tagged Map migrates at the same height as the antibody light chain, resulting in cross reactions which made it hard to discriminate between Map and artificial signal. To address this problem, one could think about several approaches. For example the use of a secondary antibody like TrueBlot® from Rockland Immunochemicals, specific against native antibodies. Furthermore a change to native conditions may prevent antibody segregation. Finally it should be considered to (ex)change the protein tags which would result in a bigger Map protein, not masked by cross reactions. Nonetheless, we are convinced that our

interaction data unambiguously demonstrate a specific interaction between the PDZ-domain of rhophilin1 and bacterial Map.

Next, we performed co-localization studies between Map and RHPN1. These (Figure 37) revealed an almost complete congruency of both proteins. In most of the cases small globular structures were observed, either close to the nucleus or distributed throughout the whole cytoplasm. After single transfection of human RHPN1 or Map, those dots were observed, too, but by far not that numerous. This result made us speculating about the compartment where both proteins are recruited to. Our first thought was mitochondria, since Map was reported to locate at mitochondria during late stages of EPEC infection (Kenny *et al.*, 2000). Therefore we performed MitoTracker® staining in RHPN or Map transfected cells (Figure 39). Interestingly the mitochondria staining revealed no co-localization with Map, suggesting, Map is not dominantly targeted to these organelles but probably at some point during infection, where further bacterial virulence factors might contribute to mitochondria targeting. Unfortunately, the simultaneous use of co-transfections and MitoTracker® did not work, because the combination of our Myc antibody together with the blue labeled secondary antibody produced such a high background signal that it was impossible to discriminate between transfected and untransfected cells. Unexpected to us, however, we observed a partial localization of human RHPN1 or its PDZ domain to mitochondria. The other tested RHPNs showed no correlation with MitoTracker®. The other putative compartment where RHPN1 and Map could meet are vesicles. We hypothesized this based on the dot like structure and, on the other hand, because it was reported that human RHPN2 is found at late endosomes (Steuve *et al*., 2006), although we scarcely observed clear localizations. Beside the full length proteins, already the RHPN1 PDZ domain is sufficient to induce a strong recruitment of Map. In this case, however no small dots were seen, but a ring like structure surrounding the nucleus, suggesting the cell endomembrane system such as the endoplasmic reticulum as interaction surface instead of mitochondria.

The fact, that RHPN1 contains a Bro1 domain lead us to the theory that RHPN1 might also interact with the endosomal sorting complex (ESCRT) required for transport. The ESCRT machinery was first described in yeast, for its crucial role in sorting membrane proteins into lysosome like vacuoles. In humans more than 20 proteins interact to form three different complexes (ESCRT I-III). They fulfill functions in endosomal sorting of ubiquitinated receptors and mediate membrane

curvature and fission processes, such as cytokinetic abscission or in the biogenesis of multivesicular bodies (MVB) (Rusten *et al.*, 2012, Jouvenet, 2012). In yeast the Bro1 protein was described to interact directly with the ESCRT component Snf7 and function with, or downstream of ESCRT III in the MVB pathway (Odorizzi *et al.*, 2003). In mammals the close related Bro homolog is called Alix (Missotten *et al.*, 1999, Vito *et al.*, 1999). We therefore suggest that Map targets RHPN1 to subsequent recruit the ESCRT III complex towards the infection side. Hijacking of the ESCRT machinery has been reported to be important for the budding of different enveloped viruses. The human parainfluenza virus HPIV1, a prominent respiratory pathogen, encodes a set of accessory C proteins, which are involved in the regulation of the virus replication rate, suppression of the IFN response and suppression of apoptosis. Furthermore, these proteins bind to Alix, a Bro1 domain containing protein, capable of recruiting the ESCRT subunit CHMP4b (Boonyaratanakornkit *et al.*, 2013). The authors suggest, that by targeting CHMP4b via Alix, the C proteins are recruited to a specific side at intracellular membranes, where they can promote virus budding. Studies on the retrovirus HIV and ESCRT III have an even longer history and the first connection between virus budding and ESCRT machinery was drawn in 2003. A few molecules of the virus protein Gag attach at one point of the membrane and accumulate more and more Gag protein. Simultaneous Alix is recruited towards the cytosolic side of Gag and the viral envelop starts to form. When the envelop is almost completed, ESCRT and the associated protein Vsp4 are recruited and fission take place. The whole procedure takes only 10 min (Strack *et al.*, 2003, Pires *et al.*, 2009, Morita *et al.*, 2011, Jouvenet, 2012). Finally, in another study the positive effect of Alix on virus was lead back to its Bro-domain (Popov *et al.*, 2009). More importantly, the Bro domain of Alix could be replaced by that of rhophilin with the same efficiency (Popov *et al.*, 2009). From this we delineate that RHPN1 may serve as alternative ESCRT adapter under specific conditions. Interestingly ESCRT is not only associated with membrane sorting but also with autophagy (Rusten *et al.*, 2009). Since autophagy is an important defense mechanism against pathogens (Mostowy *et al.*, 2011) this may be the cause of recruitment.

To see if there is any connection between human RHPN1 and ESCRT, we tested two different antibodies against CHMP4b, the ESCRT III subunit that is bound by the Bro1 domain containing protein Alix. On the one hand, we tried to perform pull down assay with endogenous CHMP4b against immobilized human RHPN1.

Unfortunately, both antibodies we used produced so many cross reactions in the western blot detection, that we were not able to identify CHMP4b (Figure 31). On the other hand, we used one of the antibodies in immunofluorescence microscopy of Hela cells transfected with human RHPN1. In this case the antibody performed well, but no co-localization was observed (Figure 44). Although we failed to show an interaction between RHPN1 and the ESCRT machinery, it still may exist. It could possibly be shown for example by the use of ectopic expressed CHMP4b instead of the endogenous. Alternatively, RHPN1 might only assemble with ESCRT-subunits under special conditions such as during bacterial attachment or during escape from autophagy. Further studies will shed light on this question. In this context, it is tempting to speculate on the potentially internalized dead bacteria observed after ectopic RHPN1 expression. However, more data are needed to confirm such a connection.

Together, the current thesis has provided evidence for several interactions of virulence factors with host cell proteins. The interaction between Map and human RHPN1 was further characterized. We mapped the interaction surface between both proteins and tried to approximate a physiologic function of RHPN1 in cells and of this interaction during infection.

To do so, we turned to run EPEC infection assays. In a first experiment we checked if the ectopic expression of any RHPN somehow affects the formation of pedestals at the infection site. Analysis of pedestal formation revealed that indeed the transfections of Map contributed positively to pedestal formation. Human RHPN1 and RHPN2 expression showed a repressive influence (Figure 41). The Map dependent growth of pedestals suggests that ectopically expressed Map amplifies the function of the endogenous protein which was translocated via the EPEC T3SS. The interpretation of the RHPN result is more difficult because human RHPN1 as well as human RHPN2 had a repressive effect and mouse RHPN1 had not. It has to be noted, that mRHPN1 should be tested in murine cells since it may be nonfunctional in our experimental background. Nevertheless, microscopic analysis of these infection assays revealed a further, unique, effect of human RHPN1.

Transfections of human RHPN1 resulted in rod shaped accumulations of our protein in the GFP channel, reminiscent of bacteria (Figure 40) accumulating the GFP tagged protein. Gentamycin protection assay (Figure 42) however revealed no increased numbers of living intracellular bacteria. Given the connection between RHPN1 and

autophagy, we analyzed if these green bacteria maybe dead and intracellular, by using inside out staining. These assays revealed co-localizations with extra and intracellular LPS positive spots. From the result we can conclude that we are indeed looking at active autophagy. The localization is a clear hint that human RHPN1 participates in EPEC infection (Figure 43). Since we could not observe any protein accumulations in the first 60 min post infection, human RHPN1 seems to take part only in later stages of the infection. It will be interesting to follow this trail to learn more about the highly regulated mechanisms behind an EPEC infection, especially with respect to the exact role of RHPN1 during this process.

3.6 Collaborative projects

During the accruement of this thesis, I participated in two collaborative projects, with our cooperation partners on related topics.

The first one was the characterization of a stable, viable mouse fibroblast cell line, genetically depleted for Rac1 (Steffen *et al*., 2013). Those cells, also lacking any detectable Rac2 and Rac3 activity, were deficient in the formation of lamellipodia and strongly affected in migration. This was shown in 2D wound healing assays and chemotaxis assays. The formation of filopodia, spreading and of focal complex assembly were assessed. Cell spreading was accomplished by filopodia formation and subsequent flow of membrane and cytoplasm in the space between them. Because earlier attempts to generate a viable genetic knock out cell line failed, it was thought that Rac1 participates essentially in cell proliferation (Vidali *et al.*, 2006, Guo *et al.*, 2006). Our cells show that this link is not essential but can be bypassed. Yet, in large parts we could confirm the current knowledge. I am sure, that with this new viable Rac1 knock out cell line, we got a strong tool to gain deeper insides into the broad functions of the important Rac1 GTPase. For infection research, it will be interesting to revisit the role of Rac for bacterial pathogenesis. Also in the case of EPEC and given the strong interaction of RHPN1 with CA Rac1, analyses with the help of these cells will be very interesting.

Within the framework of this project, I was involved in the detection of Rac2 and Rac3 levels. Furthermore I contributed in the analysis of the focal contact formation. Finally the effect of bacterial Rac1 GEFs (IpgB1) in these cells was tested.

The second collaborative project was in cooperation with Sonja Blasche from the DKFZ in Heidelberg. It was about the identification of novel targets of EHEC effector proteins with focus on Tir. Based on a Y2H screen, six novel and two already published EPEC-Tir interactors were identified and subsequently confirmed. It was my part to test the new interactors in infection assays and to perform immunofluorescence microscopy for their recruitment to the infection site. Beside the positive controls BAIAP1 and -2, which were strongly recruited, we observed the serin/threonine kinase 16 (STK16) and hippocalcin-like1 (HPCAL1) to be targeted towards the infection side. In this case STK16 is interesting, because it is known that Tir has to be phosphorylated before actin reorganization and pedestal formation is started (Campellone, 2010). These results will be submitted in due time (Blasche *et al*., in prep.)

3.7 Concluding remarks

This work provides new insides into host pathogen interaction on the protein level. We discovered human RHPN1 as a novel target of the A/E group virulence factor Map. Furthermore we showed considerable evidences that the *Shigella* effector IpgB2 is able to interact with the human protein BBS4 and finally the *Salmonella* virulence factor SifA was shown to bind the small GTPase Rab9 in pull down assays. Based on a Y2H screening, the poorly defined RhoA-interactor RHPN1 and the translocated virulence factor Map, with the ability to provoke cytoskeletal reorganizations, were found to interact with each other. By utilizing biochemical and microscopic techniques we were able to confirm this finding. Although the interaction is verified, its biological function still remains elusive and needs further studies. To get a better impression of cellular localization of the RHPN1 Map interaction, it will be instrumental to use confocal video microscopy. Also a co-staining with markers for different vesicle populations should be considered, to see if there are compartments, other than mitochondria, where the interaction takes place. An infection assay using a *ΔMap* EPEC mutant will uncover if the observe RHPN1 recruitment is indeed Map dependent. In vise versa experiment with RHPN1 knock down cells we will reveal defects in establishment of the infection. In case RHPN1 is involved in the defense mechanism of autophagy, infection may even be enhanced when RHPN1 is absent.

BBS4 is known to be involved in the formation of the primary cilium and in the recycling of different receptors on its surface. Since the cilium is almost ubiquitous in eukaryotic cells, it is imaginable that this compartment is a target of virulence factors. There is nothing known about any interference of pathogens with pathways like hedgehog or wnt, whose receptors are organized by BBS4, but it might be an interesting topic of further studies. However, for the case that centriolar satellites are sites of cell cycle control (Staples *et al.*, 2012, Kim *et al.*, 2004) it can be speculated that *Shigella* targets BBS4 to affect the host´s cell division cycle. This has been shown before (Iwai *et al.*, 2007).

The interaction between SifA and Rab9 was only shown in one directional pull down assays. So it is mandatory to spend more effort to verify this interaction. However, both proteins were reported to be involved in the formation and maintenance of Sifs. This circumstance makes an interaction plausible. Nevertheless, at least co-localization studies should be performed to confirm a relation between both proteins in time and space.

Even if the insights reported here, are just small pieces of a huge puzzle, they may contribute to the growing pool of knowledge on infectious diseases.

4 Material

4.1 Chemicals

If not further mentioned, all chemicals used in this thesis, were purchased from AppliChem, Fermentas, Invitrogen, Machery-Nagel, Merck, Millipore, New England Biolabs, Quiagen, Roche, Roth, Sigma-Aldrich, Thermo Fischer Scientific and not listed in detail. Water used in this study was purified and distilled with a Milli-Q Advantage A10 System (Merck Millipore Billerica). If not further specified, solutions were prepared in H_2O_{dd}.

4.2 Cell culture reagents and plasticware

Cell culture media and supplements were purchased, if not further mentioned from Gibco, PAA and Sigma-Aldrich. Plasticware was ordered from Greiner, Sarstedt, Techno Plastic Products and Thermo Fischer Scientific.

4.3 Bacterial strains

The following bacterial strains were used in this study.

Table 2 List of bacterial strains used in this study

Bacterial strain	Function	Source
Escherichia coli TG2	cloning	Stratagene
Escherichia coli DH5α	cloning	Invitrogen
Escherichia coli DB3.1	gateway cloning	Invitrogen
Escherichia coli BL21	protein expression	Invitrogen
Escherichia coli C600	infection assays	Stratagene
EPEC E2348/69	infection assays	Iguchy A. 2009

4.4 Cell lines

The following cell lines were used in this study. For medium (see 5.2.1)

Table 3 List of mammalian cell lines used in this study

Cell line	Organism	Type	Function	Medium
B16-F1	Mm	melanoma, skin	protein expression	1
Hela	Hs	cervical cancer	microscopy	2
Cos7	*C. aethiops*	kidney	microscopy, infection assays	3

4.5 Plasmids

Plasmids used in this study are listed below (intermediate clones not shown)

Table 4 List of plasmids used in this study

Plasmid	Number	Function	Source
pGBT9-GW	SAR 17	intermediate vector Y2H	DKFZ
pDONR-211	SAR 18	final vector Y2H	Invitrogen
pEGFP C1	SAR 34	GFP-tagged expression vector	Clontech
pEGFP C1-RhoG V12	SAR 35		this group
pEGFP C1-IpgB1	SAR 36		this group
pDONR211-GW-IpgB1-W76A	SAR 37	final clone for Y2H	this study
pDONR211-GW-IpgB2-ΔmemB-W62A	SAR 38	final clone for Y2H	this study
pDONR211-GW-IpgB2-W62A	SAR 39	final clone for Y2H	this study
pDONR211-GW-IpgB2-ΔmemB	SAR 40	final clone for Y2H	this study
pDONR211-GW-SifB-Δext 99-336	SAR 41	final clone for Y2H	this study
pDONR211-GW-EspM2-Citero	SAR 42	final clone for Y2H	this study
pDONR211-GW-IpgB1	SAR 43	final clone for Y2H	this study
pDONR211-GW-EspT-EPEC	SAR 44	final clone for Y2H	this study
pDONR211-GW-Map	SAR 45	final clone for Y2H	this study
pDONR211-GW-SifA-FL	SAR 46	final clone for Y2H	this study
pDONR211-GW-IpgB1-ΔmemB	SAR 47	final clone for Y2H	this study
pDONR211-GW-SifA-Δext	SAR 48	final clone for Y2H	this study
pDONR211-GW-EspT-Citero	SAR 49	final clone for Y2H	this study
pDONR211-GW-IpgB1-ΔmemB-W76A	SAR 50	final clone for Y2H	this study
pDONR211-GW-IpgB2	SAR 51	final clone for Y2H	this study

pRK5-Rac1 L61-Myc	SAR 54	pull down; microscopy	this group
pcDNA3-RhoGV12-3Myc	SAR 55	pull down; microscopy	this group
pDONR211-GW-SopE	SAR 68	final clone for Y2H	this study
pDONR211-GW-SopE FL	SAR 69	final clone for Y2H	this study
pDONR211-GW-SopE2	SAR 70	final clone for Y2H	this study
pDONR211-GW-SopE2 FL	SAR 71	final clone for Y2H	this study
pDONR211-GW-SopB FL	SAR 72	final clone for Y2H	this study
pDONR211-GW-SopB N 1-351	SAR 73	final clone for Y2H	this study
pDONR211-GW-SopB C 352-562	SAR 74	final clone for Y2H	this study
pDONR211-GW-IpGD	SAR 75	final clone for Y2H	this study
pDONR211-GW-IpGB1 H136A	SAR 76	final clone for Y2H	this study
pDONR211-GW-IpGB2 H121A	SAR 77	final clone for Y2H	this study
pEGFP-C2-Arf6Q67L	SAR 88	pull down; microscopy	this group
pGEX-6P-1	SAR 90	protein expression vector	Amersham
pGEX-6P-3	SAR 91	protein expression vector	Amersham
pEGFP-C1-Rac Q61L	SAR 92	pull down; microscopy	this study
pEGFP-C2	SAR 96	GFP-tagged expression vector	Clontech
pEGFP-C3	SAR 97	GFP-tagged expression vector	Clontech
pEGFP-C1-SifB-Δext 99-336	SAR 98	pull down; microscopy	this study
pEGFP-C1-EspT-EPEC	SAR 99	pull down; microscopy	this study
pEGFP-C1-Map	SAR 100	pull down; microscopy	this study
pEGFP-C1-SifA-FL	SAR 101	pull down; microscopy	this study
pEGFP-C1-SifA-Δext	SAR 102	pull down; microscopy	this study
pEGFP-C1-EspT-Citero	SAR 103	pull down; microscopy	this study
pEGFP-C1-SopB FL	SAR 104	pull down; microscopy	this study
pEGFP-C1-SopB N 1-351	SAR 105	pull down; microscopy	this study
pEGFP-C1-SopB C 352-562	SAR 106	pull down; microscopy	this study
pEGFP-C1-IpGD	SAR 107	pull down; microscopy	this study
pEGFP-C1-hum RHPN1	SAR 108	pull down; microscopy	this study
pEGFP-C3-hum RHPN2	SAR 109	pull down; microscopy	this study
pGEX-6P-3-hum RHPN1	SAR 111	protein expression	this study
pGEX-6P-1-hum RHPN2	SAR 112	protein expression	this study
pGEX-6P-1-EspT-EPEC	SAR 114	protein expression	this study
pGEX-6P-1-EspT-Citero	SAR 115	protein expression	this study
pJET1.2	SAR 116	cloning vector	Fermentas

pQE-30	SAR 117	protein expression vector	Qiagen
pQE-30-SifB-Δext 99-336	SAR 118	protein expression	this study
pQE-30-SifA-FL	SAR 119	protein expression	this study
pQE-30-SifA-d ext	SAR 120	protein expression	this study
pEGFP-N1-Arf6-WT	SAR 121	pull down; microscopy	P. Chavrier
pEGFP-N1-Arf6-T44N	SAR 122	pull down; microscopy	P. Chavrier
pEGFP-N1-Arf6-Q67L	SAR 123	pull down; microscopy	P. Chavrier
pEGFP-N1-Arf6-T157N	SAR 124	pull down; microscopy	P. Chavrier
pEGFP-N1-Arf6-T27N	SAR 125	pull down; microscopy	P. Chavrier
pGEX-6P-1-SifB-Δext 99-336	SAR 129	protein expression	this study
pGEX-6P-1-Map	SAR 130	protein expression	this study
pGEX-6P-1-SifA FL	SAR 131	protein expression	this study
pGEX-6P-1-SifA-Δext	SAR 132	protein expression	this study
pGEX-6P-1-SopB-FL	SAR 133	protein expression	this study
pGEX-6P-1-SopB N 1-351	SAR 134	protein expression	this study
pGEX-6P-1-SopB C 352-562	SAR 135	protein expression	this study
pGEX-6P-1-IpgD	SAR 136	protein expression	this study
pRK5-Cdc42-WT-myc (iso1)	SAR 137	pull down; microscopy	this group
pRK5-Rac1-WT-myc (iso1b)	SAR 138	pull down; microscopy	this group
pEGFP-C1-IpgB1-W76A	SAR 139	pull down; microscopy	this study
pEGFP-C1-IpgB2-ΔmemB-W62A	SAR 140	pull down; microscopy	this study
pEGFP-C1-IpgB2-W62A	SAR 141	pull down; microscopy	this study
pEGFP-C1-IpgB2-ΔmemB	SAR 142	pull down; microscopy	this study
pEGFP-C1-EspM2-Citero	SAR 143	pull down; microscopy	this study
pEGFP-C1-IpgB1	SAR 144	pull down; microscopy	this study
pEGFP-C1-IpgB1-ΔmemB	SAR 145	pull down; microscopy	this study
pEGFP-C1-IpgB1-ΔmemB-W76A	SAR 146	pull down; microscopy	this study
pEGFP-C1-IpgB2	SAR 147	pull down; microscopy	this study
pEGFP-C1-SopE catalytic domain	SAR 148	pull down; microscopy	this study
pEGFP-C1-SopE FL	SAR 149	pull down; microscopy	this study
pEGFP-C1-SopE2 catalytic domain	SAR 150	pull down; microscopy	this study
pEGFP-C1-SopE2 FL	SAR 151	pull down; microscopy	this study
pEGFP-C1-IpGB1 H136A	SAR 152	pull down; microscopy	this study
pEGFP-C1-IpGB2 H121A	SAR 153	pull down; microscopy	this study
pETM-41-IpgB2	SAR 161	protein expression	Sally (BS)

pETM-41-EspT (EHEC)	SAR 162	protein expression	this group
pETM-41-EspT (Citero)	SAR 163	protein expression	this group
pETM-41-Map	SAR 164	protein expression	this group
pETM-41	SAR 165	protein expression vector	EMBL
pRK5-Cdc42-Q61L-myc	SAR 166	pull down; microscopy	L. Machesky
pRK5-Cdc42-T17N-myc	SAR 167	pull down; microscopy	L. Machesky
pRK5-Rac1-Q61L-myc	SAR 168	pull down; microscopy	L. Machesky
pRK5-Rac1-T17N-myc	SAR 169	pull down; microscopy	L. Machesky
pRK5-RhoA-G14V-myc	SAR 170	pull down; microscopy	L. Machesky
pRK5-RhoA-T19N-myc	SAR 171	pull down; microscopy	L. Machesky
pEGFP-C1-hum RHPN1 Bro	SAR 172	pull down; microscopy	this study
pEGFP-C1-hum RHPN1 HR1	SAR 173	pull down; microscopy	this study
pEGFP-C1-hum RHPN1 PDZ	SAR 174	pull down; microscopy	this study
pEGFP-C1-ATP6V1E1	SAR 176	pull down; microscopy	this study
pETM-41-SifB Δext	SAR 178	protein expression	this group
pETM-41-SifA Δext	SAR 179	protein expression	this group
pmCherry-C1	SAR 180	RFP-tagged expression vector	Clontech
pmCherry-C1-Map	SAR 181	pull down; microscopy	this study
pGEX-2T-RhoA WT	SAR 182	protein expression	this group
pDONR211-GW-SseJ	SAR 184	final clone for Y2H	this study
pETM41-IpgB1	SAR 189	protein expression	this group
pETM41-SopB	SAR 190	protein expression	this group
pETM41-RhoAT17N	SAR 192	protein expression	this group
pEGFP-C1-humRHPN2-PDZ	SAR 193	pull down; microscopy	this study
pEGFP-C2-mRhoG wt	SAR 202	pull down; microscopy	this group
pEGFP-C1-hRhoG G12V	SAR 203	pull down; microscopy	this group
pEGFP-C1-hRhoG T17N	SAR 204	pull down; microscopy	this group
pEGFP-C1-RADIL-PDZ	SAR 209	pull down; microscopy	this study
pEGFP-C1-mus RHPN1-PDZ	SAR 210	pull down; microscopy	this study
pEGFP-C1-mus RHPN2-PDZ	SAR 211	pull down; microscopy	this study
pRK5-myc(new)-Map	SAR 215	pull down; microscopy	this study
pRK5-myc(new)-SifA	SAR 216	pull down; microscopy	this study
pRK5-myc(new)-EspT Citero	SAR 217	pull down; microscopy	this study
pRK5-myc(new)-IpgB2	SAR 218	pull down; microscopy	this study
pEGFP-C1-mus RHPN1	SAR 220	pull down; microscopy	this study

4.6 Oligonucleotides

Plasmids were generated using oligonucleotides listed below. Oligonucleotides were purchased from Eurofins MWG GmbH.

Table 5 List of oligonucleotides used in this study

Designation	Sequence 5' - 3'
Generation of GFP or GST tagged human RHPN1	
SAR-P3	AAGGATCCATGATCTTAGAGGAGAGGCCGG
SAR-P4	TTGAATTCTCATGGCCATCCTGGGTGCT
Generation of GFP or GST tagged human RHPN2	
SAR-P7	AACTCGAGATGACTGACGCACTGTTG
SAR-P8	TTCTCGAGTTAGTACCAAGAGCTGTCTGAG
Generation of GFP or GST tagged mouse RHPN1	
SAR-P5	ATGGATCCATGATACTTGAGGAGAGGCC
SAR-P34	TTGAATTCTCATCCTCGTGCTCGTGCT
Inverse PCR to delete an intron from mouse RHPN1	
SAR-P37	TCCGCTGGCCTGAAGGAGGG
SAR-P38	CTCAGCCTGACCCCCTGGAA
Site directed mutagenesis to solve a point mutation in mouse RHPN1	
SAR-P39	GGCTGAGTCCGCTGGCCTGAAGGAGGGCGACTACATCGTG
SAR-P40	CCAGCGGACTCAGCCTGACCCCCTGGGACGACAGCAGCGA
Generation of GFP tagged human RHPN1 BRO domain	
SAR-P11	ATGCAGGATCCATGGTCACTGTCCCTATGATCCC
SAR-P12	TGCATGTCGACACGCCACCGGTTCTTAGC
Generation of GFP tagged human RHPN1 HR1 domain	
SAR-P13	ATGCAGGATCCATGGGCTGTGACTCTCTGACGC
SAR-P14	TGCTTGTCGACATGCCGGCCAGGGTCC
Generation of GFP tagged human RHPN1 PDZ domain	
SAR-P15	ATCGAGGATCCATGGTGGGGCCCGTGCATCTG
SAR-P16	TGCATGTCGACCCGCCTCTCCCGCAGC
Generation of GFP tagged human RHPN2 PDZ domain	
SAR-P25	ATCCAAGATCTATGCCTCGAAGTATCCGCTT
SAR-P26	TGCATGTCGACCACAACTTTCATCTCGATC

Generation of His-MBP tagged human RHPN2 PDZ domain

SAR-P31	GTGCACCATGGTGCCTCGAAGTATCCGCTT
SAR-P32	TGCATGCGGCCGCCACAACTTTCATCTCGATC

4.7 Antibodies

The antibodies, antisera and fluorescent dyes used in this study are listed below. Abbreviations in this table: mouse (m), rabbit (r), goat (g), monoclonal (mc), polyclonal (pc), western blot (WB), immunoprecipitation (IP) and immunofluorescence microscopy (IF).

Table 6 List of antibodies and fluorescent dyes used in this study

Designation	Source	Application	Reference
primary antibodies			
α-CHMP4B	r/pc	WB (1:1000); IF (1:100)	Abcam
α-CHMP4B	r/pc	WB (1:1000); IF (1:100)	Santa Cruz
α-Myc	m/mc	WB (1:1); IF (1:1)	Supernatent, hybridoma clone 9E10
α-*E.coli* J5 LPS	r/pc	IF (1:200)	Novus Biologicals
α-GFP	m/mc	WB (1:1000)	Purified, hybridoma clone 101G4B2
α-mouse-HRP	g/IgG/M	WB (1:2000)	Jackson Immunoresearch Laboratories
α-rabbit-HRP	g/IgG	WB (1:2000)	Jackson Immunoresearch Laboratories
secondary antibodies			
α-mouse-Alexa 594	g/IgG	IF (1:200)	Jackson Immunoresearch Laboratories
α-rabbit-Alexa 594	g/IgG	IF (1:200)	Jackson Immunoresearch Laboratories
α-mouse-Alexa 350	g/IgG	IF (1:50)	Jackson Immunoresearch Laboratories
α-rabbit-Alexa 350	g/IgG	IF (1:50)	Jackson Immunoresearch Laboratories
fluorescent dyes			
phalloidin-Alexa 594	-	IF (1:100)	Invitrogen
phalloidin-Alexa 350	-	IF (1:50)	Invitrogen
DAPI	-	IF (1:50)	Invitrogen
MitoTracker Red	-	IF (500 nM)	Invitrogen

4.8 Kits

Kits used in this study are listed below

Table 7 List of kits used in this study

Designation	Application	Source
NucleoSpin® Extract II	DNA fragment purification	Macherey-Nagel
NucleoBond® PC100	plasmid purification	Macherey-Nagel
GeneJET Plasmid Mini	plasmid purification	Thermo FischerScientific
Anti-c-Myc Immunoprecipitation	immunoprecipitation	Sigma-Aldrich
Gatway® Cloning	DNA cloning	Invitrogen

5 Methods

5.1 Cultivation of bacteria

Bacterial strains were grown in appropriate volume of Luria Bertani broth (LB) medium at 37°C with aeration on a rotating shaking platform. If required, antibiotics were added to LB broth at the respective concentration (kanamycin (kana) 50 µg/ml; ampicillin (amp) 100 µg/ml; chloramphenicol (ch) 34 µg/ml in ethanol).

5.1.1 Preparation of RbCl competent bacteria

In the morning an *E.coli* pre culture was diluted 1:100 into 300 ml LB medium containing 300 µl of 1 M $MgCl_2$. The suspension was incubated on a shaker at 37°C for 2-3 h (until OD_{600} =0.4-0.6). Next the bacteria were pelleted for 5 min by 4500 x*g* at 4°C and resuspended in 120 ml ice cold TFB1 (do not vortex), followed by a 5 min incubation on ice. Then bacteria were pelleted again for 5 min by 4500 x*g* at 4°C and resuspended in 6-12 ml ice cold TFB2, according to the pellet size (do not vortex). After a final incubation of 15-60 min on ice, bacteria were aliquoted in 30-50 µl, shock frosted in liquid N_2 and stored at -80°C.

TFB1		**TBF2**	
30 mM KAc	set pH 5.8 by using HAc sterilize buffer by filtration	10 mM PIPES	set pH 6.5 by using 1 M KOH sterilize buffer by filtration
10 mM $CaCl_2$		75 mM $CaCl_2$ ($2H_2O$)	
50 mM $MnCl_2$		10 mM RbCl	
100 mM RbCl		15 % Glycerol	
15 % Glycerol			

5.1.2 Transformation of chemical competent *E.coli*

To transform bacteria with plasmid DNA, an aliquot of competent bacteria was defrosted on ice. Next, the DNA solution was given to the bacteria in a ratio of 1:100-1:10 and mixed carefully. Now the mixture was incubated 30-60 minutes on ice, followed by a 1 min heat shock at 42°C and a regeneration step with 1 ml LB at

37°C on a shaker for 30-60 minutes. Finally the bacteria were pelleted, resuspended in 100 µl LB and spreaded on LB-agar which contain the appropriate antibiotics.

5.2 Cell culture methods

5.2.1 Media

All media were pre warmed to 37°C before use. Sera were heat inactivated at 56°C for at least 40 min. After preparing the medium, the solution was sterilized by vacuum filtration into a sterile cell culture bottle.

1. B16 DMEM (high gluc)
10% FCS (PAA)
2 mM Glutamin
(+1% PS)

2. Hela MEM (high gluc)
10% FCS (Sigma)
2 mM Glutamin
1% 100mM Natrium-Pyruvat
1% 100x neAS
(+1% PS)

3. Cos7 DMEM (high gluc)
10% FCS (Sigma)
(+1% PS)

5.2.2 Cultivation

Cells were splited every two or three days if the cells covered 90-95% of the dish. In order to split cells, the old medium was removed completely, including 1x washing with PBS. Afterwards an incubation step with an appropriate amount of trypsin (PAA) in the cell culture incubator, to detach the cells from the surface, followed. Now the cell suspension was diluted in fresh growth medium. In case of B16 cells

this diluted cell suspension was directly seeded into a new medium containing tissue culture treated dish (1:10 and 1:20). In case of Hela and Cos7 cells the solution was centrifuged 4 min by 1000 x*g* at RT. Then the pellet was resuspended in fresh media to get rid of all trypsin. Next, those cells were also given into new medium containing dishes (1:3-1:10). For growth, cells were placed into the humid incubator at 37°C with 5 % CO_2.

5.2.3 Freezing and thawing of cells

For long time storage, 3 confluent 10 cm dishes were treated with trypsin and centrifuged as it was described in the previous paragraph. Cells were resuspended in 10 ml 4°C cold growth medium containing 10 % dimethylsulfoxide (DMSO, Sigma) and aliquoted in 1 ml into cryotubes, which where than placed, overnight, into an isopropanol filled Mr. Freeze box (Nalgene) at -80°C. On the next day, the cells were transferred for long time storage into liquid nitrogen.

To thaw cells, a tube was taken from the liquid nitrogen and unfreezed at 37°C in a water bath. Then the cell suspension was transferred into a 15 ml falcon and stepwise diluted in 10 ml fresh growth medium. After that, cells were pelleted, resuspended in fresh medium and seeded into a 10 cm dish.

5.2.4 Transfection of mammalian cells

24 h prior to transfection, the cells were seeded at a higher concentration (1:10 for B16 and 1:3 for Hela and Cos7). At the day of transfection a mixture of pure DNA (ideal concentration around 1 µg/µl) and an appropriate transfection reagent was according to the manufacturer manual made. In case double transfections the amount of each plasmid was reduced by 30 % compared to the single approach. Transfection of B16 was performed with SuperFect® (Quiagen), while Hela and Cos7 cells were transfected with X-tremeGene®HP and X-tremeGene®9 (both Roche) respectively. After 60 minutes incubation, the solution was applied to the cells. Depending on DNA and reagents toxicity, the cells were incubated with the DNA/transfection reagent solution for 6 to 16 h in order to allow DNA uptake and protein expression. In some cases of severe toxicity, a rescue by medium exchange after 2 h was necessary.

5.2.5 Cell preparation for fluorescence microscopy

Hela or Cos7 cells were splited at the evening before transfection in a 1:3 or 1:5 ratio respectively and normally and usually seeded into a 3 cm dish. The next morning, the transfection was made and incubated for 12 to 24 h. After incubation, the cells were again splited (1:1 or 1:2) on pre washed glass coverslips coated with Fibronectin (Roche) (1:40 dilution in PBS incubated for 1 h, then 3 times washed with PBS). Coverslips were usually used with 12 well plates. Within 6 to 12 h cells attach to the glass, spread and were ready for fixation.

5.2.6 Infection assay

The assay was performed as previously described by Lommel (Lommel *et al.*, 2004). Two days before the assay started, Cos7 cells were transfected in a 3 cm dish with the DNA of interest. One day later, the transfected cells were seeded 1:3 on Fibronectin coated coverslips in a 12-well plate, using medium without any antibiotics. Furthermore a LB pre culture of EPEC and *E.coli* C600 as a negative control was started. In the morning of the day of the infection assay, 0.5 ml of the overnight pre cultures were pelleted by 4000 x*g* and two times washed with 1 ml of DMEM. Now the bacteria were resuspended in 25 ml of DMEM and incubated on a shaker at 37°C. Three hours later, the medium was taken off the Cos7 cells and replaced by 1.5 ml of a 1:75 DMEM dilution of the bacteria. Now the cells were placed into an incubator under normal cell culture conditions. After 10, 30, 60 and 180 min cells were fixed by replacing the bacteria solution with pre warmed PBS containing 4 % of PFA for 30 minutes. After fixation, cells were prepared for microscopy (see 5.5). In case of incubation of cells with bacteria longer than 1 h, the medium had to be changed every 60 min in order to prevent bacterial overgrowth.

5.2.7 Gentamicin protection assay

One day before the assay Cos7 cells were seeded 1:2 in 24-well plate using medium without antibiotics. Furthermore a LB pre culture of EPEC and *E.coli* C600 as a negative control was started. In the morning of the day of the gentamicin protection assay, 0.5 ml of the overnight pre cultures were pelleted by 4000 x*g* and two times washed with 1 ml of DMEM. Now the bacteria were resuspended in 16.5 ml of DMEM and incubated on a shaker at 37°C. Three hours later, the medium on the

Cos7 cells was replaced by a 1:100 DMEM dilution of the bacteria, followed by a 3 h incubation under normal cell culture conditions. To prevent bacterial overgrowth, the medium was changed every 60 minutes. After 3 h the cells were washed twice with pre warmed PBS, followed by another 90 min incubation in 1.5 ml medium containing 50 µg/ml gentamicin. After all extracellular bacteria were killed, cells were washed twice with PBS, then incubated for 5 min with 1 ml 0.2 % Triton-X-100 in H_2O. The lysates were collected. Finally every lysate was diluted 1:10, 1:100 and 1:1000 in PBS. 100 µl of each dilution were plated on LB-agar plates without antibiotics and incubated overnight at 37°C. On the next day, the colonies of at least two dilutions were counted. The experiment was performed in triplicates, data processed with Microsoft Excel 2010.

5.3 Molecular biological methods

5.3.1 Yeast two hybrid screen

The Y2H screen was performed and the data evaluated by Manfred Kögl and Frank Schwarz from the Genomics and Proteomics Core Facilities at the German Cancer Research Center in Heidelberg as described in 2007 (Koegl *et al.*, 2007)

5.3.2 Polymerase chain reaction (PCR)

For PCR reactions, Phusion High Fidelity DNA Polymerase (Thermo Fisher) with proof-reading activity was used. Constructs were designed using ApE (Version 2.0.44, University of Utah). Primer annealing temperatures and secondary structures were analyzed with the OligoAnalyzer® web tool from the IDT homepage.

Standard PCR approach:

1 x	HF Phusion buffer
2 pmol	dNTP
2.5 pmol	primer I and II
1 pg	template DNA
1 U	Phusion DNA polymerase
ad. 50 µl	H_2O_{dd}

Standard PCR program:

98°C	30 s	
98°C	10 s	30 x
55-72°C	15 s	
72°C	30 s/1000 bp	
72°C	10 min	
4°C	∞	

5.3.3 Inverse PCR

The inverse PCR was performed like the standard PCR described in the paragraph before, only with primer directed into opposite directions and less polymerization cycles (12-15). Right after the PCR, the DNA was treated with 5 U DpnI for 2 h at 37°C to get rid of the template DNA. The next step was a gel electrophoresis, followed by DNA gel extraction (see 5.3.5). Finally a self-ligation was performed, before the transformation.

5.3.4 Site directed mutagenesis

The site directed mutagenesis was performed as described previous by Liu (Liu *et al.*, 2008).

5.3.5 DNA gel electrophoresis and gel extraction

After PCR or plasmid digestion, the DNA samples were mixed with 5 x loading dye and separated by agarose gel electrophoresis at 100 V 45-60 min. The gel consisted of 1-2 % low EEO agarose (AppliChem) in 1 x TAE buffer (from 50 x stock, AppliChem) and contained 0.5 µg/ml ethidiumbromide. As size marker the GeneRuler 1 kb Plus DNA Ladder (Thermo Fisher Scientific) was used. Separated DNA was visualized in an E-Box VX2 transilluminator (Peqlab).

DNA bands were cut out and extracted by the use of the NucleoSpin® Extract II Kit (Macherey-Nagel) according to manufacturer's protocol.

10 ml 5 x DNA loading dye

5 ml	30 % Ficoll (as to be autoclaved)
2 ml	250 mM EDTA pH 8,0
500 µl	10 % SDS
200 µl	50 x TAE pH 7,5
800 µl	0.5 % Xylenblue
800 µl	0.5 % Bromphenolblue
700 µl	H_2O

5.3.6 DNA restriction digest

Restriction enzymes were purchased from Fermentas/Thermo Fisher Scientific and used according to manufacturer's recommendations. Analytical restrictions were performed in a total volume of 20 µl using 1 µg DNA, incubated for 1 h at the recommended temperature. Preparative restriction digests were performed in a total volume of 50 µl using 2 µg DNA, incubated for 3 h or overnight at the recommended temperature. The amount of enzyme used for each digestion was individually calculated according to unit definition and number of restriction sites within the respective plasmid.

5.3.7 Ligation of DNA fragments

Ligation was performed in a total volume of 20 µl using 1 µg vector DNA, 16 µl insert DNA and 1 Weiss U T4 DNA ligase (Fermentas/ Thermo Fisher Scientific). The ligation mix was incubated at 16°C overnight, inactivated at 65°C for 10 min. Finally competent *E.coli* were transformed with the ligation mix (see 5.1.2).

5.3.8 Gateway cloning

The procedure was done as described in the Gateway cloning protocol of Invitrogen.

5.3.9 DNA amplification

E.coli DH5α were transformed (see 5.1.2) with the respective plasmid. On the next day bacteria were inoculated into LB medium containing an appropriate antibiotic and the cultures were grown overnight at 37°C on a shaker. On the next day, the

DNA was extracted by using the NucleoBond PC-100 Kit (Macherey-Nagel) or the GeneJet Plasmid Miniprep Kit (Thermo Fisher Scientific) according to the manufacturer's protocol. After cleanup, the plasmid concentration and purity was measured with a WPA Biowave S2100 Diode Array Spectrophotometer (Biochrom).

5.3.10 DNA sequencing

After cloning involving a PCR step, constructs were sequenced. The DNA sequencing was performed by Eurofins MWG GmbH.

5.4 Biochemical methods

5.4.1 Recombinant protein purification

The protein expression strain *E. coli* BL21 was transformed with the expression plasmids, which carried the gene for the protein that should be expressed. On the next day a 50 ml LB pre culture was inoculated and grown overnight, shaking at 37°C. The whole suspension was transferred into a baffled flask containing 500 ml LB medium supplemented with 2 g/l glucose on the next morning. At an OD_{600} of 0.5-0.8, protein expression was induced by adding 0.5 mM IPTG (AppliChem) and the culture was grown at 20-37°C for 8-20 h, depending on the respective protein.
All preparation steps were performed at 4°C to avoid protein degradation and at every step of the preparation 50 µl samples were taken for a SDS-PAGE. The cells were harvested by 20 min centrifugation at 4,000 x*g*, the pellet was resuspended in 10 ml ice cold lysis buffer, a small amount of lysozyme (Roth) was added and then the suspension was incubated at 4°C under mixing for 15 min. The cells were opened by sonification using an ultrasonic device (UP100H, Hielscher) first time for 1 min, followed by 5 x 30 s, between each round of sonification the samples were put on ice. The insoluble fraction was removed by 60 min centrifugation at 20,000 x*g*. During centrifugation, 500 µl beads were loaded onto a column, washed twice with 1 x PBS buffer and once with lysis buffer to equilibrate the beads. The equilibrated beads were mixed with the protein-containing supernatant and incubated overnight under constant rotation. The next day, the beads were washed four times with 5 ml lysis buffer, resuspended in 2 ml resuspension buffer, aliquoted, shock frozen in liquid nitrogen and stored at -80°C for long time storage.

Successful protein expression, concentration and purity was accessed by mixing each sample, taken at each step of the procedure, and 30 µl beads with 10 µl 4 x SDS sample buffer and boiled for 5 min at 95°C. Finally 10 µl of these samples were loaded on a SDS polyacrylamide gel, 2.5 µl, 5 µl and 10 µl in case of the beads. Additionally, three different amounts of bovine serum albumin (BSA), 5, 10 and 20 µg were loaded on the gel and separated by SDS-PAGE (see 5.4.4). The amount of protein bound to the beads was estimated compared to the BSA control.

Buffers for Ni^{2+}-NTA beads

lysis buffer

50 mM	NaH_2PO_4	
300 mM	NaCl	
10 mM	Imidazol	
set pH 8.0 using NaOH		
10 mM	β-Mercaptoethanol	add always fresh
	Protease inhibitors cocktail EDTA free	
	Benzonase	

washing buffer

50 mM	NaH_2PO_4	
300 mM	NaCl	
10 mM	Imidazol	
set pH 8.0 using NaOH		
10 mM	β-Mercaptoethanol	add always fresh

Buffers for GST beads

lysis buffer

50 mM	Tris HCl pH 8.5
20 %	Sucrose
200 mM	N_2S

2 mM	$MgCl_2$	
2 mM	DTT	add always fresh
	Protease inhibitor cocktail EDTA free	

washing buffer

50 mM	Tris HCl pH 7.6
0.1 %	Triton X-100
150 mM	NaCl
10 mM	$MgCl_2$

5.4.2 Pull down analysis

All steps were performed at 4°C. On the day before the pull down assay, B16 cells were transfected with plasmids of interest and incubated overnight under normal cell culture conditions (see 5.2.2). The next day in the morning, cells were washed twice with PBS and scraped of the dish in 300 µl IP-buffer containing 1 % Triton X-100 and protease inhibitor cocktail. The lysate was incubated on ice for at least 15 min, including several times vortexting. After incubation, the insoluble fraction was pelleted by centrifugation at 15,000 x*g* for 15 min. 30 µl of the supernatant were taken and mixed with 4 x SDS-sample buffer as "load control". 150 µl of the supernatant were mixed with 30 µl prey-protein coupled beads and incubated for at least 60 min on a rotating wheel in the cool room. Now the beads were pelleted (3 min, 500 x*g*) and washed three times with IP-buffer containing 1 % Triton X-100 but no protease inhibitor. From the supernatant after the first centrifugation step a 30 µl sample was taken and mixed with 4 x SDS-sample buffer as "supernatant control". After the last centrifugation step, the beads were resuspended in 30 µl 4 x SDS-sample buffer "pull down", boiled for 5 min at 95°C for subsequent SDS-PAGE.

IP-buffer

15 mM	KCl
50 mM	NaCl
8 mM	Tris, free base
12 mM	Hepes, free base

5 mM	$MgCl_2$	
1 %	Triton X-100	add always
	Protease inhibitor cocktail EDTA free	fresh

5.4.3 Co-immunoprecipitation

Co-immunoprecipitations of Myc-tagged proteins were performed by using the Anti-c-Myc Immunoprecipitation Kit (Sigma Aldrich) according to manufacturer's recommendations, or by using 5 µg of GFP antibody.

5.4.4 Protein gel electrophoresis (SDS-PAGE)

To separate proteins according to their size 9.5 x 6.5 cm, SDS containing polyacrylamide gels were used. Gels were poured in customized blocs of 10 to 15 gels. First the 10 or 15 % separation gels were poured and covered with a layer of isopropanol. After 30 min, the gels were polymerized, the isopropanol discarded and washed 10 times with water. Then the 5 % stacking gels were poured and the combs inserted. Again, after 30 min, polymerization was over and the gels could be assembled into customized, SDS-running buffer filed SDS-chambers and loaded with SDS-protein samples and pre- or unstained protein ladder (Thermo Fischer Scientific). Gels were run at 100 V/gel for 2-3 h

10 x 5 % stacking gel

23 ml	H_2O
10 ml	0.5 M Tris HCl pH 6.8
6.8 ml	30 % Acrylamid / Bisacrylamid
400 µl	10 % SDS
80 µl	TEMED
80 µl	25 % APS

10 x 10 % (15 %) collection gel

49 (29) ml	H_2O
30 (30) ml	1.5 M Tris HCl pH 8.8

37 (60) ml	30 % Acrylamid / Bisacrylamid
1.2 (1.2) ml	10 % SDS
160 (160) µl	TEMED
160 (160) µl	25 % APS

SDS-running buffer

25 mM	Tris base
192 mM	Glycin
0.1 % (v/v)	SDS

4 x SDS-sample buffer

25 mM	Tris pH 6.8 (HCl)
29 % (v/v)	Glycerol
3.3 % (v/v)	SDS
3.3 % (v/v)	β-Mercaptoethanol
0.17 % (w/v)	Bromphenolblue

5.4.5 Coomassie staining

To visualize proteins on gels after SDS-PAGE or on PVDF membranes after Western blotting, they were shaken in Coomassie staining solution for several hours. Excess dye was extracted by shaking the gel or membrane in Coomassie destaining solution for 3 h.

Coomassie staining solution

25 %	Methanol
10 % (v/v)	Acetic acid
0.1 % (w/v)	Coomassie Brilliant Blue R250

Coomassie destaining solution

40 %	Methanol
10 % (v/v)	Acetic acid

5.4.6 Western blotting and protein detection

After protein separation by SDS-PAGE, the proteins were transferred from the gel to PVDF membranes (Merck-Millipore), using a semi dry blotting system. Prior assembling the blotting sandwich in a Semi-dry blotting Biometra Fastblot B44 (Analytik Jena), filter papers were equilibrated in blotting buffer, the membrane was activated in methanol. The blot was run at 150 mA/membrane for 3 h. Blotting efficiency was checked by reversible protein staining of the membrane in Ponceau S staining solution.

If the transfer was successful, the membrane was blocked in 10 % milk/TBS-T for 30 min, incubated with a primary antibody at 4°C overnight on a shaker, followed by three 15 min washing steps with TBS-T and another hour shaking incubation with the second antibody at room temperature. Finally the membrane was washed again three times with TBS-T and once with H_2O_{dd}, before the membrane was covered with 8 ml LumiLight Western Blotting Substrate (Roche) to detect HRP activity of second antibodies in a Geliance 600 Imaging System (Perkin Elmer).

The resulting image was saved as a TIF-file and processed in Adobe® Photoshop CS6 Extended (Adobe Systems).

Ponceau S solution

5 g	Ponceau S
0.4 % (v/v)	Methanol
15 % (v/v)	Acetic acid

Blotting buffer

50 mM	Tris base
38.5 mM	Glycine
1.3 mM	SDS
20 % (v/v)	Methanol

TBS (-T)

200 mM	Tris base
1.37 M	NaCl

pH 7.6 (HCl)

(0.1 % (v/v) Tween 20)

5.4.7 Stripping of PVDF membranes

In order to remove antibodies from PVDF membranes, they were 5 min shaken in buffer A at room temperature and subsequent 10 min in buffer B, followed by two washing steps in TBS-T. After blocking, the membrane was ready for another antibody.

Stripping buffer A

500 mM NaCl

200 mM Glycine

pH 2.0 (HCl)

Stripping buffer B

500 mM Tris base

pH 11.0 (NaOH)

5.5 Microscopy techniques

5.5.1 Coverslip washing

To clarify glass coverslips from production residues, they were shaken for 1 h in washing solution at room temperature and washed ten times with H_2O_{dd}. After sterilization the coverslips were 30 min coated with Fibronectin (25 µg/ml in PBS; stock 1 g/l in 2 M urea; Roche) and then washed twice with PBS.

Coverslip washing solution

60 % (v/v) Ethanol

40 % (v/v) conc. HCl

5.5.2 Staining of mitochondria

Mitochondria were stained by using 500 nM MitoTracker®Red (Invitrogen) according to the manufacturer's manual.

5.5.3 Fixation and immuno-staining of cells

In order to fixate cells, the medium was quickly replaced by pre warmed 4 % PFA in PBS at room temperature. After 20 min cells were permeabilized one minute in 0.05-1% Triton X-100 (depending on the subsequent antibody staining) in PBS. Then the coverslips were three times washed with PBS, followed by a blocking step with 5 % horse serum (v/v) in PBS containing 1 % BSA (w/v) for 1 h at room temperature or overnight at 4°C.

Subsequently the coverslips were washed several times in PBS and the immune-staining was performed by placing a coverslip upside down on a 20 µl drop of primary antibody diluted (see 4.7) in PBS containing 1 % BSA. To avoid drying, the drop was placed on parafilm in a dark humid chamber. After one hour the coverslips were washed again and placed on another drop containing the diluted secondary antibody and additional fluorescent dyes. 45 min later the coverslips were washed a last time and placed on a 20 µl drop of Mowiol on an ethanol cleaned microscope glass slide. The fixation hardened overnight at 4°C.

Mowiol

0.4 g/ml	Mowiol 7200
1 g/ml	Glycerol
0.2 M	Tris pH 9.0
2.5 %	DABCO

5.5.4 Imaging and image processing

All pictures were taken by using either a PALM IX70 microscope (Olympus) in combination with a HXP-120 Light Source (Visitron Systems), a 18.0 Monochrome camera w/o IR (Diagnostics Instruments Inc.) and the 60 x objective lens UPLFLN60XOI (Olympus) or an Axiovert 200 microscope (Zeiss), equipped with a sensicam® qe high performance cooled digital 12bit CCD camera, a pE-2 LED

excitation system (CoolLED) light source and the 63 x or 100 x Plan-Neofluar (Zeiss). Both microscopes were run with VisiVIEW software (Visitron Systems).
Images were processed with Adobe® Photoshop CS6 Extended (Adobe Systems) or ImageJ 1.43m (National Institute of Health, USA) containing the MBF ImageJ plug-in bundle for microscopy (McMaster University, Biophotonics Facility).

6 Picture credits

7 Literatur

Abercrombie, M., Heaysman, J.E. and Pegrum, S.M. (1970a). The locomotion of fibroblasts in culture. I. Movements of the leading edge. *Exp Cell Res* **59,** 393-398.

Abercrombie, M., Heaysman, J.E. and Pegrum, S.M. (1970b). The locomotion of fibroblasts in culture. II. "Ruffling". *Exp Cell Res* **60,** 437-444.

Aktories, K. (2011). Bacterial protein toxins that modify host regulatory GTPases. *Nat Rev Microbiol* **9,** 487-498.

Albers, M., Kranz, H., Kober, I., Kaiser, C., Klink, M., Suckow, J., *et al.* (2005). Automated yeast two-hybrid screening for nuclear receptor-interacting proteins. *Mol Cell Proteomics* **4,** 205-213.

Aleman, A., Rodriguez-Escudero, I., Mallo, G.V., Cid, V.J., Molina, M. and Rotger, R. (2005). The amino-terminal non-catalytic region of Salmonella typhimurium SigD affects actin organization in yeast and mammalian cells. *Cell Microbiol* **7,** 1432-1446.

Alto, N.M., Shao, F., Lazar, C.S., Brost, R.L., Chua, G., Mattoo, S., *et al.* (2006). Identification of a bacterial type III effector family with G protein mimicry functions. *Cell* **124,** 133-145.

Arbeloa, A., Blanco, M., Moreira, F.C., Bulgin, R., Lopez, C., Dahbi, G., *et al.* (2009). Distribution of espM and espT among enteropathogenic and enterohaemorrhagic Escherichia coli. *J Med Microbiol* **58,** 988-995.

Balaban, N.Q., Schwarz, U.S., Riveline, D., Goichberg, P., Tzur, G., Sabanay, I., *et al.* (2001). Force and focal adhesion assembly: a close relationship studied using elastic micropatterned substrates. *Nat Cell Biol* **3,** 466-472.

Berger, C.N., Crepin, V.F., Jepson, M.A., Arbeloa, A. and Frankel, G. (2009). The mechanisms used by enteropathogenic Escherichia coli to control filopodia dynamics. *Cell Microbiol* **11,** 309-322.

Bernardini, M.L., Mounier, J., d'Hauteville, H., Coquis-Rondon, M. and Sansonetti, P.J. (1989). Identification of icsA, a plasmid locus of Shigella flexneri that governs bacterial intra- and intercellular spread through interaction with F-actin. *Proc Natl Acad Sci U S A* **86,** 3867-3871.

Beuzon, C.R., Meresse, S., Unsworth, K.E., Ruiz-Albert, J., Garvis, S., Waterman, S.R., *et al.* (2000). Salmonella maintains the integrity of its intracellular vacuole through the action of SifA. *EMBO J* **19,** 3235-3249.

Boonyaratanakornkit, J., Schomacker, H., Collins, P. and Schmidt, A. (2013). Alix Serves as an Adaptor That Allows Human Parainfluenza Virus Type 1 to Interact with the Host Cell ESCRT System. *PLoS One* **8,** e59462.

Botelho, R.J. and Grinstein, S. (2011). Phagocytosis. *Curr Biol* **21,** R533-538.

Boucrot, E., Henry, T., Borg, J.P., Gorvel, J.P. and Meresse, S. (2005). The intracellular fate of Salmonella depends on the recruitment of kinesin. *Science* **308,** 1174-1178.

Boulter, E., Garcia-Mata, R., Guilluy, C., Dubash, A., Rossi, G., Brennwald, P.J. and Burridge, K. (2010). Regulation of Rho GTPase crosstalk, degradation and activity by RhoGDI1. *Nat Cell Biol* **12,** 477-483.

Brumell, J.H. and Scidmore, M.A. (2007). Manipulation of rab GTPase function by intracellular bacterial pathogens. *Microbiol Mol Biol Rev* **71,** 636-652.

Bulgin, R., Arbeloa, A., Goulding, D., Dougan, G., Crepin, V.F., Raymond, B. and Frankel, G. (2009a). The T3SS effector EspT defines a new category of

invasive enteropathogenic E. coli (EPEC) which form intracellular actin pedestals. *PLoS Pathog* **5,** e1000683.

Bulgin, R., Raymond, B., Garnett, J.A., Frankel, G., Crepin, V.F., Berger, C.N. and Arbeloa, A. (2010). Bacterial guanine nucleotide exchange factors SopE-like and WxxxE effectors. *Infect Immun* **78,** 1417-1425.

Bulgin, R.R., Arbeloa, A., Chung, J.C. and Frankel, G. (2009b). EspT triggers formation of lamellipodia and membrane ruffles through activation of Rac-1 and Cdc42. *Cell Microbiol* **11,** 217-229.

Burkinshaw, B.J., Prehna, G., Worrall, L.J. and Strynadka, N.C. (2012). Structure of Salmonella effector protein SopB N-terminal domain in complex with host Rho GTPase Cdc42. *J Biol Chem* **287,** 13348-13355.

Burridge, K. and Wittchen, E.S. (2013). The tension mounts: stress fibers as force-generating mechanotransducers. *J Cell Biol* **200,** 9-19.

Campellone, K.G. (2010). Cytoskeleton-modulating effectors of enteropathogenic and enterohaemorrhagic Escherichia coli: Tir, EspFU and actin pedestal assembly. *FEBS J* **277,** 2390-2402.

Campellone, K.G., Rankin, S., Pawson, T., Kirschner, M.W., Tipper, D.J. and Leong, J.M. (2004). Clustering of Nck by a 12-residue Tir phosphopeptide is sufficient to trigger localized actin assembly. *J Cell Biol* **164,** 407-416.

Campellone, K.G. and Welch, M.D. (2010). A nucleator arms race: cellular control of actin assembly. *Nat Rev Mol Cell Biol* **11,** 237-251.

Caron, E. and Hall, A. (1998). Identification of two distinct mechanisms of phagocytosis controlled by different Rho GTPases. *Science* **282,** 1717-1721.

Chardin, P., Boquet, P., Madaule, P., Popoff, M.R., Rubin, E.J. and Gill, D.M. (1989). The mammalian G protein rhoC is ADP-ribosylated by Clostridium botulinum exoenzyme C3 and affects actin microfilaments in Vero cells. *EMBO J* **8,** 1087-1092.

Cherfils, J. and Zeghouf, M. (2013). Regulation of small GTPases by GEFs, GAPs, and GDIs. *Physiol Rev* **93,** 269-309.

Cornelis, G.R. (2006). The type III secretion injectisome. *Nat Rev Microbiol* **4,** 811-825.

Cossart, P. and Sansonetti, P.J. (2004). Bacterial invasion: the paradigms of enteroinvasive pathogens. *Science* **304,** 242-248.

Cox, A.D. and Der, C.J. (2010). Ras history: The saga continues. *Small GTPases* **1,** 2-27.

Cramer, L.P., Siebert, M. and Mitchison, T.J. (1997). Identification of novel graded polarity actin filament bundles in locomoting heart fibroblasts: implications for the generation of motile force. *J Cell Biol* **136,** 1287-1305.

D'Souza-Schorey, C., Boshans, R.L., McDonough, M., Stahl, P.D. and Van Aelst, L. (1997). A role for POR1, a Rac1-interacting protein, in ARF6-mediated cytoskeletal rearrangements. *EMBO J* **16,** 5445-5454.

D'Souza-Schorey, C. and Chavrier, P. (2006). ARF proteins: roles in membrane traffic and beyond. *Nat Rev Mol Cell Biol* **7,** 347-358.

Donaldson, J.G. (2003). Multiple roles for Arf6: sorting, structuring, and signaling at the plasma membrane. *J Biol Chem* **278,** 41573-41576.

Dowrick, P., Kenworthy, P., McCann, B. and Warn, R. (1993). Circular ruffle formation and closure lead to macropinocytosis in hepatocyte growth factor/scatter factor-treated cells. *Eur J Cell Biol* **61,** 44-53.

Faix, J., Breitsprecher, D., Stradal, T.E. and Rottner, K. (2009). Filopodia: Complex models for simple rods. *Int J Biochem Cell Biol* **41,** 1656-1664.

Francis, C.L., Starnbach, M.N. and Falkow, S. (1992). Morphological and cytoskeletal changes in epithelial cells occur immediately upon interaction with Salmonella typhimurium grown under low-oxygen conditions. *Mol Microbiol* **6,** 3077-3087.

Freeman, J.A., Ohl, M.E. and Miller, S.I. (2003). The Salmonella enterica serovar typhimurium translocated effectors SseJ and SifB are targeted to the Salmonella-containing vacuole. *Infect Immun* **71,** 418-427.

Friebel, A., Ilchmann, H., Aepfelbacher, M., Ehrbar, K., Machleidt, W. and Hardt, W.D. (2001). SopE and SopE2 from Salmonella typhimurium activate different sets of RhoGTPases of the host cell. *J Biol Chem* **276,** 34035-34040.

Fu, Y. and Galan, J.E. (1999). A salmonella protein antagonizes Rac-1 and Cdc42 to mediate host-cell recovery after bacterial invasion. *Nature* **401,** 293-297.

Garai, P., Gnanadhas, D.P. and Chakravortty, D. (2012). Salmonella enterica serovars Typhimurium and Typhi as model organisms: revealing paradigm of host-pathogen interactions. *Virulence* **3,** 377-388.

Garcia-del Portillo, F., Foster, J.W. and Finlay, B.B. (1993a). Role of acid tolerance response genes in Salmonella typhimurium virulence. *Infect Immun* **61,** 4489-4492.

Garcia-del Portillo, F., Zwick, M.B., Leung, K.Y. and Finlay, B.B. (1993b). Salmonella induces the formation of filamentous structures containing lysosomal membrane glycoproteins in epithelial cells. *Proc Natl Acad Sci U S A* **90,** 10544-10548.

Gerdes, J.M., Davis, E.E. and Katsanis, N. (2009). The vertebrate primary cilium in development, homeostasis, and disease. *Cell* **137,** 32-45.

Glacy, S.D. (1983). Subcellular distribution of rhodamine-actin microinjected into living fibroblastic cells. *J Cell Biol* **97,** 1207-1213.

Goldberg, M.B. and Theriot, J.A. (1995). Shigella flexneri surface protein IcsA is sufficient to direct actin-based motility. *Proc Natl Acad Sci U S A* **92,** 6572-6576.

Goley, E.D., Rodenbusch, S.E., Martin, A.C. and Welch, M.D. (2004). Critical conformational changes in the Arp2/3 complex are induced by nucleotide and nucleation promoting factor. *Mol Cell* **16,** 269-279.

Goley, E.D. and Welch, M.D. (2006). The ARP2/3 complex: an actin nucleator comes of age. *Nat Rev Mol Cell Biol* **7,** 713-726.

Gouin, E., Welch, M.D. and Cossart, P. (2005). Actin-based motility of intracellular pathogens. *Curr Opin Microbiol* **8,** 35-45.

Gu, Y., Filippi, M.D., Cancelas, J.A., Siefring, J.E., Williams, E.P., Jasti, A.C., *et al.* (2003). Hematopoietic cell regulation by Rac1 and Rac2 guanosine triphosphatases. *Science* **302,** 445-449.

Guo, F., Debidda, M., Yang, L., Williams, D.A. and Zheng, Y. (2006). Genetic deletion of Rac1 GTPase reveals its critical role in actin stress fiber formation and focal adhesion complex assembly. *J Biol Chem* **281,** 18652-18659.

Hachani, A., Biskri, L., Rossi, G., Marty, A., Menard, R., Sansonetti, P., *et al.* (2007). IpgB1 and IpgB2, two homologous effectors secreted via the Mxi-Spa type III secretion apparatus, cooperate to mediate polarized cell invasion and inflammatory potential of Shigella flexenri. *Microbes Infect* **10,** 260-268.

Hachani, A., Biskri, L., Rossi, G., Marty, A., Menard, R., Sansonetti, P., *et al.* (2008). IpgB1 and IpgB2, two homologous effectors secreted via the Mxi-Spa type III secretion apparatus, cooperate to mediate polarized cell invasion and inflammatory potential of Shigella flexenri. *Microbes Infect* **10,** 260-268.

Hall, A. (1998). Rho GTPases and the actin cytoskeleton. *Science* **279,** 509-514.

Handa, Y., Suzuki, M., Ohya, K., Iwai, H., Ishijima, N., Koleske, A.J., *et al.* (2007). Shigella IpgB1 promotes bacterial entry through the ELMO-Dock180 machinery. *Nat Cell Biol* **9,** 121-128.

Hänisch, J., Kölm, R., Wozniczka, M., Bumann, D., Rottner, K. and Stradal, T.E. (2011). Activation of a RhoA/myosin II-dependent but Arp2/3 complex-independent pathway facilitates Salmonella invasion. *Cell Host Microbe* **9,** 273-285.

Haraga, A., Ohlson, M.B. and Miller, S.I. (2007). Salmonellae interplay with host cells. *Nat Rev Microbiol* **6,** 53-66.

Hardt, W.D., Chen, L.M., Schuebel, K.E., Bustelo, X.R. and Galan, J.E. (1998). S. typhimurium encodes an activator of Rho GTPases that induces membrane ruffling and nuclear responses in host cells. *Cell* **93,** 815-826.

Hartland, E.L., Daniell, S.J., Delahay, R.M., Neves, B.C., Wallis, T., Shaw, R.K., *et al.* (2000). The type III protein translocation system of enteropathogenic Escherichia coli involves EspA-EspB protein interactions. *Mol Microbiol* **35,** 1483-1492.

Heasman, S.J. and Ridley, A.J. (2008). Mammalian Rho GTPases: new insights into their functions from in vivo studies. *Nat Rev Mol Cell Biol* **9,** 690-701.

Heath, J.P. and Dunn, G.A. (1978). Cell to substratum contacts of chick fibroblasts and their relation to the microfilament system. A correlated interference-reflexion and high-voltage electron-microscope study. *J Cell Sci* **29,** 197-212.

Henderson, I.R., Navarro-Garcia, F., Desvaux, M., Fernandez, R.C. and Ala'Aldeen, D. (2004). Type V protein secretion pathway: the autotransporter story. *Microbiol Mol Biol Rev* **68,** 692-744.

Hernandez-Hernandez, V., Pravincumar, P., Diaz-Font, A., May-Simera, H., Jenkins, D., Knight, M. and Beales, P.L. (2013). Bardet-Biedl syndrome proteins control the cilia length through regulation of actin polymerization. *Hum Mol Genet*.

Hoon, J.L., Wong, W.K. and Koh, C.G. (2012). Functions and regulation of circular dorsal ruffles. *Mol Cell Biol* **32,** 4246-4257.

Hotulainen, P. and Lappalainen, P. (2006). Stress fibers are generated by two distinct actin assembly mechanisms in motile cells. *J Cell Biol* **173,** 383-394.

Huang, Z., Sutton, S.E., Wallenfang, A.J., Orchard, R.C., Wu, X., Feng, Y., *et al.* (2009). Structural insights into host GTPase isoform selection by a family of bacterial GEF mimics. *Nat Struct Mol Biol* **16,** 853-860.

Ide, T., Laarmann, S., Greune, L., Schillers, H., Oberleithner, H. and Schmidt, M.A. (2001). Characterization of translocation pores inserted into plasma membranes by type III-secreted Esp proteins of enteropathogenic Escherichia coli. *Cell Microbiol* **3,** 669-679.

Ingram, V.M. (1969). A side view of moving fibroblasts. *Nature* **222,** 641-644.

Iwai, H., Kim, M., Yoshikawa, Y., Ashida, H., Ogawa, M., Fujita, Y., *et al.* (2007). A bacterial effector targets Mad2L2, an APC inhibitor, to modulate host cell cycling. *Cell* **130,** 611-623.

Jackson, L.K., Nawabi, P., Hentea, C., Roark, E.A. and Haldar, K. (2008). The Salmonella virulence protein SifA is a G protein antagonist. *Proc Natl Acad Sci U S A* **105,** 14141-14146.

Jelen, F., Oleksy, A., Smietana, K. and Otlewski, J. (2003). PDZ domains - common players in the cell signaling. *Acta Biochim Pol* **50,** 985-1017.

Jouvenet, N. (2012). Dynamics of ESCRT proteins. *Cell Mol Life Sci* **69,** 4121-4133.

Kagan, J.C. and Iwasaki, A. (2012). Phagosome as the organelle linking innate and adaptive immunity. *Traffic* **13,** 1053-1061.

Kenny, B., DeVinney, R., Stein, M., Reinscheid, D.J., Frey, E.A. and Finlay, B.B. (1997). Enteropathogenic E. coli (EPEC) transfers its receptor for intimate adherence into mammalian cells. *Cell* **91,** 511-520.

Kenny, B., Ellis, S., Leard, A.D., Warawa, J., Mellor, H. and Jepson, M.A. (2002). Co-ordinate regulation of distinct host cell signalling pathways by multifunctional enteropathogenic Escherichia coli effector molecules. *Mol Microbiol* **44,** 1095-1107.

Kenny, B. and Jepson, M. (2000). Targeting of an enteropathogenic Escherichia coli (EPEC) effector protein to host mitochondria. *Cell Microbiol* **2,** 579-590.

Kim, J.C., Badano, J.L., Sibold, S., Esmail, M.A., Hill, J., Hoskins, B.E., *et al.* (2004). The Bardet-Biedl protein BBS4 targets cargo to the pericentriolar region and is required for microtubule anchoring and cell cycle progression. *Nat Genet* **36,** 462-470.

Kim, S. and Tsiokas, L. (2011). Cilia and cell cycle re-entry: more than a coincidence. *Cell Cycle* **10,** 2683-2690.

Klink, B.U., Barden, S., Heidler, T.V., Borchers, C., Ladwein, M., Stradal, T.E., *et al.* (2010). Structure of Shigella IpgB2 in complex with human RhoA: implications for the mechanism of bacterial guanine nucleotide exchange factor mimicry. *J Biol Chem* **285,** 17197-17208.

Knutton, S., Rosenshine, I., Pallen, M.J., Nisan, I., Neves, B.C., Bain, C., *et al.* (1998). A novel EspA-associated surface organelle of enteropathogenic Escherichia coli involved in protein translocation into epithelial cells. *EMBO J* **17,** 2166-2176.

Koegl, M. and Uetz, P. (2007). Improving yeast two-hybrid screening systems. *Brief Funct Genomic Proteomic* **6,** 302-312.

Koleske, A.J. (2003). Do filopodia enable the growth cone to find its way? *Sci STKE* **2003,** pe20.

Köstler, S.A., Auinger, S., Vinzenz, M., Rottner, K. and Small, J.V. (2008). Differentially oriented populations of actin filaments generated in lamellipodia collaborate in pushing and pausing at the cell front. *Nat Cell Biol* **10,** 306-313.

Kozma, R., Ahmed, S., Best, A. and Lim, L. (1995). The Ras-related protein Cdc42Hs and bradykinin promote formation of peripheral actin microspikes and filopodia in Swiss 3T3 fibroblasts. *Mol Cell Biol* **15,** 1942-1952.

Kureishy, N., Sapountzi, V., Prag, S., Anilkumar, N. and Adams, J.C. (2002). Fascins, and their roles in cell structure and function. *Bioessays* **24,** 350-361.

Ladwein, M. and Rottner, K. (2008). On the Rho'd: the regulation of membrane protrusions by Rho-GTPases. *FEBS Lett* **582,** 2066-2074.

Lazarides, E. and Burridge, K. (1975). Alpha-actinin: immunofluorescent localization of a muscle structural protein in nonmuscle cells. *Cell* **6,** 289-298.

Leung, T., Manser, E., Tan, L. and Lim, L. (1995). A novel serine/threonine kinase binding the Ras-related RhoA GTPase which translocates the kinase to peripheral membranes. *J Biol Chem* **270,** 29051-29054.

Liu, H. and Naismith, J.H. (2008). An efficient one-step site-directed deletion, insertion, single and multiple-site plasmid mutagenesis protocol. *BMC Biotechnol* **8,** 91.

Loktev, A.V., Zhang, Q., Beck, J.S., Searby, C.C., Scheetz, T.E., Bazan, J.F.*, et al.* (2008). A BBSome subunit links ciliogenesis, microtubule stability, and acetylation. *Dev Cell* **15,** 854-865.

Lommel, S., Benesch, S., Rohde, M., Wehland, J. and Rottner, K. (2004). Enterohaemorrhagic and enteropathogenic Escherichia coli use different mechanisms for actin pedestal formation that converge on N-WASP. *Cell Microbiol* **6,** 243-254.

Lozano, R., Naghavi, M., Foreman, K., Lim, S., Shibuya, K., Aboyans, V.*, et al.* (2012). Global and regional mortality from 235 causes of death for 20 age groups in 1990 and 2010: a systematic analysis for the Global Burden of Disease Study 2010. *Lancet* **380,** 2095-2128.

Ma, L., Rohatgi, R. and Kirschner, M.W. (1998). The Arp2/3 complex mediates actin polymerization induced by the small GTP-binding protein Cdc42. *Proc Natl Acad Sci U S A* **95,** 15362-15367.

Machesky, L.M., Atkinson, S.J., Ampe, C., Vandekerckhove, J. and Pollard, T.D. (1994). Purification of a cortical complex containing two unconventional actins from Acanthamoeba by affinity chromatography on profilin-agarose. *J Cell Biol* **127,** 107-115.

Mallavarapu, A. and Mitchison, T. (1999). Regulated actin cytoskeleton assembly at filopodium tips controls their extension and retraction. *J Cell Biol* **146,** 1097-1106.

Martinez-Lorenzo, M.J., Meresse, S., de Chastellier, C. and Gorvel, J.P. (2001). Unusual intracellular trafficking of Salmonella typhimurium in human melanoma cells. *Cell Microbiol* **3,** 407-416.

Mattila, P.K. and Lappalainen, P. (2008). Filopodia: molecular architecture and cellular functions. *Nat Rev Mol Cell Biol* **9,** 446-454.

Mattoo, S., Lee, Y.M. and Dixon, J.E. (2007). Interactions of bacterial effector proteins with host proteins. *Curr Opin Immunol* **19,** 392-401.

McGhie, E.J., Brawn, L.C., Hume, P.J., Humphreys, D. and Koronakis, V. (2009). Salmonella takes control: effector-driven manipulation of the host. *Curr Opin Microbiol* **12,** 117-124.

Medzhitov, R. (2009). Approaching the asymptote: 20 years later. *Immunity* **30,** 766-775.

Mellström, K., Höglund, A.S., Nistér, M., Heldin, C.H., Westermark, B. and Lindberg, U. (1983). The effect of platelet-derived growth factor on morphology and motility of human glial cells. *J. of Muscle Res. Cell Motil.* **4,** 589-609.

Missotten, M., Nichols, A., Rieger, K. and Sadoul, R. (1999). Alix, a novel mouse protein undergoing calcium-dependent interaction with the apoptosis-linked-gene 2 (ALG-2) protein. *Cell Death Differ* **6,** 124-129.

Morita, E., Sandrin, V., McCullough, J., Katsuyama, A., Baci Hamilton, I. and Sundquist, W.I. (2011). ESCRT-III protein requirements for HIV-1 budding. *Cell Host Microbe* **9,** 235-242.

Mostowy, S. and Cossart, P. (2011). Autophagy and the cytoskeleton: new links revealed by intracellular pathogens. *Autophagy* **7,** 780-782.

Mullins, R.D., Heuser, J.A. and Pollard, T.D. (1998). The interaction of Arp2/3 complex with actin: nucleation, high affinity pointed end capping, and formation of branching networks of filaments. *Proc Natl Acad Sci U S A* **95,** 6181-6186.

Murata, T., Delprato, A., Ingmundson, A., Toomre, D.K., Lambright, D.G. and Roy, C.R. (2006). The Legionella pneumophila effector protein DrrA is a Rab1 guanine nucleotide-exchange factor. *Nat Cell Biol* **8,** 971-977.

Mykytyn, K., Braun, T., Carmi, R., Haider, N.B., Searby, C.C., Shastri, M.*, et al.* (2001). Identification of the gene that, when mutated, causes the human obesity syndrome BBS4. *Nat Genet* **28,** 188-191.

Mykytyn, K., Mullins, R.F., Andrews, M., Chiang, A.P., Swiderski, R.E., Yang, B.*, et al.* (2004). Bardet-Biedl syndrome type 4 (BBS4)-null mice implicate Bbs4 in flagella formation but not global cilia assembly. *Proc Natl Acad Sci U S A* **101,** 8664-8669.

Nachury, M.V., Loktev, A.V., Zhang, Q., Westlake, C.J., Peranen, J., Merdes, A.*, et al.* (2007). A core complex of BBS proteins cooperates with the GTPase Rab8 to promote ciliary membrane biogenesis. *Cell* **129,** 1201-1213.

Nickas, M.E. and Yaffe, M.P. (1996). BRO1, a novel gene that interacts with components of the Pkc1p-mitogen-activated protein kinase pathway in Saccharomyces cerevisiae. *Mol Cell Biol* **16,** 2585-2593.

Nobes, C.D. and Hall, A. (1995). Rho, rac, and cdc42 GTPases regulate the assembly of multimolecular focal complexes associated with actin stress fibers, lamellipodia, and filopodia. *Cell* **81,** 53-62.

Nordenfelt, P., Grinstein, S., Bjorck, L. and Tapper, H. (2012). V-ATPase-mediated phagosomal acidification is impaired by Streptococcus pyogenes through Mga-regulated surface proteins. *Microbes Infect* **14,** 1319-1329.

Norris, F.A., Wilson, M.P., Wallis, T.S., Galyov, E.E. and Majerus, P.W. (1998). SopB, a protein required for virulence of Salmonella dublin, is an inositol phosphate phosphatase. *Proc Natl Acad Sci U S A* **95,** 14057-14059.

Odorizzi, G., Katzmann, D.J., Babst, M., Audhya, A. and Emr, S.D. (2003). Bro1 is an endosome-associated protein that functions in the MVB pathway in Saccharomyces cerevisiae. *J Cell Sci* **116,** 1893-1903.

Ogawa, M., Handa, Y., Ashida, H., Suzuki, M. and Sasakawa, C. (2008). The versatility of Shigella effectors. *Nat Rev Microbiol* **6,** 11-16.

Ohlson, M.B., Huang, Z., Alto, N.M., Blanc, M.P., Dixon, J.E., Chai, J. and Miller, S.I. (2008). Structure and function of Salmonella SifA indicate that its interactions with SKIP, SseJ, and RhoA family GTPases induce endosomal tubulation. *Cell Host Microbe* **4,** 434-446.

Ohya, K., Handa, Y., Ogawa, M., Suzuki, M. and Sasakawa, C. (2005). IpgB1 is a novel Shigella effector protein involved in bacterial invasion of host cells. Its activity to promote membrane ruffling via Rac1 and Cdc42 activation. *J Biol Chem* **280,** 24022-24034.

Orchard, R.C. and Alto, N.M. (2012a). Mimicking GEFs: a common theme for bacterial pathogens. *Cell Microbiol* **14,** 10-18.

Orchard, R.C., Kittisopikul, M., Altschuler, S.J., Wu, L.F., Suel, G.M. and Alto, N.M. (2012b). Identification of F-actin as the dynamic hub in a microbial-induced GTPase polarity circuit. *Cell* **148,** 803-815.

Pan, J., You, Y., Huang, T. and Brody, S.L. (2007). RhoA-mediated apical actin enrichment is required for ciliogenesis and promoted by Foxj1. *J Cell Sci* **120,** 1868-1876.

Parsot, C. (2005). Shigella spp. and enteroinvasive Escherichia coli pathogenicity factors. *FEMS Microbiol Lett* **252,** 11-18.

Partridge, M.A. and Marcantonio, E.E. (2006). Initiation of attachment and generation of mature focal adhesions by integrin-containing filopodia in cell spreading. *Mol Biol Cell* **17,** 4237-4248.

Patel, J.C. and Galan, J.E. (2005). Manipulation of the host actin cytoskeleton by Salmonella--all in the name of entry. *Curr Opin Microbiol* **8,** 10-15.

Paterson, H.F., Self, A.J., Garrett, M.D., Just, I., Aktories, K. and Hall, A. (1990). Microinjection of recombinant p21rho induces rapid changes in cell morphology. *J Cell Biol* **111,** 1001-1007.

Peck, J.W., Oberst, M., Bouker, K.B., Bowden, E. and Burbelo, P.D. (2002). The RhoA-binding protein, rhophilin-2, regulates actin cytoskeleton organization. *J Biol Chem* **277,** 43924-43932.

Pellegrin, S. and Mellor, H. (2007). Actin stress fibres. *J Cell Sci* **120,** 3491-3499.

Perez-Sayans, M., Suarez-Penaranda, J.M., Barros-Angueira, F., Diz, P.G., Gandara-Rey, J.M. and Garcia-Garcia, A. (2012). An update in the structure, function, and regulation of V-ATPases: the role of the C subunit. *Braz J Biol* **72,** 189-198.

Pires, R., Hartlieb, B., Signor, L., Schoehn, G., Lata, S., Roessle, M., *et al.* (2009). A crescent-shaped ALIX dimer targets ESCRT-III CHMP4 filaments. *Structure* **17,** 843-856.

Pollard, T.D. and Borisy, G.G. (2003). Cellular motility driven by assembly and disassembly of actin filaments. *Cell* **112,** 453-465.

Popov, S., Popova, E., Inoue, M. and Gottlinger, H.G. (2009). Divergent Bro1 domains share the capacity to bind human immunodeficiency virus type 1 nucleocapsid and to enhance virus-like particle production. *J Virol* **83,** 7185-7193.

Prehoda, K.E., Scott, J.A., Mullins, R.D. and Lim, W.A. (2000). Integration of multiple signals through cooperative regulation of the N-WASP-Arp2/3 complex. *Science* **290,** 801-806.

Pukatzki, S., Ma, A.T., Sturtevant, D., Krastins, B., Sarracino, D., Nelson, W.C., *et al.* (2006). Identification of a conserved bacterial protein secretion system in Vibrio cholerae using the Dictyostelium host model system. *Proc Natl Acad Sci U S A* **103,** 1528-1533.

Radhakrishna, H., Al-Awar, O., Khachikian, Z. and Donaldson, J.G. (1999). ARF6 requirement for Rac ruffling suggests a role for membrane trafficking in cortical actin rearrangements. *J Cell Sci* **112 (Pt 6),** 855-866.

Raymond, B., Crepin, V.F., Collins, J.W. and Frankel, G. (2011). The WxxxE effector EspT triggers expression of immune mediators in an Erk/JNK and NF-kappaB-dependent manner. *Cell Microbiol* **13,** 1881-1893.

Ridley, A.J. (2011). Life at the leading edge. *Cell* **145,** 1012-1022.

Ridley, A.J., Paterson, H.F., Johnston, C.L., Diekmann, D. and Hall, A. (1992). The small GTP-binding protein rac regulates growth factor-induced membrane ruffling. *Cell* **70,** 401-410.

Robins-Browne, R.M. and Hartland, E.L. (2002). Escherichia coli as a cause of diarrhea. *J Gastroenterol Hepatol* **17,** 467-475.

Rodriguez-Escudero, I., Ferrer, N.L., Rotger, R., Cid, V.J. and Molina, M. (2011). Interaction of the Salmonella Typhimurium effector protein SopB with host cell Cdc42 is involved in intracellular replication. *Mol Microbiol* **80,** 1220-1240.

Rohatgi, R., Ma, L., Miki, H., Lopez, M., Kirchhausen, T., Takenawa, T. and Kirschner, M.W. (1999). The interaction between N-WASP and the Arp2/3 complex links Cdc42-dependent signals to actin assembly. *Cell* **97,** 221-231.

Roppenser, B., Grinstein, S. and Brumell, J.H. (2012). Modulation of host phosphoinositide metabolism during Salmonella invasion by the type III secreted effector SopB. *Methods Cell Biol* **108,** 173-186.

Rottner, K. and Stradal, T.E. (2011). Actin dynamics and turnover in cell motility. *Curr Opin Cell Biol* **23,** 569-578.

Rottner, K., Stradal, T.E. and Wehland, J. (2005). Bacteria-host-cell interactions at the plasma membrane: stories on actin cytoskeleton subversion. *Dev Cell* **9,** 3-17.

Rotty, J.D., Wu, C. and Bear, J.E. (2013). New insights into the regulation and cellular functions of the ARP2/3 complex. *Nat Rev Mol Cell Biol* **14,** 7-12.

Rouiller, I., Xu, X.P., Amann, K.J., Egile, C., Nickell, S., Nicastro, D.*, et al.* (2008). The structural basis of actin filament branching by the Arp2/3 complex. *J Cell Biol* **180,** 887-895.

Ruiz-Albert, J., Yu, X.J., Beuzon, C.R., Blakey, A.N., Galyov, E.E. and Holden, D.W. (2002). Complementary activities of SseJ and SifA regulate dynamics of the Salmonella typhimurium vacuolar membrane. *Mol Microbiol* **44,** 645-661.

Rusten, T.E. and Stenmark, H. (2009). How do ESCRT proteins control autophagy? *J Cell Sci* **122,** 2179-2183.

Rusten, T.E., Vaccari, T. and Stenmark, H. (2012). Shaping development with ESCRTs. *Nat Cell Biol* **14,** 38-45.

Sacher, M., Kim, Y.G., Lavie, A., Oh, B.H. and Segev, N. (2008). The TRAPP complex: insights into its architecture and function. *Traffic* **9,** 2032-2042.

Sarantis, H. and Grinstein, S. (2012). Subversion of phagocytosis for pathogen survival. *Cell Host Microbe* **12,** 419-431.

Schoebel, S., Oesterlin, L.K., Blankenfeldt, W., Goody, R.S. and Itzen, A. (2009). RabGDI displacement by DrrA from Legionella is a consequence of its guanine nucleotide exchange activity. *Mol Cell* **36,** 1060-1072.

Schroeder, G.N. and Hilbi, H. (2008). Molecular pathogenesis of Shigella spp.: controlling host cell signaling, invasion, and death by type III secretion. *Clin Microbiol Rev* **21,** 134-156.

Shen, Y., Kawamura, I., Nomura, T., Tsuchiya, K., Hara, H., Dewamitta, S.R., *et al.* (2010). Toll-like receptor 2- and MyD88-dependent phosphatidylinositol 3-kinase and Rac1 activation facilitates the phagocytosis of Listeria monocytogenes by murine macrophages. *Infect Immun* **78,** 2857-2867.

Sigal, Y.J., Quintero, O.A., Cheney, R.E. and Morris, A.J. (2007). Cdc42 and ARP2/3-independent regulation of filopodia by an integral membrane lipid-phosphatase-related protein. *J Cell Sci* **120,** 340-352.

Simpson, N., Shaw, R., Crepin, V.F., Mundy, R., FitzGerald, A.J., Cummings, N., *et al.* (2006). The enteropathogenic Escherichia coli type III secretion system effector Map binds EBP50/NHERF1: implication for cell signalling and diarrhoea. *Mol Microbiol* **60,** 349-363.

Small, J.V., Isenberg, G. and Celis, J.E. (1978). Polarity of actin at the leading edge of cultured cells. *Nature* **272,** 638-639.

Small, J.V., Rottner, K., Kaverina, I. and Anderson, K.I. (1998). Assembling an actin cytoskeleton for cell attachment and movement. *Biochim Biophys Acta* **1404,** 271-281.

Small, J.V., Stradal, T., Vignal, E. and Rottner, K. (2002). The lamellipodium: where motility begins. *Trends Cell Biol* **12,** 112-120.

Smith, A.C., Cirulis, J.T., Casanova, J.E., Scidmore, M.A. and Brumell, J.H. (2005). Interaction of the Salmonella-containing vacuole with the endocytic recycling system. *J Biol Chem* **280,** 24634-24641.

Smith, A.C., Heo, W.D., Braun, V., Jiang, X., Macrae, C., Casanova, J.E., *et al.* (2007). A network of Rab GTPases controls phagosome maturation and is modulated by Salmonella enterica serovar Typhimurium. *J Cell Biol* **176,** 263-268.

Spalluto, C., Wilson, D.I. and Hearn, T. (2013). Evidence for centriolar satellite localization of CDK1 and cyclin B2. *Cell Cycle* **12,** 1802-1803.

Srikanth, C.V., Mercado-Lubo, R., Hallstrom, K. and McCormick, B.A. (2011). Salmonella effector proteins and host-cell responses. *Cell Mol Life Sci* **68,** 3687-3697.

Staples, C.J., Myers, K.N., Beveridge, R.D., Patil, A.A., Lee, A.J., Swanton, C., *et al.* (2012). The centriolar satellite protein Cep131 is important for genome stability. *J Cell Sci* **125,** 4770-4779.

Steffen, A., Faix, J., Resch, G.P., Linkner, J., Wehland, J., Small, J.V., *et al.* (2006). Filopodia formation in the absence of functional WAVE- and Arp2/3-complexes. *Mol Biol Cell* **17,** 2581-2591.

Steffen, A., Ladwein, M., Dimchev, G.A., Hein, A., Schwenkmezger, L., Arens, S., *et al.* (2013). Rac function is critical for cell migration but not required for spreading and focal adhesion formation. *J Cell Sci*.

Stein, M.A., Leung, K.Y., Zwick, M., Garcia-del Portillo, F. and Finlay, B.B. (1996). Identification of a Salmonella virulence gene required for formation of filamentous structures containing lysosomal membrane glycoproteins within epithelial cells. *Mol Microbiol* **20,** 151-164.

Steuve, S., Devosse, T., Lauwers, E., Vanderwinden, J.M., Andre, B., Courtoy, P.J. and Pirson, I. (2006). Rhophilin-2 is targeted to late-endosomal structures of the vesicular machinery in the presence of activated RhoB. *Exp Cell Res* **312,** 3981-3989.

Strack, B., Calistri, A., Craig, S., Popova, E. and Gottlinger, H.G. (2003). AIP1/ALIX is a binding partner for HIV-1 p6 and EIAV p9 functioning in virus budding. *Cell* **114,** 689-699.

Suetsugu, S., Yamazaki, D., Kurisu, S. and Takenawa, T. (2003). Differential roles of WAVE1 and WAVE2 in dorsal and peripheral ruffle formation for fibroblast cell migration. *Dev Cell* **5,** 595-609.

Sugihara, K., Nakatsuji, N., Nakamura, K., Nakao, K., Hashimoto, R., Otani, H., *et al.* (1998). Rac1 is required for the formation of three germ layers during gastrulation. *Oncogene* **17,** 3427-3433.

Svitkina, T.M., Bulanova, E.A., Chaga, O.Y., Vignjevic, D.M., Kojima, S., Vasiliev, J.M. and Borisy, G.G. (2003). Mechanism of filopodia initiation by reorganization of a dendritic network. *J Cell Biol* **160,** 409-421.

Swanson, J.A. (2008). Shaping cups into phagosomes and macropinosomes. *Nat Rev Mol Cell Biol* **9,** 639-649.

Vazquez-Torres, A., Jones-Carson, J., Baumler, A.J., Falkow, S., Valdivia, R., Brown, W., *et al.* (1999). Extraintestinal dissemination of Salmonella by CD18-expressing phagocytes. *Nature* **401,** 804-808.

Vidali, L., Chen, F., Cicchetti, G., Ohta, Y. and Kwiatkowski, D.J. (2006). Rac1-null mouse embryonic fibroblasts are motile and respond to platelet-derived growth factor. *Mol Biol Cell* **17,** 2377-2390.

Vignjevic, D., Kojima, S., Aratyn, Y., Danciu, O., Svitkina, T. and Borisy, G.G. (2006). Role of fascin in filopodial protrusion. *J Cell Biol* **174,** 863-875.

Vito, P., Pellegrini, L., Guiet, C. and D'Adamio, L. (1999). Cloning of AIP1, a novel protein that associates with the apoptosis-linked gene ALG-2 in a Ca2+-dependent reaction. *J Biol Chem* **274,** 1533-1540.

Watanabe, G., Saito, Y., Madaule, P., Ishizaki, T., Fujisawa, K., Morii, N., *et al.* (1996). Protein kinase N (PKN) and PKN-related protein rhophilin as targets of small GTPase Rho. *Science* **271,** 645-648.

Watanabe, N., Kato, T., Fujita, A., Ishizaki, T. and Narumiya, S. (1999). Cooperation between mDia1 and ROCK in Rho-induced actin reorganization. *Nat Cell Biol* **1,** 136-143.

Watanabe, N., Madaule, P., Reid, T., Ishizaki, T., Watanabe, G., Kakizuka, A., *et al.* (1997). p140mDia, a mammalian homolog of Drosophila diaphanous, is a target protein for Rho small GTPase and is a ligand for profilin. *EMBO J* **16,** 3044-3056.

Weber, K. and Groeschel-Stewart, U. (1974). Antibody to myosin: the specific visualization of myosin-containing filaments in nonmuscle cells. *Proc Natl Acad Sci U S A* **71,** 4561-4564.

Wehrle-Haller, B. (2012). Structure and function of focal adhesions. *Curr Opin Cell Biol* **24,** 116-124.

Wei, Q., Zhang, Y., Li, Y., Zhang, Q., Ling, K. and Hu, J. (2012). The BBSome controls IFT assembly and turnaround in cilia. *Nat Cell Biol* **14,** 950-957.

Welch, M.D., Iwamatsu, A. and Mitchison, T.J. (1997). Actin polymerization is induced by Arp2/3 protein complex at the surface of Listeria monocytogenes. *Nature* **385,** 265-269.

Welch, M.D., Rosenblatt, J., Skoble, J., Portnoy, D.A. and Mitchison, T.J. (1998). Interaction of human Arp2/3 complex and the Listeria monocytogenes ActA protein in actin filament nucleation. *Science* **281,** 105-108.

Wong, A.R., Pearson, J.S., Bright, M.D., Munera, D., Robinson, K.S., Lee, S.F., *et al.* (2011a). Enteropathogenic and enterohaemorrhagic Escherichia coli: even more subversive elements. *Mol Microbiol* **80,** 1420-1438.

Wong, D., Bach, H., Sun, J., Hmama, Z. and Av-Gay, Y. (2011b). Mycobacterium tuberculosis protein tyrosine phosphatase (PtpA) excludes host vacuolar-H+-ATPase to inhibit phagosome acidification. *Proc Natl Acad Sci U S A* **108,** 19371-19376.

Wood, W., Jacinto, A., Grose, R., Woolner, S., Gale, J., Wilson, C. and Martin, P. (2002a). Wound healing recapitulates morphogenesis in Drosophila embryos. *Nat Cell Biol* **4,** 907-912.

Wood, W. and Martin, P. (2002b). Structures in focus - filopodia. *Int J Biochem Cell Biol* **34,** 726-730.

Yang, C. and Svitkina, T. (2011). Filopodia initiation: focus on the Arp2/3 complex and formins. *Cell Adh Migr* **5,** 402-408.

Yuk, J.M., Yoshimori, T. and Jo, E.K. (2012). Autophagy and bacterial infectious diseases. *Exp Mol Med* **44,** 99-108.

Zerial, M. and McBride, H. (2001). Rab proteins as membrane organizers. *Nat Rev Mol Cell Biol* **2,** 107-117.

Zhang, J., Zhu, J., Bu, X., Cushion, M., Kinane, T.B., Avraham, H. and Koziel, H. (2005). Cdc42 and RhoB activation are required for mannose receptor-mediated phagocytosis by human alveolar macrophages. *Mol Biol Cell* **16,** 824-834.

Zhou, D., Chen, L.M., Hernandez, L., Shears, S.B. and Galan, J.E. (2001). A Salmonella inositol polyphosphatase acts in conjunction with other bacterial effectors to promote host cell actin cytoskeleton rearrangements and bacterial internalization. *Mol Microbiol* **39,** 248-259.

Vordruck für die Versicherungen nach § 6 Abs. 3, Nr. 5, 6, 9

Hiermit versichere ich, dass ich bisher noch keinen Promotionsversuch unternommen habe.

Münster, 23.09.2013 .....

Hiermit versichere ich, dass ich die vorgelegte Dissertation selbst und ohne unerlaubte Hilfe angefertigt, alle in Anspruch genommenen Quellen und Hilfsmittel in der Dissertation angegeben habe und die Dissertation nicht bereits anderweitig als Prüfungsarbeit vorgelegen hat.

Münster, 23.09.2013 .....

Hiermit erkläre ich mich mit der Zulassung von Zuhörerinnen/Zuhörern beim öffentlichen Teil der Disputation einverstanden.

Münster, 23.09.2013 .....

Vordruck für die Versicherung nach § 6 Abs. 3 (2)

Hiermit versichere ich, dass ich nicht wegen einer Straftat zu einer Strafe von mehr als einem Jahr Freiheitsentzug verurteilt worden bin, zu deren Begehung ich meine wissenschaftliche Qualifikation missbraucht habe.

Münster, 23.09.2013 .....

Curriculum vitae

Danksagung